Assessment of Ground Effects on the Propagation of Aircraft Noise: The T-38A Flight Experiment

FOR REFERENCE

NOT TO BE TAKEN FROM THIS ROOM

William L. Willshire, Jr.

DECEMBER 1980

NASA

NASA Technical Paper 1747

Assessment of Ground Effects on the Propagation of Aircraft Noise: The T-38A Flight Experiment

William L. Willshire, Jr.
Langley Research Center
Hampton, Virginia

SUMMARY

A flight experiment was conducted to investigate air-to-ground propagation of sound at grazing angles of incidence. A turbojet-powered airplane was flown at low altitudes over two microphone arrays. The first array consisted of 8 microphones positioned along a 2500-m concrete runway. The second array consisted of 12 microphones positioned over grass parallel to the runway. Twenty-eight flights were made at altitudes ranging from 10 to 160 m. The acoustic data have been reduced to 1/3-octave band spectra and time correlated with the tracking and weather information. Acoustic, tracking, and weather information are presented in the appendices in a form which will allow independent analysis of the data.

The dependence of ground effects on frequency, incidence angle, and slant range has been determined using two analysis methods. In the first, referred to as the near/far comparison method, acoustic data from a microphone close to the flight track are compared with data from down-range microphones positioned over grass. The second method used is a direct comparison between two microphones equidistant from the flight track but positioned over the two different surfaces. In both methods, source directivity angle was the criterion by which portions of the microphone signals were compared.

The results of the two analysis methods were in general agreement. The ground effects were largest in the frequency range of 200 to 400 Hz and were found to be dependent on incidence angle and on slant range. Ground effects measured for angles of incidence greater than 10° to 15° were near zero. Measured attenuation increased with increasing slant range for slant ranges less than 750 m. Theoretical predictions were found to be in good agreement with the major details of the measured results.

INTRODUCTION

The levels of noise received on the ground from an aircraft are strongly influenced by the ground as a reflecting-absorbing boundary. When the aircraft is close to the ground during takeoff and landing, noise is emitted at grazing angles to a sideline observer. The signal received at the sideline is different, by as much as 20 dB for certain frequencies, from what would be expected considering only the effects of spherical spreading and atmospheric absorption. The difference between measured and expected sideline noise levels is referred to as lateral attenuation.

Lateral attenuation is not due solely to ground effects. At low elevation angles, shielding effects of the aircraft on the emitted noise may substantially alter the received signal. Lateral attenuation should be separated into shielding effects and ground effects because of their differing physical origins. Shielding effects are aircraft dependent, while ground effects are functions of

ground properties such as porosity and roughness. A basic understanding of the effects contributing to lateral attenuation is required for accurate prediction of aircraft noise.

A procedure for predicting propagation effects on aircraft noise was given by Putnam (ref. 1) in 1975. For predicting ground attenuation, Putnam recommended the empirical curves developed by Franken and Bishop (ref. 2) for ground-to-ground propagation in conjunction with civil noise-exposure-forecast (NEF) transition curves (given in ref. 3) for air-to-ground propagation. The NEF curve, which illustrates the dependence of ground attenuation on aircraft elevation angle, has a sharp cutoff of ground effects above about 7° elevation; whereas, other estimates have been made that ground effects persist for elevation angles up to 30°, 50°, or even 70° (ref. 1).

Pao, Wenzel, and Oncley (ref. 4) have proposed an analytically based prediction method for ground effects to replace Putnam's empirical method. Ground reflection and attenuation are included in the analytical method for ground-to-ground and air-to-ground propagation. The empirical ground-impedance formula by Delany and Bazley (ref. 5) is used in the prediction method. In agreement with Putnam's method, the analytical procedure predicts that ground attenuation of aircraft noise decreases quickly, but smoothly, with increasing elevation angles.

A widely used data set on ground-to-ground propagation over large distances was developed by Parkin and Scholes (refs. 6 and 7) in the middle 1950's. They used a small turbojet engine as a noise source and made measurements at logarithmically spaced intervals, to distances of 7 km, over a grassy terrain. Data were recorded under varying weather conditions over a period of one year at two sites in England. Zorumski (ref. 8) has found fair-to-good agreement between the prediction method of Pao, Wenzel, and Oncley and the data of Parkin and Scholes. Although data scatter is large (due to variable weather and terrain conditions), the theory and the data show that ground attenuation effects are largest in a frequency range from about 200 to 2000 Hz. The theory also correctly predicts the magnitude of the ground attenuation and the ground reflection effects.

A flight experiment was conducted by Benson, Karplus, Burkhard, Sabine, and Raelson (refs. 9 to 12) to study the influence of weather on air-to-ground propagation. The results of their study indicated that ground attenuation was a function of angle, with little attenuation measured for elevation angles greater than 14°, and that the ground attenuation increased linearly with frequency from 75 to 2400 Hz. Walker has gathered data from several aircraft and developed empirical curves for the ground attenuation as a function of frequency and elevation angle (ref. 13). His curves indicate large attenuation effects (10 to 20 dB) at frequencies below 200 Hz. This is in sharp disagreement with the predictions and with the Parkin and Scholes data. Mashita and Bauer (ref. 14) have analyzed data from three aircraft and found attenuation effects in the frequency range from 200 to 2000 Hz, which roughly agree with the low-angle predictions. However, their results do not show the predicted rapid decrease of attenuation with elevation angle. Mashita and Bauer also isolated aircraft-dependent lateral attenuation effects and recommended that the curve with least lateral attenuation be used for the ground attenuation.

2

The purpose of this paper is to analyze a comprehensive data base, the T-38 excess-ground-attenuation-experiment data, for ground effects on air-to-ground noise propagation. The T-38 experiment is described in detail in reference 15 and was intended to complement the data of Parkin and Scholes by including the elevation angle of the acoustic source as a variable. Shallow angles are emphasized since data are needed in this regime to settle the questions of the dependence of ground attenuation on angle. A turbojet airplane, powered by a single rear-mounted engine, is used as a noise source in order to minimize shielding effects. Ground effects are calculated from the data to determine the variation of these effects with frequency, elevation angle, and slant range. A theoretical model is chosen and used to make predictions of the ground effects to compare with the measured results. Basic data on the airplane flights, the weather, and the noise are included as appendices so that independent studies of these data may be conducted by other researchers.

SYMBOLS

a	dimensionless nonnegative number
A	complex number
c_o	speed of sound
f	frequency
$F(\tau)$	function defined by equation (4)
$Im(A)$	imaginary part of complex number A
k	wave number
k_o	wave number of 1/3-octave bandcenter frequency
p^2	mean square pressure
$p_o{}^2$	free-field mean square pressure
r_2	total path length of reflected wave
R	magnitude of complex reflection coefficient
W	complex error function
X,Y,Z	data reduction coordinates
z	acoustic ground impedance
α	phase of complex reflection

β	elevation angle
Γ	plane wave reflection coefficient
Δr	difference in length between reflected and direct paths
η	defined by equation (8)
θ	angle between reflected wave path and ground
ν	normalized acoustic admittance of ground
ρ_o	ground level density
σ	ground flow resistance
τ	defined by equation (5)

Abbreviations:

EPNL	effective perceived noise level
G.m.t.	Greenwich mean time
NEF	noise exposure forecast
SPL	sound pressure level
SR	slant range

DESCRIPTION OF EXPERIMENT

Test Site

The flight program was conducted during the first week of November 1978 at the NASA Wallops Flight Center. Figure 1 is a photograph of the general experimental site. The aircraft flight track was along runway 10-28; the flight track direction was from the top left to the top right of the figure. The microphone arrays were located along runway 04-22, a 2500-m long, 50-m wide, landing research runway and in the grassy area to the left (north), between the runway and the taxiway. The radar tracking site was located to the left of the intersection of runways 04-22 and 10-28.

The grassy area may be described as covered with institutional grass which was cut every week. The width of the grassy area was 115 m for the wider portion and 70 m for the narrower portion, close to the flight track. The soil under the grass was a mixture of sand and clay and was dry because the area had received less than 1.3 cm of rain within the 30 days before the test.

Aircraft

The airplane used in the experiment is shown in figure 2. The airplane was powered by two turbojet engines with afterburners. Each engine develops 11 930 N of thrust at military power setting, 17 130 N of thrust with after-burning, and 490 N of thrust at flight idle. Listed in table I are additional engine parameters. A laser tracker was used to determine aircraft position, which was calculated in Cartesian coordinates oriented with respect to the runways as shown in figure 3, every 1/2 sec Greenwich mean time (G.m.t.).

Constraints for unambiguous tracking are: ranges between 100 m and 36 000 m; radial velocities less than 3048 m/sec; and radial acceleration less than 0.45 rad/sec. Tracking system accuracy is estimated to be ±0.5 m.

The airplane was equipped with two laser reflector cube housings. The main reflector was located on a centerline pylon 7.2 m forward of the exhaust nozzle exit and 0.6 m below the engine centerline. A secondary reflector was located on the aft fuselage 2.2 m forward of the nozzle exit, 0.2 m above the engine centerline, and 0.7 m laterally from the centerline. Speed brakes are shown in figure 2 in the deployed position behind the main laser reflector. Exhaust nozzles are 0.4 m in diameter with 0.5-m centerline spacing. The nozzle centers are 1.4 m above the ground plane and protrude 0.6 m behind the aircraft fuselage.

In order to minimize flight speeds, the landing gear and speed brakes were deployed. During the incoming flight, the laser tracker locked onto the main reflector. However, the speed brakes and main-landing-gear doors obstructed the line of sight to the main reflector after the aircraft passed the tracking station. Hence, the aircraft was tracked during the outgoing flight by the secondary reflector. The loss of track introduced gaps in the tracking information ranging from 3 to 7 sec. In processing the flight tracks, a straight line was interpolated between the gap endpoints.

There were 28 flights (runs) in 2 days of testing. For every run, the flight path of the airplane was from west to east above the centerline of run-way 10-28 at a prescribed altitude. The airplane was flying at the particular run conditions at least 800 m before and after the intersection of runways 04-22 and 10-28. The various runs and their corresponding flight conditions are listed in table II. For the majority of the flights, the number one (left) engine was at flight idle and the number two (right) engine was at a nominal power setting of 100 percent. Two runs were flown at an altitude of 18 m with the number two engine in full afterburner. Run 28 was done under ground-static conditions.

Figure 4 is an illustration of the laser track for run 26. In the fig-ure, the three-dimensional tracking information is split into 2 two-dimensional views: an X-Y view and an X-Z view. The X-Y view includes an outline of the Wallops runways used in the test and the microphone positions, labeled 1 to 20, to be discussed in the next section. The microphone locations are along run-way 04-22, and the aircraft's ground track is the dashed line along runway 10-28. Evident in the X-Z view is the straight line that has been computed to fill in a gap in the tracking information due to loss of track.

Acoustic Instrumentation

The acoustic instrumentation consisted of 20 microphone systems located in 5 mobile vans. The microphone positions are illustrated in figure 5, and their Cartesian coordinates are listed in table III (in the runway-fixed coordinate system). The components of a microphone system are illustrated in block form in figure 6.

To document the system's linearity, sensitivity, distortion, and noise floor, each acoustic instrumentation system was laboratory calibrated prior to going into the field. The results of the laboratory calibrations were used to insure that the equipment operated within the manufacturer's specifications. A piston phone was used in the field for level calibration, and a pink noise source was used for frequency response calibration. The acoustic signals recorded were time correlated with G.m.t.

Weather Instrumentation

Weather measurements were made at a number of locations along runway 04-22. Wind speed, wind direction, temperature, and relative humidity were measured with portable 1.2-m weather stations located near vans 1 and 5 (see fig. 5) in the open areas south of runway 04-22. A 10-m-high portable weather station located near van 2 measured barometric pressure in addition to the variables measured by the 1.2-m stations. The output of the 1.2-m stations was in the form of strip charts, while the output of the 10-m station was digitally encoded and recorded on the magnetic tape recorder in van 2. The output of the 10-m station could also be conveniently read in a real-time mode inside the van. Detailed descriptions of both types of weather stations may be found in reference 16.

A retrievable balloon was used to raise one weather measuring instrument package. Profiles of temperature, relative humidity, and wind speed, up to an altitude of 500 m, were measured with the balloon package. The altitude of the package was computed from pressure differences between the measured ground pressure and the pressure measured aloft. The output of the package was telemetered down to an instrument van on the ground, where it was displayed in a real-time mode and was encoded and recorded on magnetic tape. The balloon weather station is described in more detail in reference 17.

Additional weather information was obtained from three permanent weather stations located in building N-159, in building C-15, and in the triangle area. The station at N-159 has a sensor height of 10 m, the sensor height at C-15 is 4 m, and the triangle station sensors have heights of 3, 6, 9, 12, and 15 m. Each station was instrumented to measure wind speed, wind direction, and temperature. The N-159 site was also equipped for the measurement of dew point and barometric pressure. The outputs of the N-159 and C-15 sites were in the form of strip charts, while the triangle site output was in the form of computer listings.

A representative sample of the weather information obtained from the ground stations is illustrated in table IV for run 27. Weather data for each run, as

well as profiles of wind speed, temperature, and relative humidity taken through use of the instrumented balloon package, are given in appendix B.

Acoustic Data

The analog tapes of the flyover noise were reduced by 1/3-octave band analysis. The frequency range of the analysis was from 20 Hz to 10 kHz with an averaging time of 1/8 sec. The 1/8-sec averaging time was necessary because of the large angular velocity of the aircraft with respect to the microphones closest to the flight path. The 1/3-octave band analysis was initiated for each run when the incoming aircraft was approximately 800 m from the intersection of runways 04-22 and 10-28. The analysis was stopped when the amplitude of the noise received from the aircraft approached that of the background noise. Associated with each 1/3-octave spectrum is a G.m.t., an overall sound pressure level (SPL), and a dBA level.

The piston-phone calibration was used to calibrate the amplitude of the 1/3-octave band analysis system. The pink-noise calibration was used to correct for deviations from a flat frequency response of the record/playback system.

The quality of the reduced acoustic data was first checked by inspection of the overall time histories for each microphone for each run. Overall time histories for microphones 2, 4, 6, and 8 for run number 27 are illustrated in figure 7. Broadening of the shape of the airplane noise time history occurs as the distance from microphone to flight path increases with microphone number. This may be seen in figure 7. The effect of atmospheric propagation anomalies are noted by the roughness in the signals from the further microphone locations because of the longer propagation distances and the smaller signal-to-noise ratios.

Ambiguities may exist in the results of the lower frequency 1/3-octave bands because of the 1/8-sec averaging time. The 1/3-octave band analyzer used in the data reduction process passes an input signal in parallel through various, active 1/3-octave band filters and selectively samples the output of the filters. The limiting feature of this analysis for the present application is the response time of the filters. A customary manner of characterizing filter response is to compute a so-called "BT" product (bandwidth multiplied by time width of the signal); a BT product greater than 50 is considered satisfactory. For the 100-Hz 1/3-octave band at an analysis time of 1/8 sec, the BT product is 6. The reduced data at the lower frequency bands must be viewed with the limited response times of the filters in mind. However, the lower frequency results to be given later appear to be consistent with the higher frequency results.

Spectra from run 27 for microphones 2, 4, 8, and 16, at the time of their respective maximum overall sound pressure levels, are shown in figure 8. Observed in the last three spectra of figure 8 is a double hump formation which broadens (over a number of 1/3-octave bands) and deepens with increasing propagation distance.

METHODS OF ANALYSIS AND THEORY

Various methods may be used to determine ground effects. Most methods are comparative in nature in that a relative difference is determined between two microphone signals. After a methodology is chosen, the manner in which the portions of the signals to be compared are selected becomes a critical issue. Criteria which may be used to select the portions of the signals are maximum overall level, maximum level in a particular 1/3-octave band, closest point of approach, and sound emission angle, to name a few. From a trial-and-error approach, two methods to compute ground effects were found to be the most reliable and consistent. They are described in this section. Included in the discussion is the criteria used to select the portions of the signals to be compared.

Comparison of Near and Far Microphones

The method used by Parkin and Scholes (refs. 6 and 7) to calculate ground effects was a comparison in the frequency domain of near and far microphones positioned over the same terrain. In this method, a microphone close to the acoustic source is chosen as a reference microphone, and its signal is compared to the signals from the remaining microphone locations, referred to as measurement microphones. Corrections are made to the reference microphone signal for differences in spherical spreading and atmospheric absorption between the measurement and reference microphone locations. The difference between the corrected reference spectrum and the measurement spectrum is a measure of the relative difference in ground effects between the two positions. If the reference microphone signal is free of ground effects, the procedure results in a measure of the absolute ground effect at the measurement location.

In practice, the method of comparing near and far microphones must account for the directivity of the source. With a static experiment like that of Parkin and Scholes, the problem of differences in source directivity was not large. In their experiment, all of the microphones were of the same height and were placed on a radial line from the source, and the dimensions of the source were small compared to the distance to the first microphone. As an aircraft flies by a microphone, however, the emission directivity angle of the received signal is constantly changing. For flight work, the solution is to insure that the signals from the two microphones to be compared have the identical source emission angle. The problem of directivity synchronization involved in comparing two signals from different microphones in a flight experiment is a major one.

For the present study, implementation of the near/far comparison method was accomplished with the aid of a computer. A free-field source spectrum was used as the reference spectrum. This source spectrum was determined by averaging spectra from runs 17 to 24, 26, and 27 for microphone 15. These 10 runs were selected because they were taken under more ideal weather conditions. For the results to be given later, the following subset of the 10 runs was selected (the subset represents 1 run for each altitude): 17, 21, 24, 26, and 27. Microphone 15, a 10-m microphone positioned over concrete close to flight path, was selected because it had more readily predictable ground effects. The

spectra for each run to be averaged were selected from an emission angle criterion. Before averaging the 10 spectra, the effect of ground reflections were removed, as detailed below, and the spectra were corrected for atmospheric absorption and spherical spreading to a slant range of 10 m.

Because of the oblique angle between the microphone arrays and the flight track in the T-38A flight experiment, the sound emitted from the airplane at an emission angle of 122.5° (referenced to the forward inlet direction) propagated parallel to the microphone arrays. For a particular run, values were calculated for the time and position of the aircraft at which the sound emitted propagated parallel to and over the microphone array containing microphone 15 (the sound emitted at a directivity angle of 122.5°, see fig. 9). These values are referred to as the emission time and position. The propagation time from this aircraft position to microphone 15 was then calculated using an average speed of sound, which was calculated using a layered model of the atmosphere incorporating measured weather parameter profiles. The reception time was defined as the sum of the emission time and the propagation time. The two 1/3-octave band spectra of the time history for microphone 15 located on either side of the reception time were averaged together to form a spectrum for the particular run. The averaging of two 1/8-sec spectra gives an effective averaging time of 1/4 sec for the resulting spectrum.

Corrections computed with the ground-effects prediction procedure (to be discussed later in this section) were applied to the spectra to remove the influence of ground reflections. The value of the input parameters necessary for the procedure were set to the same values as those used in a later section of this report for a microphone positioned over concrete. Atmospheric absorption corrections were calculated using the American National Standards Institute (ANSI) standard method for the determination of molecular absorption (ref. 18). The resulting reference spectrum is illustrated in figure 10. The solid curve is the average spectrum at 10.m with ground effects removed and is the spectrum used as the reference spectrum in the near/far comparison method.

After the reference spectrum has been determined, the near/far method is implemented by selecting a measurement microphone for a particular run and determining the measurement spectrum in a similar fashion. The reference spectrum is brought to the same slant range as the measurement spectrum by incorporating losses for spherical spreading and atmospheric absorption. The measurement spectrum is subtracted from the reference spectrum to yield a ground effects spectrum for the particular geometry (measurement microphone and run) chosen. Subtracting the measurement spectrum from the reference spectrum defines a positive sign for an attenuation and a negative sign for an amplification for the ground effects at the measurement microphone.

Comparison of Microphones Over Concrete and Grass

The second method used to analyze ground effects is a direct comparison between two microphones equally distant from the acoustic source but positioned over different surfaces. An advantage of the direct comparison method is that there is no need to use corrections for differences in spherical spreading and atmospheric absorption between the two signals to be compared. The direct

9

comparison method has the same source directivity problem as the previous comparative method. To solve the problem, the source emission angles of the two signals to be compared are again constrained to be equal. The difference is then taken between the signals of the two microphones in the frequency domain. The result is a spectrum which is a measure of the relative difference in ground effects between the two microphone locations.

Implementation of the direct comparison method begins with the selection of a microphone pair and a run number. For the present study, the possible microphone pairs which are equal distance from the flight path and positioned over grass and concrete, respectively, are microphones 1-13, 2-14, 3-15, 8-18, 9-19, and 11-20. The emission angle criterion of 122.5° is again used to determine a spectrum from each microphone of a pair for the chosen run. The spectrum for the microphone positioned over grass is subtracted from the spectrum for the microphone over concrete to yield a ground effects spectrum. The spectrum represents the differences in ground effects between the two locations for the two surfaces with similar geometry between the microphones and the aircraft. A positive value signifies a lower level received at the microphone over grass as compared to the microphone over concrete.

Theoretical Predictions of Ground Effects

The theoretical model chosen to make ground effects predictions is the procedure recommended by Pao, Wenzel, and Oncley (ref. 4). This prediction method was employed by Zorumski (ref. 8) to make comparisons with the Parkin and Scholes (refs. 6 and 7) ground effects data and some aircraft flight data. The formulation of the method is based on work by Chien and Soroka (ref. 19) and Thomasson (ref. 20). The predicted mean square pressure p^2 at the observer position is

$$\frac{p^2}{p_o^2} = 1 + 2R \exp(-ak \, \Delta r)^2 \cos (\alpha + k \, \Delta r) + R^2 \tag{1}$$

where p_o^2 is the mean square pressure without ground effect (free-field mean square pressure), R and α are the magnitude and phase of the complex reflection coefficient, a is a dimensionless nonnegative number, k is the wave number, and Δr is the difference in length between the reflected path and the direct path.

The complex reflection coefficient is defined here as

$$Re^{i\alpha} \equiv \Gamma + (1 - \Gamma) \, F(\tau) \tag{2}$$

where Γ is the plane-wave reflection coefficient

$$\Gamma = \frac{\sin \theta - \nu}{\sin \theta + \nu} \tag{3}$$

θ is the angle between the reflected wave path and the ground (see fig. 9), and ν is the normalized acoustic admittance of the ground. The function $F(\tau)$ is given by

$$F(\tau) = 1 - \tau W(i\tau)\sqrt{\pi} \tag{4}$$

with

$$\tau = (\sin \theta + \nu) \sqrt{\frac{kr_2}{2i}} \tag{5}$$

where r_2 is the total path length of the reflected wave, and W is the complex error function defined by

$$W(A) = \frac{i}{\pi} \int_{-\infty}^{\infty} \frac{e^{-t^2}}{A - t} dt \qquad \text{Im}(A) > 0 \tag{6}$$

where $\text{Im}(A)$ represents the imaginary part of the complex number A.

The input for the formulation outlined above is the geometry of a source/receiver combination, the frequency, the constant a, and the normalized acoustic admittance of the ground. A two-parameter model given by Delany and Bazley (ref. 5) was used to describe the normalized acoustic admittance. The two-parameter model given in a dimensionless form after Zorumski (ref. 8) is

$$\nu = \frac{\rho_0 c_0}{z} = \left[1 + (6.86\eta)^{-0.75} + (4.36\eta)^{-0.73} \right]^{-1} \tag{7}$$

where ρ_0 and c_0 are the ground-level density and the speed of sound, respectively, z is the acoustical impedance, and η is given by

$$\eta \equiv \pi \rho_0 f / \sigma \tag{8}$$

where f is the frequency and σ is the ground flow resistance. A rough range of the value of σ for commonly encountered surfaces is from 750 Mg/(s-m^3) for an acoustically hard surface to 50 Mg/(s-m^3) for an acoustically soft surface.

Equation (1) is for discrete frequency prediction of ground effects. The acoustic data have been analyzed with 1/3-octave band analysis techniques. To make predictions comparable to the results of the 1/3-octave band analysis of the data, equation (1) must be changed to incorporate 1/3-octave band averaging. If the assumption is made that the complex reflection coefficient and the coherence factor vary little within a 1/3-octave band, the integration of equation (1) over a 1/3-octave band reduces to the integration of the cosine term. The integration yields

$$\frac{p2}{p_o{}^2} = 1 + 2R \exp(-ak \; \Delta r)^2 \; \frac{\cos \; (\alpha + k_o \; \Delta r) \; \sin \; (0.115 k_o \; \Delta r)}{0.115 k_o \; \Delta r} \tag{9}$$

where k_o is the wave number of the 1/3-octave bandcenter frequency.

RESULTS

Variation With Frequency

Results of the near/far comparison method are compared with predictions in the frequency domain in figure 11. Results are presented for microphones 4, 6, 8, and 11, representing a lateral distance from the flight track ranging from 460 m to 1650 m, and for a subset of the ten "best" runs (runs 24, 21, 17, 27 and 26) which correspond to one flight for each altitude flown. The same run sequence will be used for all of the results to be given. The microphones were all 1.2-m microphones positioned over grass.

The geometry between the airplane and the measurement microphones at the calculated emission times was entered into the prediction procedure. The values assigned to the ground flow resistance and the constant a were optimized for the best agreement between theory and experiment. The range of values tried was from 30 to 500 Mg/(s-m^3) for ground flow resistance and from 0 to 1 for the constant a. The smallest standard error between the measured and predicted results was obtained with a value of 62.5 Mg/(s-m^3) for the ground flow resistance of grass and a value of 0.1 for a.

Plotted along the ordinate in figure 11 is ground attenuation in decibels (dB) and along the abscissa is frequency in Hz. The data are cut off at 2 kHz because the signal-to-noise ratio for higher frequencies was poor for the microphones positioned far from the flight track. The solid curves are the measured results, and the dashed lines are the predicted curves. The legend to the right of each plot identifies the run and measurement microphone as well as the slant range (SR) and the elevation angle β from the aircraft to the microphone at the emission time. (See fig. 9.) The plots in the figure are grouped according to the altitudes of the runs, beginning with the highest altitude run in figure 11(a) and ending with the lowest altitude run in figure 11(e).

As the measurement microphones get farther away from the flight track (as microphone number increases), the measured excess attenuation generally increases for a particular run in figure 11. Also, greater excess attenuations are observed for a particular microphone for the lower altitude flights. Restated, a trend of greater ground attenuation for smaller β is generally observed in the plots. The largest values of excess attenuation, greater than 20 dB, are found in the frequency range of 200 to 400 Hz. The agreement between the predicted frequency dependence and the measured dependence is good, while the predicted curves generally fall beneath the measured curves.

Results for the direct comparison method, along with predictions, are illustrated in figure 12 in a fashion similar to that presented for the near/far method. Results are given for the same run sequence as in the near/far method for microphone pairs 2-14 and 9-19, representing lateral distances from the flight track of 250 m and 1600 m, respectively. The predictions were made by computing ground effects spectra for each microphone of a pair and then subtracting the spectrum of the microphone over grass from the spectrum of the microphone over concrete. The values of the input parameters pertaining to the grass were the same as those selected to make the near/far comparison predictions, namely a value of 62.5 Mg/(s-m^3) for the ground flow resistance of grass and a value of 0.1 for a. A range of values from 125 to 1000 Mg/(s-m^3) was tried for the ground flow resistance of concrete. The smallest standard error of estimate was obtained between the measured and predicted results with a value of 750 Mg/(s-m^3) for the ground flow resistance of concrete, and hence, this value was used in the predictions of figure 12.

The same general trends are observed in the direct comparison results as in the near/far comparison results: increased measured attenuation with decreasing β and maximum attenuation frequency in the range of 200 to 400 Hz. However, the measured spectra are more erratic than those obtained from the near/far method, and the predicted frequency of maximum attenuation is generally lower than the measured frequency. The direct comparison results are, in general, more complicated and not as easy to interpret as the near/far results. The direct comparison results represent the difference in ground effects between two locations, while the near/far results represent the absolute ground effects for one microphone location. From a prediction viewpoint, direct comparison predictions are also more complex and subject to larger errors, since errors in the two predicted ground effects spectra may be amplified when the spectra are subtracted.

Variations With Elevation Angle

Plotted in figure 13 are the measured and predicted excess ground attenuations obtained by the near/far comparison method given as a function of elevation angle β for the four 1/3-octave bands of center frequencies: 100, 250, 500, and 1000 Hz. Illustrated in the figure are results for all of the 1.2-m microphones over grass for the same run sequence as the earlier results. The excess ground attenuation results are divided into four slant-range groups: 230, 440, 900, and 1600 m. The average deviation of the slant range of a data point in a particular slant-range group is less than 10 percent. Division of the data by the chosen slant ranges partitions the data into the following

microphone combinations; 2, 4, 5-6-7, and 8-9-11, respectively. Plotted along the abscissa in each figure is β in degrees, ranging from 0.5 to 40; along the ordinate, ground attenuation in decibels. The measured results are denoted in the figure by the symbols; the dashed lines are the predictions.

Although scatter is evident in the measured results, similar trends are seen in the predicted results. The measured and predicted attenuations generally show a rapid decrease, approaching zero, with increasing β larger than 10° to 15°. The predicted curves generally fall beneath the majority of the data points.

Comparison of predictions with results from the direct comparison method for all the applicable 1.2-m microphone pairs for the same run sequence are given in figure 14 as a function of β. The results have been separated into a 230-m slant-range group and a 1600-m slant-range group. The average deviation of the slant range of a data point in a particular slant-range group is less than 10 percent. Results for microphone pair 2-14 are in the shorter slant-range group while the results from microphone pairs 8-18, 9-19, and 11-20 fall in the longer slant-range group. The large scatter and lack of trend seen in these plots, particularly in the 1600-m slant-range group, indicate the difficulty and complexity in the direct comparison method with respect to the near/far method in measuring excess ground attenuation.

Integrated Measure of Excess Ground Attenuation

An integrated noise metrics analysis was applied to the T-38A acoustic data base. Effective perceived noise level (EPNL) was calculated for a number of runs and microphones, and a measure of lateral attenuation in terms of EPNL units was determined using the near/far comparison method. The measurement microphones used were the 1.2-m microphones positioned over grass. The results of the EPNL calculations for the same run sequence as the results given before are illustrated in figure 15. Plotted along the ordinate is lateral attenuation in EPNL (dB) and along the abscissa is elevation angle β in degrees. Elevation angle is redefined for the integrated measures to be the angle between the source and the receiver at the point of closest approach. A 20 decibel spread is seen in the data for small elevation angles. Even with the spread, the trend observed earlier of increasing attenuation with decreasing elevation angle is clearly seen in the data. The corresponding closest-approach slant ranges associated with the data points plotted in figure 15 vary from 180 m to 1530 m.

The data from figure 15 have been subdivided and replotted in four slant-range groups: 190, 370, 765, and 1330 m. The average deviation of the slant range of a data point in a particular slant-range group is less than 10 percent. A third-order least-square fit, constrained to be zero at an elevation angle of 90 degrees, has been calculated for each slant-range group and plotted in figure 16 along with a lateral attenuation curve obtained from flight data gathered by Cooper (ref. 21). As a result of the subdivision into slant-range groups, a family of lateral attenuation curves is formed, and a slant-range dependence may be observed. As slant range decreases, less lateral attenuation is measured for the same elevation angles. For large elevation angles, the curves (or the extensions of the curves) merge, showing little measured attenuation. The two

largest slant-range curves collapse together on top of the curve for small elevation angles determined by Cooper. The slant ranges of the small elevation angle data of the curve in reference 21 were greater than 1330 m.

CONCLUDING REMARKS

Ground effects on aircraft noise were measured in a flight experiment over a wide range of elevation angles and slant ranges. A theoretical model chosen for comparison adequately predicted the measured ground effects on actual aircraft noise. Owing to the use of an airplane and practical propagation conditions, the results of the investigation are directly applicable to aircraft noise propagation problems.

The ground attenuation values were determined with two analysis methods; the near/far method and the direct comparison method. Results from the two methods agreed in general but exhibited considerable scatter, particularly for the direct comparison method which was found to be the inferior of the two methods. The scatter was due to many contributing factors, including atmospheric parameter gradients and fluctuations, the data sampling rate in the data reduction, and the finite dimensions of the test surfaces. Different atmospheric conditions over the grass and the runway were an additional factor contributing to the scatter in the direct comparison results.

The theoretical model employed was the ground effect prediction procedure recommended by Pao, Wenzel, and Oncley. The agreement between the measured and predicted results was good considering an outdoor environment, a moving noise source, and the long slant ranges. The predicted frequency of maximum ground attenuation agreed very well with the measured frequency, particularly for the near/far comparison results. The amplitudes of the predicted ground attenuation were generally smaller than the measured amplitudes.

The largest ground attenuations, in excess of 20 dB, were found for the 1/3-octave bands in the frequency range of 200 to 400 Hz. The measured ground attenuation quickly diminished with increasing elevation angle β. The measured ground attenuations were close to zero for β greater than 10° to 15°. A strong dependence of ground attenuation on slant range was observed, particularly in the effective perceived noise level results for small slant ranges. The farther the receiver was from the aircraft, the greater the measured ground attenuation for the same β. This slant-range dependence disappeared for slant ranges greater than about 750 m.

Langley Research Center
National Aeronautics and Space Administration
Hampton, VA 23665
October 27, 1980

APPENDIX A

FLIGHT DATA

Listed herein are the emission (EMIT) time, the emission position coordinates (X,Y,Z), the velocity (VEL), and the magnetic heading of the aircraft at the emission time. Emission times were calculated using a directivity angle criteria of 122.5°. Data are listed for every microphone and for every run. The data for a particular run and microphone are identified with the following nomenclature EGFR ##.M**, where ## is the run number and ** is the microphone number.

DIRECTIVITY ANGLE = 122.5 deg

FILENAME	EMIT TIME	X	Y (m)	Z	VEL (m/s)	HEADING (deg)
EGFR01.M01	11:46:38.07	-31.1	50.0	11.9	89.6	99.6
EGFR01.M02	11:46:38.07	-31.1	50.0	11.9	89.6	99.6
EGFR01.M03	11:46:38.07	-31.2	50.1	11.9	89.6	99.6
EGFR01.M04	11:46:38.11	-29.2	46.9	11.9	89.6	99.6
EGFR01.M05	11:46:38.16	-26.5	42.5	11.9	89.6	99.6
EGFR01.M06	11:46:37.86	-41.1	66.1	11.9	89.6	99.6
EGFR01.M07	11:46:37.90	-39.0	62.8	11.9	89.6	99.6
EGFR01.M08	11:46:37.95	-36.8	59.3	11.9	89.6	99.6
EGFR01.M09	11:46:37.99	-34.8	56.0	11.9	89.6	99.6
EGFR01.M10	11:46:38.04	-32.6	52.4	11.9	89.6	99.6
EGFR01.M11	11:46:38.04	-32.6	52.4	11.9	89.6	99.6
EGFR01.M12	11:46:38.04	-32.6	52.3	11.9	89.6	99.6
EGFR01.M18	11:46:39.00	12.5	-23.7	12.0	89.6	99.6
EGFR01.M19	11:46:39.04	14.5	-24.0	12.0	89.6	99.6
EGFR01.M20	11:46:39.09	16.7	-27.6	12.0	89.6	99.6

16

DIRECTIVITY ANGLE = 122,5 deg

FILENAME	EMIT TIME	X	Y (m)	Z	VEL (m/s)	HEADING (deg)
EGFR02.M01	11:54:27.57	-27.4	50.0	11.8	88.5	99.6
EGFR02.M02	11:54:27.57	-27.3	50.0	11.8	88.5	99.6
EGFR02.M03	11:54:27.57	-27.4	50.1	11.8	88.5	99.6
EGFR02.M04	11:54:27.61	-25.4	46.8	11.8	88.5	99.6
EGFR02.M05	11:54:27.67	-22.8	42.5	11.8	88.5	99.6
EGFR02.M06	11:54:27.36	-37.3	66.1	11.8	88.5	99.6
EGFR02.M07	11:54:27.40	-35.3	62.8	11.8	88.5	99.6
EGFR02.M08	11:54:27.45	-33.1	59.2	11.8	88.5	99.6
EGFR02.M09	11:54:27.49	-31.1	56.0	11.8	88.5	99.6
EGFR02.M10	11:54:27.54	-28.9	52.4	11.8	88.5	99.6
EGFR02.M11	11:54:27.54	-28.8	52.4	11.8	88.5	99.6
EGFR02.M12	11:54:27.54	-28.8	52.3	11.8	88.5	99.6
EGFR02.M13	11:54:28.29	5.8	-3.8	11.9	88.5	99.6
EGFR02.M14	11:54:28.29	5.8	-3.9	11.9	88.5	99.6
EGFR02.M15	11:54:28.28	5.8	-3.8	11.9	88.5	99.6
EGFR02.M16	11:54:28.29	6.0	-4.2	11.9	88.5	99.6
EGFR02.M17	11:54:28.29	6.2	-4.5	11.9	88.5	99.6
EGFR02.M18	11:54:28.51	16.2	-20.7	11.9	88.5	99.6
EGFR02.M19	11:54:28.55	18.2	-24.0	11.9	88.5	99.6
EGFR02.M20	11:54:28.60	20.5	-27.6	11.9	88.5	99.6

DIRECTIVITY ANGLE = 122.5 deg

FILENAME	EMIT TIME	X	Y (m)	Z	VEL (m/s)	HEADING (deg)
EGFR03.M01	11:58:54.52	-29.8	49.3	11.9	89.4	99.7
EGFR03.M02	11:58:54.52	-29.8	49.3	11.9	89.4	99.7
EGFR03.M03	11:58:54.52	-29.9	49.4	11.9	89.4	99.7
EGFR03.M04	11:58:54.57	-27.5	45.5	11.9	89.4	99.7
EGFR03.M05	11:58:54.64	-24.3	40.2	11.9	89.4	99.7
EGFR03.M06	11:58:54.34	-38.4	63.3	11.9	89.4	99.7
EGFR03.M07	11:58:54.39	-36.0	59.3	11.9	89.4	99.7
EGFR03.M08	11:58:54.45	-33.3	55.0	11.9	89.4	99.7
EGFR03.M09	11:58:54.50	-30.9	51.0	11.9	89.4	99.7
EGFR03.M10	11:58:54.55	-28.2	46.7	11.9	89.4	99.7
EGFR03.M11	11:58:54.55	-28.2	46.6	11.9	89.4	99.7
EGFR03.M12	11:58:54.55	-28.2	46.6	11.9	89.4	99.7
EGFR03.M13	11:58:55.23	3.2	-4.6	11.9	89.4	99.7
EGFR03.M14	11:58:55.23	3.2	-4.6	11.9	89.4	99.7
EGFR03.M15	11:58:55.23	3.1	-4.5	11.9	89.4	99.7
EGFR03.M16	11:58:55.24	3.7	-5.4	11.9	89.4	99.7
EGFR03.M17	11:58:55.24	3.8	-5.6	11.9	89.4	99.7
EGFR03.M18	11:58:55.50	15.7	-25.2	11.9	89.4	99.7
EGFR03.M19	11:58:55.55	18.4	-28.9	11.9	93.2	96.2
EGFR03.M20	11:58:55.60	21.4	-33.2	11.9	93.2	96.2

APPENDIX A

DIRECTIVITY ANGLE = 122,5 deg

FILENAME	EMIT TIME	X	Y (m)	Z	VEL (m/s)	HEADING (deg)
EGFR04.M01	12: 2:47.68	-40.6	46.5	12.9	89.2	100.6
EGFR04.M02	12: 2:47.68	-40.6	46.4	12.9	89.2	100.6
EGFR04.M03	12: 2:47.68	-40.7	46.5	12.9	89.2	100.6
EGFR04.M04	12: 2:47.78	-36.4	39.4	12.9	89.2	100.6
EGFR04.M05	12: 2:47.90	-30.7	29.8	12.9	89.2	100.6
EGFR04.M06	12: 2:47.63	-43.0	50.5	12.9	89.2	100.6
EGFR04.M07	12: 2:47.73	-38.7	43.2	12.9	89.2	100.6
EGFR04.M08	12: 2:47.83	-34.0	35.2	12.9	89.2	100.6
EGFR04.M09	12: 2:47.93	-29.7	28.0	12.9	89.2	100.6
EGFR04.M10	12: 2:48.03	-25.0	20.0	12.9	91.1	100.9
EGFR04.M11	12: 2:48.03	-24.9	19.9	12.9	91.1	100.9
EGFR04.M12	12: 2:48.03	-24.9	19.8	12.9	91.1	100.9
EGFR04.M13	12: 2:48.38	-8.6	-7.9	12.5	91.1	100.9
EGFR04.M14	12: 2:48.38	-8.6	-8.0	12.5	91.1	100.9
EGFR04.M15	12: 2:48.38	-8.6	-7.9	12.5	91.1	100.9
EGFR04.M16	12: 2:48.47	-4.7	-14.6	12.4	91.1	100.9
EGFR04.M17	12: 2:48.47	-4.6	-14.8	12.4	91.1	100.9
EGFR04.M18	12: 2:48.97	18.2	-53.8	11.8	91.1	100.9
EGFR04.M19	12: 2:49.07	23.2	-62.3	11.6	91.1	100.9
EGFR04.M20	12: 2:49.20	28.8	-71.9	11.5	91.1	100.9

DIRECTIVITY ANGLE = 122.5 deg

FILENAME	EMIT TIME	X	Y (m)	Z	VEL (m/s)	HEADING (deg)
EGFR05.M01	12: 6:59.17	-23.8	50.8	12.4	91.8	99.3
EGFR05.M02	12: 6:59.17	-23.8	50.8	12.4	91.8	99.3
EGFR05.M03	12: 6:59.17	-23.9	50.9	12.4	91.8	99.3
EGFR05.M04	12: 6:59.20	-22.4	48.5	12.4	91.8	99.3
EGFR05.M05	12: 6:59.24	-20.5	45.4	12.4	91.8	99.3
EGFR05.M06	12: 6:58.93	-35.6	69.7	12.4	91.8	99.3
EGFR05.M07	12: 6:58.96	-34.1	67.3	12.4	91.8	99.3
EGFR05.M08	12: 6:59.00	-32.5	64.7	12.4	91.8	99.3
EGFR05.M09	12: 6:59.02	-31.0	62.3	12.4	91.8	99.3
EGFR05.M10	12: 6:59.06	-29.4	59.7	12.4	91.8	99.3
EGFR05.M11	12: 6:59.06	-29.4	59.7	12.4	91.8	99.3
EGFR05.M12	12: 6:59.06	-29.3	59.7	12.4	91.8	99.3
EGFR05.M13	12: 6:59.86	9.6	-2.9	12.4	91.8	99.3
EGFR05.M14	12: 6:59.86	9.6	-2.9	12.4	91.8	99.3
EGFR05.M15	12: 6:59.86	9.5	-2.8	12.4	91.8	99.3
EGFR05.M16	12: 6:59.87	9.8	-3.3	12.4	91.8	99.3
EGFR05.M17	12: 6:59.87	10.0	-3.6	12.4	91.8	99.3
EGFR05.M18	12: 7: 0.02	17.2	-15.1	12.4	91.8	99.3
EGFR05.M19	12: 7: 0.05	18.6	-17.4	12.4	91.8	99.3
EGFR05.M20	12: 7: 0.08	20.3	-20.1	12.4	91.8	99.3

DIRECTIVITY ANGLE = 122.5 deg

FILENAME	EMIT TIME	X	Y (m)	Z	VEL (m/s)	HEADING (deg)
EGFR06.M01	19:37:37.79	-24.5	51.8	13.1	90.7	99.0
EGFR06.M02	19:37:37.79	-24.5	51.8	13.1	90.7	99.0
EGFR06.M03	19:37:37.79	-24.6	52.0	13.1	90.7	99.0
EGFR06.M04	19:37:37.80	-23.7	50.7	13.1	90.7	99.0
EGFR06.M05	19:37:37.83	-22.7	49.0	13.1	90.7	99.0
EGFR06.M06	19:37:37.50	-38.4	74.0	13.1	90.7	99.0
EGFR06.M07	19:37:37.52	-37.6	72.7	13.1	90.7	99.0
EGFR06.M08	19:37:37.53	-36.7	71.3	13.1	90.7	99.0
EGFR06.M09	19:37:37.55	-35.9	70.0	13.1	90.7	99.0
EGFR06.M10	19:37:37.45	-13.4	80.5	17.0	86.4	105.5
EGFR06.M11	19:37:37.45	-13.4	80.5	17.0	86.4	105.5
EGFR06.M12	19:37:37.45	-13.4	80.5	17.0	86.4	105.5
EGFR06.M13	19:37:38.48	9.2	-1.7	13.2	90.7	99.0
EGFR06.M14	19:37:38.48	9.2	-1.7	13.2	90.7	99.0
EGFR06.M15	19:37:38.48	9.1	-1.5	13.2	90.7	99.0
EGFR06.M16	19:37:38.51	10.3	-3.5	13.2	90.7	99.0
EGFR06.M17	19:37:38.52	10.5	-3.8	13.2	90.7	99.0
EGFR06.M18	19:37:38.57	13.3	-8.3	13.2	90.7	99.0
EGFR06.M19	19:37:38.59	14.1	-9.5	13.2	90.7	99.0
EGFR06.M20	19:37:38.61	15.0	-11.0	13.2	90.7	99.0

DIRECTIVITY ANGLE = 122.5 deg

FILENAME	EMIT TIME	X	Y (m)	Z	VEL (m/s)	HEADING (deg)
EGFR07.M01	19:42:47.95	-28.7	50.8	6.9	92.8	99.4
EGFR07.M02	19:42:47.95	-28.7	50.8	6.9	92.8	99.4
EGFR07.M03	19:42:47.95	-28.7	50.8	6.9	92.8	99.4
EGFR07.M04	19:42:47.98	-27.2	48.4	6.9	92.8	99.4
EGFR07.M05	19:42:48.02	-25.1	45.0	6.9	92.8	99.4
EGFR07.M06	19:42:47.72	-40.1	69.2	6.9	92.8	99.4
EGFR07.M07	19:42:47.75	-38.5	66.6	6.9	92.8	99.4
EGFR07.M08	19:42:47.78	-36.8	63.9	6.9	92.8	99.4
EGFR07.M09	19:42:47.82	-35.3	61.4	6.9	92.8	99.4
EGFR07.M10	19:42:47.85	-33.6	58.6	6.9	92.8	99.4
EGFR07.M11	19:42:47.85	-33.5	58.6	6.9	92.8	99.4
EGFR07.M12	19:42:47.85	-33.5	58.5	6.9	92.8	99.4
EGFR07.M13	19:42:48.63	4.6	-2.9	6.9	92.8	99.4
EGFR07.M14	19:42:48.63	4.7	-2.9	6.9	92.8	99.4
EGFR07.M15	19:42:48.63	4.6	-2.9	6.9	92.8	99.4
EGFR07.M16	19:43: 3.66	-181.9	-1882.2	-384.3	102.1	71.9
EGFR07.M17	19:43: 3.66	-181.9	-1882.3	-384.3	102.1	71.9
EGFR07.M18	19:42:48.80	12.8	-15.9	6.9	92.8	99.4
EGFR07.M19	19:42:48.83	14.3	-18.4	6.9	92.8	99.4
EGFR07.M20	19:42:48.87	16.0	-21.2	6.9	92.8	99.4

DIRECTIVITY ANGLE = 122.5 deg

FILENAME	EMIT TIME	X	Y (m)	Z	VEL (m/s)	HEADING (deg)
EGFR08.M01	19:48:45.80	-30.0	50.5	8.3	93.6	99.4
EGFR08.M02	19:48:45.80	-30.0	50.5	8.3	93.6	99.4
EGFR08.M03	19:48:45.79	-30.0	50.5	8.3	93.6	99.4
EGFR08.M04	19:48:45.83	-28.3	47.7	8.3	93.6	99.4
EGFR08.M05	19:48:45.88	-26.0	44.0	8.3	93.6	99.4
EGFR08.M06	19:48:45.58	-40.8	67.9	8.3	93.6	99.4
EGFR08.M07	19:48:45.61	-39.0	65.0	8.3	93.6	99.4
EGFR08.M08	19:48:45.65	-37.1	61.9	8.3	93.6	99.4
EGFR08.M09	19:48:45.69	-35.3	59.1	8.3	93.6	99.4
EGFR08.M10	19:48:45.73	-33.4	55.9	8.3	93.6	99.4
EGFR08.M11	19:48:45.73	-33.4	55.9	8.3	93.6	99.4
EGFR08.M12	19:48:45.73	-33.3	55.9	8.3	93.6	99.4
EGFR08.M13	19:48:46.47	3.3	-3.3	8.3	93.6	99.4
EGFR08.M14	19:48:46.47	3.3	-3.3	8.3	93.6	99.4
EGFR08.M15	19:48:46.47	3.3	-3.2	8.3	93.6	99.4
EGFR08.M16	19:48:46.47	3.2	-3.1	8.3	93.6	99.4
EGFR08.M17	19:48:46.47	3.3	-3.3	8.3	93.6	99.4
EGFR08.M18	19:48:46.66	12.4	-18.0	8.3	93.6	99.4
EGFR08.M19	19:48:46.69	14.1	-20.8	8.3	93.6	99.4
EGFR08.M20	19:48:46.73	16.1	-24.0	8.3	93.6	99.4

DIRECTIVITY ANGLE = 122.5 deg

FILENAME	EMIT TIME	X	Y (m)	Z	VEL (m/s)	HEADING (deg)
EGFR09.M01	19:52:38.40	-28.9	50.1	5.7	93.4	99.6
EGFR09.M02	19:52:38.40	-28.9	50.1	5.7	93.4	99.6
EGFR09.M03	19:52:38.40	-28.9	50.1	5.7	93.4	99.6
EGFR09.M04	19:52:38.44	-26.9	46.9	5.7	93.4	99.6
EGFR09.M05	19:52:38.49	-24.3	42.6	5.7	93.4	99.6
EGFR09.M06	19:52:38.20	-38.8	66.2	5.7	93.4	99.6
EGFR09.M07	19:52:38.23	-36.8	62.9	5.7	93.4	99.6
EGFR09.M08	19:52:38.28	-34.6	59.4	5.7	93.4	99.6
EGFR09.M09	19:52:38.32	-32.6	56.1	5.7	93.4	99.6
EGFR09.M10	19:52:38.37	-30.4	52.5	5.7	93.4	99.6
EGFR09.M11	19:52:38.37	-30.4	52.5	5.7	93.4	99.6
EGFR09.M12	19:52:38.37	-30.4	52.5	5.7	93.4	99.6
EGFR09.M13	19:52:39.08	4.3	-3.7	5.6	93.4	99.6
EGFR09.M14	19:52:39.08	4.3	-3.7	5.6	93.4	99.6
EGFR09.M15	19:52:39.08	4.3	-3.7	5.6	93.4	99.6
EGFR09.M16	19:52:39.05	2.9	-1.4	5.6	93.4	99.6
EGFR09.M17	19:52:39.05	3.0	-1.7	5.6	93.4	99.6
EGFR09.M18	19:52:38.53	-3.6	44.4	9.9	90.3	104.6
EGFR09.M19	19:52:39.33	16.7	-23.8	5.5	93.4	99.6
EGFR09.M20	19:52:39.38	18.9	-27.5	5.5	93.4	99.6

DIRECTIVITY ANGLE = 122.5 deg

FILENAME	EMIT TIME	X	Y (m)	Z	VEL (m/s)	HEADING (deg)
EGFR10.M01	19:56:24.14	-27.2	50.7	18.5	93.4	99.3
EGFR10.M02	19:56:24.14	-27.2	50.7	18.5	93.4	99.3
EGFR10.M03	19:56:24.13	-27.4	51.0	18.5	93.4	99.3
EGFR10.M04	19:56:24.16	-26.0	48.7	18.5	93.4	99.3
EGFR10.M05	19:56:24.20	-24.2	45.8	18.5	93.4	99.3
EGFR10.M06	19:56:23.89	-39.4	70.2	18.5	93.4	99.3
EGFR10.M07	19:56:23.92	-37.9	67.9	18.5	93.4	99.3
EGFR10.M08	19:56:23.95	-36.4	65.5	18.5	93.4	99.3
EGFR10.M09	19:56:23.98	-35.1	63.3	18.5	93.4	99.3
EGFR10.M10	19:56:24.02	-33.5	60.8	18.5	93.4	99.3
EGFR10.M11	19:56:24.02	-33.5	60.8	18.5	93.4	99.3
EGFR10.M12	19:56:24.02	-33.5	60.8	18.5	93.4	99.3
EGFR10.M13	19:56:24.82	6.2	-2.9	18.6	93.4	99.3
EGFR10.M14	19:56:24.82	6.2	-2.9	18.6	93.4	99.3
EGFR10.M15	19:56:24.81	6.0	-2.7	18.6	93.4	99.3
EGFR10.M16	19:56:24.88	9.0	-7.4	18.6	93.4	99.3
EGFR10.M17	19:56:24.88	9.1	-7.6	18.6	93.4	99.3
EGFR10.M18	19:56:24.96	13.2	-14.2	18.6	93.4	99.3
EGFR10.M19	19:56:24.98	14.6	-16.5	18.6	93.4	99.3
EGFR10.M20	19:56:25.02	16.2	-18.9	18.6	93.4	99.3

DIRECTIVITY ANGLE = 122.5 deg

FILENAME	EMIT TIME	X	Y (m)	Z	VEL (m/s)	HEADING (deg)
EGFR11.M01	20: 0: 2.09	-33.9	48.5	21.2	94.1	99.9
EGFR11.M02	20: 0: 2.09	-33.9	48.5	21.2	94.1	99.9
EGFR11.M03	20: 0: 2.09	-34.1	48.8	21.2	94.1	99.9
EGFR11.M04	20: 0: 2.14	-31.4	44.4	21.2	94.1	99.9
EGFR11.M05	20: 0: 2.21	-27.9	38.7	21.1	94.1	99.9
EGFR11.M06	20: 0: 1.92	-41.8	61.5	21.2	94.1	99.9
EGFR11.M07	20: 0: 1.98	-39.1	57.0	21.2	94.1	99.9
EGFR11.M08	20: 0: 2.04	-36.1	52.2	21.2	94.1	99.9
EGFR11.M09	20: 0: 2.09	-33.5	47.8	21.2	94.1	99.9
EGFR11.M10	20: 0: 2.16	-30.5	42.9	21.2	94.1	99.9
EGFR11.M11	20: 0: 2.16	-30.5	42.9	21.2	94.1	99.9
EGFR11.M12	20: 0: 2.16	-30.4	42.9	21.2	94.1	99.9
EGFR11.M13	20: 0: 2.76	-1.0	-5.4	21.1	94.1	99.9
EGFR11.M14	20: 0: 2.76	-1.0	-5.4	21.1	94.1	99.9
EGFR11.M15	20: 0: 2.76	-1.2	-5.1	21.1	94.1	99.9
EGFR11.M16	20: 0: 2.85	3.4	-12.7	21.1	94.1	99.9
EGFR11.M17	20: 0: 2.85	3.6	-12.9	21.1	94.1	99.9
EGFR11.M18	20: 0: 3.04	12.8	-28.0	21.1	94.1	99.9
EGFR11.M19	20: 0: 3.09	15.4	-32.4	21.1	94.1	99.9
EGFR11.M20	20: 0: 3.16	18.4	-37.3	21.1	94.1	99.9

APPENDIX A

DIRECTIVITY ANGLE = 122.5 deg

FILENAME	EMIT TIME	X	Y (m)	Z	VEL (m/s)	HEADING (deg)
EGFR12.M01	20: 3:59.09	-29.2	50.1	22.3	95.4	99.4
EGFR12.M02	20: 3:59.09	-29.2	50.1	22.3	95.4	99.4
EGFR12.M03	20: 3:59.09	-29.5	50.5	22.3	95.4	99.4
EGFR12.M04	20: 3:59.13	-27.8	47.8	22.3	95.4	99.4
EGFR12.M05	20: 3:59.16	-25.7	44.4	22.3	95.4	99.4
EGFR12.M06	20: 3:58.87	-40.7	68.5	22.3	95.4	99.4
EGFR12.M07	20: 3:58.90	-39.0	65.9	22.3	95.4	99.4
EGFR12.M08	20: 3:58.94	-37.2	63.0	22.3	95.4	99.4
EGFR12.M09	20: 3:58.97	-35.6	60.4	22.3	95.4	99.4
EGFR12.M10	20: 3:59.01	-33.8	57.5	22.3	95.4	99.4
EGFR12.M11	20: 3:59.01	-33.8	57.4	22.3	95.4	99.4
EGFR12.M12	20: 3:59.01	-33.8	57.4	22.3	95.4	99.4
EGFR12.M13	20: 3:59.76	4.1	-3.6	22.4	95.4	99.4
EGFR12.M14	20: 3:59.76	4.0	-3.5	22.4	95.4	99.4
EGFR12.M15	20: 3:59.75	3.9	-3.2	22.4	95.4	99.4
EGFR12.M16	20: 3:59.84	8.3	-10.4	22.4	95.4	99.4
EGFR12.M17	20: 3:59.84	8.4	-10.6	22.4	95.4	99.4
EGFR12.M18	20: 3:59.92	12.3	-16.8	22.4	95.4	99.4
EGFR12.M19	20: 3:59.95	13.9	-19.5	22.4	95.4	99.4
EGFR12.M20	20: 3:59.99	15.7	-22.4	22.4	95.4	99.4

DIRECTIVITY ANGLE = 122.5 deg

FILENAME	EMIT TIME	X	Y (m)	Z	VEL (m/s)	HEADING (deg)
EGFR13.M01	21: 2:30.04	-39.9	45.9	19.6	102.5	100.6
EGFR13.M02	21: 2:30.04	-39.9	45.9	19.6	102.5	100.6
EGFR13.M03	21: 2:30.04	-40.0	46.1	19.6	102.5	100.6
EGFR13.M04	21: 2:30.13	-35.7	38.7	19.6	102.5	100.6
EGFR13.M05	21: 2:30.23	-29.8	28.8	19.6	102.5	100.6
EGFR13.M06	21: 2:30.00	-42.0	49.4	19.6	102.5	100.6
EGFR13.M07	21: 2:30.09	-37.4	41.8	19.6	102.5	100.6
EGFR13.M08	21: 2:30.18	-32.6	33.6	19.6	102.5	100.6
EGFR13.M09	21: 2:30.27	-28.2	26.1	19.6	102.5	100.6
EGFR13.M10	21: 2:30.36	-23.3	17.8	19.7	102.5	100.6
EGFR13.M11	21: 2:30.36	-23.2	17.7	19.7	102.5	100.6
EGFR13.M12	21: 2:30.36	-23.2	17.6	19.7	102.5	100.6
EGFR13.M13	21: 2:30.66	-7.8	-8.4	19.7	102.5	100.6
EGFR13.M14	21: 2:30.66	-7.8	-8.5	19.7	102.5	100.6
EGFR13.M15	21: 2:30.66	-7.9	-8.3	19.7	102.5	100.6
EGFR13.M16	21: 2:30.76	-2.6	-17.2	19.7	102.5	100.6
EGFR13.M17	21: 2:30.76	-2.5	-17.4	19.7	102.5	100.6
EGFR13.M18	21: 2:31.10	15.2	-47.3	19.8	102.5	100.6
EGFR13.M19	21: 2:31.18	19.6	-54.7	19.8	102.5	100.6
EGFR13.M20	21: 2:31.28	24.5	-63.1	19.8	102.5	100.6

APPENDIX A

DIRECTIVITY ANGLE = 122.5 deg

FILENAME	EMIT TIME	X	Y (m)	Z	VEL (m/s)	HEADING (deg)
EGFR14.M01	21: 6:19.05	-27.6	50.4	20.7	92.0	99.3
EGFR14.M02	21: 6:19.05	-27.6	50.5	20.7	92.0	99.3
EGFR14.M03	21: 6:19.05	-27.8	50.8	20.7	92.0	99.3
EGFR14.M04	21: 6:19.08	-26.3	48.4	20.7	92.0	99.3
EGFR14.M05	21: 6:19.12	-24.5	45.4	20.7	92.0	99.3
EGFR14.M06	21: 6:18.80	-39.6	69.7	20.7	92.0	99.3
EGFR14.M07	21: 6:18.84	-38.1	67.3	20.7	92.0	99.3
EGFR14.M08	21: 6:18.87	-36.5	64.8	20.7	92.0	99.3
EGFR14.M09	21: 6:18.90	-35.1	62.4	20.7	92.0	99.3
EGFR14.M10	21: 6:18.93	-33.5	59.9	20.7	92.0	99.3
EGFR14.M11	21: 6:18.93	-33.4	59.8	20.7	92.0	99.3
EGFR14.M12	21: 6:18.93	-33.4	59.8	20.7	92.0	99.3
EGFR14.M13	21: 6:19.73	5.8	-3.2	20.7	92.0	99.3
EGFR14.M14	21: 6:19.73	5.8	-3.2	20.7	92.0	99.3
EGFR14.M15	21: 6:19.73	5.6	-2.9	20.7	92.0	99.3
EGFR14.M16	21: 6:19.80	9.2	-8.8	20.7	92.0	99.3
EGFR14.M17	21: 6:19.81	9.4	-9.0	20.7	92.0	99.3
EGFR14.M18	21: 6:19.89	13.1	-15.0	20.7	92.0	99.3
EGFR14.M19	21: 6:19.91	14.6	-17.3	20.7	92.0	99.3
EGFR14.M20	21: 6:19.95	16.2	-19.9	20.7	92.0	99.3

DIRECTIVITY ANGLE = 122.5 deg

FILENAME	EMIT TIME	X	Y	Z	VEL	HEADING
			(m)		(m/s)	(deg)
EGFR15.M01	21: 9:53.39	-39.3	47.9	18.6	94.3	100.1
EGFR15.M02	21: 9:53.39	-39.3	47.9	18.6	94.3	100.1
EGFR15.M03	21: 9:53.39	-39.5	48.2	18.6	94.3	100.1
EGFR15.M04	21: 9:53.45	-36.3	42.9	18.6	94.3	100.1
EGFR15.M05	21: 9:53.54	-32.1	36.0	18.6	96.0	100.3
EGFR15.M06	21: 9:53.27	-45.6	58.3	18.7	94.3	100.1
EGFR15.M07	21: 9:53.33	-42.3	53.0	18.7	94.3	100.1
EGFR15.M08	21: 9:53.40	-38.9	47.2	18.6	94.3	100.1
EGFR15.M09	21: 9:53.47	-35.8	42.1	18.6	94.3	100.1
EGFR15.M10	21: 9:53.54	-32.3	36.3	18.6	96.0	100.3
EGFR15.M11	21: 9:53.54	-32.2	36.2	18.6	96.0	100.3
EGFR15.M12	21: 9:53.54	-32.2	36.2	18.6	96.0	100.3
EGFR15.M13	21: 9:54.06	-6.4	-6.9	18.8	96.0	100.3
EGFR15.M14	21: 9:54.06	-6.4	-6.9	18.8	96.0	100.3
EGFR15.M15	21: 9:54.06	-6.5	-6.7	18.8	96.0	100.3
EGFR15.M16	21: 9:54.16	-1.4	-15.2	18.8	96.0	100.3
EGFR15.M17	21: 9:54.16	-1.3	-15.4	18.8	96.0	100.3
EGFR15.M18	21: 9:54.45	12.5	-38.4	18.9	96.0	100.3
EGFR15.M19	21: 9:54.52	16.1	-44.5	19.0	96.0	100.3
EGFR15.M20	21: 9:54.60	20.2	-51.3	19.0	96.0	100.3

DIRECTIVITY ANGLE = 122.5 deg

FILENAME	EMIT TIME	X	Y	Z	VEL	HEADING
			(m)		(m/s)	(deg)
EGFR16.M01	21:13:54.52	-42.4	45.5	37.7	95.3	100.4
EGFR16.M02	21:13:54.52	-42.4	45.6	37.7	95.3	100.4
EGFR16.M03	21:13:54.52	-42.8	46.3	37.7	95.3	100.4
EGFR16.M04	21:13:54.59	-39.2	40.3	37.7	95.3	100.4
EGFR16.M05	21:13:54.69	-34.3	32.1	37.7	95.3	100.4
EGFR16.M06	21:13:54.42	-47.2	53.5	37.6	95.3	100.4
EGFR16.M07	21:13:54.50	-43.3	47.0	37.6	95.3	100.4
EGFR16.M08	21:13:54.59	-39.1	40.1	37.7	95.3	100.4
EGFR16.M09	21:13:54.66	-35.3	33.7	37.7	95.3	100.4
EGFR16.M10	21:13:54.75	-31.1	26.6	37.8	95.3	100.4
EGFR16.M11	21:13:54.75	-31.0	26.5	37.8	95.3	100.4
EGFR16.M12	21:13:54.75	-31.0	26.5	37.8	95.3	100.4
EGFR16.M13	21:13:55.17	-10.1	-8.5	38.1	100.2	100.4
EGFR16.M14	21:13:55.17	-10.1	-8.5	38.1	100.2	100.4
EGFR16.M15	21:13:55.16	-10.5	-7.9	38.1	100.2	100.4
EGFR16.M16	21:13:55.40	1.3	-27.7	38.5	100.2	100.4
EGFR16.M17	21:13:55.40	1.4	-27.9	38.5	100.2	100.4
EGFR16.M18	21:13:55.55	8.9	-40.2	38.7	96.5	98.7
EGFR16.M19	21:13:55.62	12.9	-46.5	38.8	96.5	98.7
EGFR16.M20	21:13:56.52	56.0	-119.5	40.2	93.3	99.5

DIRECTIVITY ANGLE = 122.5 deg

FILENAME	EMIT TIME	X	Y (m)	Z	VEL (m/s)	HEADING (deg)
EGFR17.M01	21:17:35.52	-33.3	47.4	39.3	96.3	99.7
EGFR17.M02	21:17:35.52	-33.4	47.5	39.3	96.3	99.7
EGFR17.M03	21:17:35.51	-33.9	48.3	39.3	96.3	99.7
EGFR17.M04	21:17:35.55	-31.8	44.9	39.2	96.3	99.7
EGFR17.M05	21:17:35.60	-29.0	40.4	39.2	96.3	99.7
EGFR17.M06	21:17:35.32	-43.4	63.8	39.3	96.3	99.7
EGFR17.M07	21:17:35.36	-41.1	60.1	39.3	96.3	99.7
EGFR17.M08	21:17:35.41	-38.7	56.1	39.3	96.3	99.7
EGFR17.M09	21:17:35.45	-36.4	52.5	39.3	96.3	99.7
EGFR17.M10	21:17:35.51	-33.9	48.4	39.3	96.3	99.7
EGFR17.M11	21:17:35.51	-33.9	48.3	39.3	96.3	99.7
EGFR17.M12	21:17:35.51	-33.9	48.4	39.3	96.3	99.7
EGFR17.M13	21:17:36.17	-0.4	-6.2	39.1	96.3	99.7
EGFR17.M14	21:17:36.17	-0.5	-6.1	39.1	96.3	99.7
EGFR17.M15	21:17:36.16	-0.9	-5.4	39.1	96.3	99.7
EGFR17.M16	21:17:36.37	9.5	-22.4	39.0	96.3	99.7
EGFR17.M17	21:17:36.37	9.7	-22.6	39.0	96.3	99.7
EGFR17.M18	21:17:36.38	10.5	-24.0	39.0	96.3	99.7
EGFR17.M19	21:17:36.43	12.7	-27.6	39.0	96.3	99.7
EGFR17.M20	21:17:36.48	15.2	-31.7	39.0	96.3	99.7

DIRECTIVITY ANGLE = 122.5 deg

FILENAME	EMIT TIME	X	Y (m)	Z	VEL (m/s)	HEADING (deg)
EGFR18.M01	21:20:57.65	-31.0	47.3	37.8	96.9	99.7
EGFR18.M02	21:20:57.65	-31.0	47.4	37.8	96.9	99.7
EGFR18.M03	21:20:57.64	-31.5	48.2	37.8	96.9	99.7
EGFR18.M04	21:20:57.68	-29.3	44.6	37.8	96.9	99.7
EGFR18.M05	21:20:57.74	-26.5	39.9	37.7	96.9	99.7
EGFR18.M06	21:20:57.46	-40.7	63.2	37.9	96.9	99.7
EGFR18.M07	21:20:57.51	-38.4	59.4	37.9	96.9	99.7
EGFR18.M08	21:20:57.55	-35.9	55.3	37.8	96.9	99.7
EGFR18.M09	21:20:57.60	-33.6	51.5	37.8	96.9	99.7
EGFR18.M10	21:20:57.65	-31.0	47.3	37.8	96.9	99.7
EGFR18.M11	21:20:57.65	-31.0	47.3	37.8	96.9	99.7
EGFR18.M12	21:20:57.65	-31.0	47.4	37.8	96.9	99.7
EGFR18.M13	21:20:58.30	1.9	-6.3	37.4	96.9	99.7
EGFR18.M14	21:20:58.30	1.8	-6.2	37.4	96.9	99.7
EGFR18.M15	21:20:58.29	1.4	-5.6	37.4	96.9	99.7
EGFR18.M16	21:20:58.48	10.6	-20.6	37.3	96.9	99.7
EGFR18.M17	21:20:58.48	10.7	-20.8	37.3	96.9	99.7
EGFR18.M18	21:20:58.52	13.2	-24.8	37.3	96.9	99.7
EGFR18.M19	21:20:58.57	15.5	-28.6	37.2	96.9	99.7
EGFR18.M20	21:20:58.62	18.1	-32.8	37.2	96.9	99.7

DIRECTIVITY ANGLE = 122.5 deg

FILENAME	EMIT TIME	X	Y (m)	Z	VEL (m/s)	HEADING (deg)
EGFR19.M01	21:25:57.80	-35.8	41.8	70.4	98.2	99.9
EGFR19.M02	21:25:57.80	-36.0	42.1	70.4	98.2	99.9
EGFR19.M03	21:25:57.78	-36.9	43.6	70.4	98.2	99.9
EGFR19.M04	21:25:57.81	-35.4	41.1	70.4	98.2	99.9
EGFR19.M05	21:25:57.87	-32.5	36.4	70.4	98.2	99.9
EGFR19.M06	21:25:57.59	-46.5	59.4	70.3	98.2	99.9
EGFR19.M07	21:25:57.64	-43.8	55.0	70.3	98.2	99.9
EGFR19.M08	21:25:57.70	-40.9	50.2	70.3	98.2	99.9
EGFR19.M09	21:25:57.75	-38.2	45.8	70.4	98.2	99.9
EGFR19.M10	21:25:57.81	-35.1	40.7	70.4	98.2	99.9
EGFR19.M11	21:25:57.81	-35.1	40.7	70.4	98.2	99.9
EGFR19.M12	21:25:57.81	-35.2	40.8	70.4	98.2	99.9
EGFR19.M13	21:25:58.43	-3.5	-11.3	70.6	98.2	99.9
EGFR19.M14	21:25:58.43	-3.7	-11.0	70.6	98.2	99.9
EGFR19.M15	21:25:58.41	-4.4	-9.7	70.6	98.2	99.9
EGFR19.M16	21:25:58.80	15.3	-42.3	70.7	98.2	99.9
EGFR19.M17	21:25:58.80	15.5	-42.5	70.7	98.2	99.9
EGFR19.M18	21:25:58.66	7.9	-30.0	70.6	98.2	99.9
EGFR19.M19	21:25:58.71	10.6	-34.5	70.7	98.2	99.9
EGFR19.M20	21:25:58.77	13.7	-39.6	70.7	98.2	99.9

DIRECTIVITY ANGLE = 122.5 deg

FILENAME	EMIT TIME	X	Y (m)	Z	VEL (m/s)	HEADING (deg)
EGFR20.M01	21:29:39.57	-32.1	39.9	85.4	98.2	99.7
EGFR20.M02	21:29:39.56	-32.3	40.2	85.4	98.2	99.7
EGFR20.M03	21:29:39.55	-33.3	42.0	85.3	98.2	99.7
EGFR20.M04	21:29:39.55	-33.0	41.4	85.3	98.2	99.7
EGFR20.M05	21:29:39.59	-31.0	38.2	85.4	98.2	99.7
EGFR20.M06	21:29:39.30	-45.5	61.9	85.1	98.2	99.7
EGFR20.M07	21:29:39.35	-43.3	58.3	85.1	98.2	99.7
EGFR20.M08	21:29:39.40	-40.9	54.3	85.2	98.2	99.7
EGFR20.M09	21:29:39.44	-38.6	50.6	85.2	98.2	99.7
EGFR20.M10	21:29:39.49	-36.0	46.3	85.3	98.2	99.7
EGFR20.M11	21:29:39.49	-36.0	46.3	85.3	98.2	99.7
EGFR20.M12	21:29:39.49	-36.0	46.4	85.3	98.2	99.7
EGFR20.M13	21:29:40.20	0.2	-12.8	86.0	98.2	99.7
EGFR20.M14	21:29:40.20	0.0	-12.5	86.0	98.2	99.7
EGFR20.M15	21:29:40.17	-0.9	-11.0	86.0	98.2	99.7
EGFR20.M16	21:29:40.64	22.1	-48.6	86.1	87.7	99.9
EGFR20.M17	21:29:40.64	22.2	-48.8	86.1	87.7	99.9
EGFR20.M18	21:29:40.35	8.1	-25.8	86.2	98.2	99.7
EGFR20.M19	21:29:40.40	10.4	-29.5	86.2	98.2	99.7
EGFR20.M20	21:29:40.45	13.1	-33.8	86.3	98.2	99.7

DIRECTIVITY ANGLE = 122.5 deg

FILENAME	EMIT TIME	X	Y (m)	Z	VEL (m/s)	HEADING (deg)
EGFR21.M01	21:33:13.24	-38.6	38.2	76.6	97.2	100.5
EGFR21.M02	21:33:13.24	-38.7	38.5	76.6	97.2	100.5
EGFR21.M03	21:33:13.22	-39.7	40.1	76.6	97.2	100.5
EGFR21.M04	21:33:13.27	-37.2	35.8	76.6	97.2	100.5
EGFR21.M05	21:33:13.37	-32.6	28.1	76.6	97.2	100.5
EGFR21.M06	21:33:13.11	-45.2	49.4	76.6	97.2	100.5
EGFR21.M07	21:33:13.20	-41.2	42.6	76.6	97.2	100.5
EGFR21.M08	21:33:13.28	-36.7	35.1	76.6	97.2	100.5
EGFR21.M09	21:33:13.36	-32.7	28.2	76.6	97.2	100.5
EGFR21.M10	21:33:13.45	-28.1	20.5	76.7	97.2	100.5
EGFR21.M11	21:33:13.45	-28.0	20.5	76.7	97.2	100.5
EGFR21.M12	21:33:13.45	-28.1	20.5	76.7	97.2	100.5
EGFR21.M13	21:33:13.88	-7.0	-15.1	76.8	97.2	100.5
EGFR21.M14	21:33:13.88	-7.1	-14.8	76.8	97.2	100.5
EGFR21.M15	21:33:13.86	-8.0	-13.4	76.8	97.2	100.5
EGFR21.M16	21:33:14.28	13.0	-48.7	76.9	97.2	100.5
EGFR21.M17	21:33:14.29	13.1	-48.9	76.9	97.2	100.5
EGFR21.M18	21:33:14.25	11.1	-45.6	76.9	97.2	100.5
EGFR21.M19	21:33:14.33	15.2	-52.5	76.9	97.2	100.5
EGFR21.M20	21:33:14.42	19.9	-60.3	76.9	97.2	100.5

DIRECTIVITY ANGLE = 122.5 deg

FILENAME	EMIT TIME	X	Y (m)	Z	VEL (m/s)	HEADING (deg)
EGFR22.M01	21:36:48.78	-29.2	18.0	150.3	101.1	100.4
EGFR22.M02	21:36:48.77	-29.6	18.7	150.3	101.1	100.4
EGFR22.M03	21:36:48.74	-31.4	21.7	150.3	101.1	100.4
EGFR22.M04	21:36:48.69	-34.2	26.5	150.2	101.1	100.4
EGFR22.M05	21:36:48.71	-32.7	24.0	150.2	101.1	100.4
EGFR22.M06	21:36:48.45	-46.4	46.9	149.9	101.1	100.4
EGFR22.M07	21:36:48.51	-43.2	41.6	150.0	101.1	100.4
EGFR22.M08	21:36:48.59	-39.5	35.3	150.1	101.1	100.4
EGFR22.M09	21:36:48.65	-35.9	29.3	150.2	101.1	100.4
EGFR22.M10	21:36:48.65	-17.8	29.7	161.5	96.5	105.5
EGFR22.M11	21:36:48.65	-17.8	29.7	161.5	96.5	105.5
EGFR22.M12	21:36:48.65	-17.9	29.9	161.5	96.5	105.5
EGFR22.M13	21:36:49.37	1.2	-33.1	151.1	101.1	100.4
EGFR22.M14	21:36:49.37	0.9	-32.5	151.1	101.1	100.4
EGFR22.M15	21:36:49.34	-0.7	-29.8	151.1	101.1	100.4
EGFR22.M16	21:36:50.01	34.2	-88.5	151.9	101.1	100.4
EGFR22.M17	21:36:50.01	34.4	-88.7	152.0	101.1	100.4
EGFR22.M18	21:36:49.51	8.5	-45.3	151.3	101.1	100.4
EGFR22.M19	21:36:49.58	12.1	-51.3	151.4	101.1	100.4
EGFR22.M20	21:36:49.66	16.2	-58.3	151.5	101.1	100.4

DIRECTIVITY ANGLE = 122.5 deg

FILENAME	EMIT TIME	X	Y (m)	Z	VEL (m/s)	HEADING (deg)
EGFR23.M01	21:40:11.81	-31.4	18.4	139.9	97.3	100.9
EGFR23.M02	21:40:11.80	-31.7	19.1	139.9	97.3	100.9
EGFR23.M03	21:40:11.77	-33.4	21.9	139.9	97.3	100.9
EGFR23.M04	21:40:11.75	-34.3	23.5	139.9	97.3	100.9
EGFR23.M05	21:40:11.82	-30.9	17.7	139.9	97.3	100.9
EGFR23.M06	21:40:11.57	-43.4	39.0	139.8	97.3	100.9
EGFR23.M07	21:40:11.66	-39.0	31.6	139.9	97.3	100.9
EGFR23.M08	21:40:11.76	-34.1	23.1	139.9	97.3	100.9
EGFR23.M09	21:40:11.85	-29.4	15.1	139.9	97.3	100.9
EGFR23.M10	21:40:11.96	-24.1	6.0	140.0	97.3	100.9
EGFR23.M11	21:40:11.96	-24.1	5.9	140.0	97.3	100.9
EGFR23.M12	21:40:11.96	-24.2	6.2	140.0	97.3	100.9
EGFR23.M13	21:40:12.43	-1.3	-33.1	140.2	97.3	100.9
EGFR23.M14	21:40:12.42	-1.6	-32.6	140.2	97.3	100.9
EGFR23.M15	21:40:12.39	-3.1	-30.0	140.2	97.3	100.9
EGFR23.M16	21:40:13.05	29.2	-85.2	140.5	97.3	100.9
EGFR23.M17	21:40:13.05	29.3	-85.4	140.5	97.3	100.9
EGFR23.M18	21:40:12.72	13.2	-57.9	140.4	97.3	100.9
EGFR23.M19	21:40:12.82	17.9	-65.9	140.4	97.3	100.9
EGFR23.M20	21:40:12.93	23.2	-75.1	140.5	97.3	100.9

DIRECTIVITY ANGLE = 122.5 deg

FILENAME	EMIT TIME	X	Y	Z	VEL	HEADING
			(m)		(m/s)	(deg)
EGFR24.M01	21:43:26.70	-18.7	23.5	146.6	101.8	99.6
EGFR24.M02	21:43:26.69	-19.1	24.1	146.6	101.8	99.6
EGFR24.M03	21:43:26.65	-20.9	26.9	146.5	101.8	99.6
EGFR24.M04	21:43:26.58	-25.0	33.6	146.4	101.8	99.6
EGFR24.M05	21:43:26.56	-25.8	35.0	146.4	101.8	99.6
EGFR24.M06	21:43:26.27	-41.3	60.1	146.0	101.8	99.6
EGFR24.M07	21:43:26.29	-40.1	58.2	146.1	101.8	99.6
EGFR24.M08	21:43:26.32	-38.4	55.5	146.1	101.8	99.6
EGFR24.M09	21:43:26.35	-36.8	52.8	146.1	101.8	99.6
EGFR24.M10	21:43:26.39	-34.8	49.5	146.2	101.8	99.6
EGFR24.M11	21:43:26.39	-34.8	49.5	146.2	101.8	99.6
EGFR24.M12	21:43:26.39	-34.9	49.8	146.2	101.8	99.6
EGFR24.M13	21:43:27.28	12.6	-27.5	147.3	101.8	99.6
EGFR24.M14	21:43:27.27	12.3	-26.9	147.3	101.8	99.6
EGFR24.M15	21:43:27.24	10.7	-24.3	147.2	101.8	99.6
EGFR24.M16	21:43:27.88	44.5	-79.3	148.0	101.8	99.6
EGFR24.M17	21:43:27.88	44.6	-79.5	148.0	101.8	99.6
EGFR24.M18	21:43:27.24	10.7	-24.4	147.2	101.8	99.6
EGFR24.M19	21:43:27.27	12.4	-27.2	147.3	101.8	99.6
EGFR24.M20	21:43:27.31	14.5	-30.4	147.3	101.8	99.6

DIRECTIVITY ANGLE = 122.5 deg

FILENAME	EMIT TIME	X	Y (m)	Z	VEL (m/s)	HEADING (deg)
EGFR25.M01	21:48:18.16	38.9	36.7	9.4	103.1	102.1
EGFR25.M02	21:48:18.17	38.9	36.5	9.4	103.1	102.1
EGFR25.M03	21:48:18.17	39.0	36.4	9.4	103.1	102.1
EGFR25.M04	21:48:18.31	46.2	23.5	9.4	103.1	102.1
EGFR25.M05	21:48:18.51	56.1	5.8	9.4	103.1	102.1
EGFR25.M06	21:48:18.33	46.9	22.3	9.4	103.1	102.1
EGFR25.M07	21:48:18.48	54.4	8.8	9.4	103.1	102.1
EGFR25.M08	21:48:18.64	62.5	-5.7	9.3	103.1	102.1
EGFR25.M09	21:48:15.16	-108.0	291.9	9.9	57.8	90.6
EGFR25.M10	21:48:14.46	-134.2	322.5	9.6	57.8	90.6
EGFR25.M11	21:48:14.45	-134.6	322.9	9.6	57.8	90.6
EGFR25.M12	21:48:14.44	-134.9	323.3	9.6	57.8	90.6
EGFR25.M13	21:48:18.78	69.6	-18.4	9.3	103.1	102.1
EGFR25.M14	21:48:18.78	69.7	-18.6	9.3	103.1	102.1
EGFR25.M15	21:48:18.78	69.7	-18.7	9.3	103.1	102.1
EGFR25.M16	21:48:18.62	61.4	-3.7	9.3	103.1	102.1
EGFR25.M17	21:48:18.62	61.5	-4.0	9.3	103.1	102.1
EGFR25.M18	21:48:19.55	108.2	-87.6	9.1	103.1	102.1
EGFR25.M19	21:48:19.70	115.5	-100.8	9.1	103.1	102.1
EGFR25.M20	21:48:19.86	123.8	-115.6	9.1	103.1	102.1

APPENDIX A

DIRECTIVITY ANGLE = 122.5 deg

FILENAME	EMIT TIME	X	Y (m)	Z	VEL (m/s)	HEADING (deg)
EGFR26.M01	21:52:20.44	-30.2	49.4	10.4	93.3	99.7
EGFR26.M02	21:52:20.44	-30.2	49.4	10.4	93.3	99.7
EGFR26.M03	21:52:20.44	-30.2	49.5	10.4	93.3	99.7
EGFR26.M04	21:52:20.48	-27.9	45.6	10.4	93.3	99.7
EGFR26.M05	21:52:20.55	-24.7	40.5	10.5	93.3	99.7
EGFR26.M06	21:52:20.26	-38.9	63.6	10.4	93.3	99.7
EGFR26.M07	21:52:20.31	-36.5	59.7	10.4	93.3	99.7
EGFR26.M08	21:52:20.37	-33.9	55.4	10.4	93.3	99.7
EGFR26.M09	21:52:20.41	-31.5	51.6	10.4	93.3	99.7
EGFR26.M10	21:52:20.47	-28.9	47.3	10.4	93.3	99.7
EGFR26.M11	21:52:20.47	-28.9	47.2	10.4	93.3	99.7
EGFR26.M12	21:52:20.47	-28.8	47.2	10.4	93.3	99.7
EGFR26.M13	21:52:21.12	2.8	-4.5	10.5	93.3	99.7
EGFR26.M14	21:52:21.12	2.8	-4.5	10.5	93.3	99.7
EGFR26.M15	21:52:21.12	2.8	-4.4	10.5	93.3	99.7
EGFR26.M16	21:52:21.13	3.0	-4.8	10.5	93.3	99.7
EGFR26.M17	21:52:21.13	3.1	-5.0	10.5	93.3	99.7
EGFR26.M18	21:52:21.38	15.2	-24.7	10.6	93.3	99.7
EGFR26.M19	21:52:21.42	17.6	-28.6	10.6	93.3	99.7
EGFR26.M20	21:52:21.48	20.2	-32.9	10.6	93.3	99.7

DIRECTIVITY ANGLE = 122.5 deg

FILENAME	EMIT TIME	X	Y (m)	Z	VEL (m/s)	HEADING (deg)
EGFR27.M01	21:55:42.94	-29.6	50.1	23.7	97.6	99.4
EGFR27.M02	21:55:42.94	-29.6	50.2	23.7	97.6	99.4
EGFR27.M03	21:55:42.93	-29.8	50.5	23.7	97.6	99.4
EGFR27.M04	21:55:42.96	-28.2	48.0	23.7	97.6	99.4
EGFR27.M05	21:55:43.00	-26.2	44.7	23.7	97.6	99.4
EGFR27.M06	21:55:42.71	-41.2	68.8	23.6	97.6	99.4
EGFR27.M07	21:55:42.74	-39.5	66.2	23.6	97.6	99.4
EGFR27.M08	21:55:42.78	-37.8	63.4	23.6	97.6	99.4
EGFR27.M09	21:55:42.81	-36.2	60.8	23.6	97.6	99.4
EGFR27.M10	21:55:42.84	-34.4	58.0	23.6	97.6	99.4
EGFR27.M11	21:55:42.84	-34.4	58.0	23.6	97.6	99.4
EGFR27.M12	21:55:42.84	-34.4	57.9	23.6	97.6	99.4
EGFR27.M13	21:55:43.59	3.7	-3.5	23.9	99.7	99.4
EGFR27.M14	21:55:43.59	3.7	-3.5	23.9	99.7	99.4
EGFR27.M15	21:55:43.58	3.5	-3.2	23.9	99.7	99.4
EGFR27.M16	21:55:43.67	8.6	-11.3	23.9	99.7	99.4
EGFR27.M17	21:55:43.68	8.7	-11.6	23.9	99.7	99.4
EGFR27.M18	21:55:43.73	11.7	-16.4	23.9	99.7	99.4
EGFR27.M19	21:55:43.77	13.3	-19.0	23.9	99.7	99.4
EGFR27.M20	21:55:43.80	15.1	-21.9	23.9	99.7	99.4

DIRECTIVITY ANGLE = 122.5 deg

FILENAME	EMIT TIME	X	Y (m)	Z	VEL (m/s)	HEADING (deg)
EGFR28.M01	22:22:30.00	510.0	0.0	1.4	0.0	85.0
EGFR28.M02	22:22:30.00	510.0	0.0	1.4	0.0	85.0
EGFR28.M03	22:22:30.00	510.0	0.0	1.4	0.0	85.0
EGFR28.M04	22:22:30.00	510.0	0.0	1.4	0.0	85.0
EGFR28.M05	22:22:48.00	510.0	0.0	1.4	0.0	85.0
EGFR28.M06	22:22:48.00	510.0	0.0	1.4	0.0	85.0
EGFR28.M07	22:22:48.00	510.0	0.0	1.4	0.0	85.0
EGFR28.M08	22:22:38.00	510.0	0.0	1.4	0.0	85.0
EGFR28.M09	22:22:30.00	510.0	0.0	1.4	0.0	85.0
EGFR28.M10	22:22:30.00	510.0	0.0	1.4	0.0	85.0
EGFR28.M11	22:22:30.00	510.0	0.0	1.4	0.0	85.0
EGFR28.M12	22:22:30.00	510.0	0.0	1.4	0.0	85.0
EGFR28.M13	22:22:29.00	510.0	0.0	1.4	0.0	85.0
EGFR28.M14	22:22:29.00	510.0	0.0	1.4	0.0	85.0
EGFR28.M15	22:22:29.00	510.0	0.0	1.4	0.0	85.0
EGFR28.M16	22:22:29.00	510.0	0.0	1.4	0.0	85.0
EGFR28.M17	22:22:29.00	510.0	0.0	1.4	0.0	85.0
EGFR28.M18	22:22:35.00	510.0	0.0	1.4	0.0	85.0
EGFR28.M19	22:22:35.00	510.0	0.0	1.4	0.0	85.0
EGFR28.M20	22:22:35.00	510.0	0.0	1.4	0.0	85.0

APPENDIX B

WEATHER DATA

    Average values of weather data for each run are presented herein for the
following weather stations: all stations in the triangle area, the 4-m station
at building C-15, the 1.2-m station at van 1, the 1.2-m station at van 5, and
the 10-m station at van 3. The weather profile data is presented with the
beginning and ending Greenwich mean time of each profile run.

TRIANGLE AREA WEATHER STATION

Date	Run no.	Wind speed, m/sec					Average wind direction, deg	Temperature, °C	
		Station						Station	
		3 m	6 m	9 m	12 m	15 m		3 m	15 m
11/1/78	1	3.8	4.0	4.1	4.1	4.7	314	7.4	9.4
	2	3.9	4.1	4.5	4.2	4.7	316	7.0	9.4
	3	3.9	4.4	4.3	4.4	4.7	315	6.8	9.5
	4	3.6	3.8	4.3	4.1	4.8	317	6.8	9.5
	5	3.7	4.4	4.2	4.4	4.5	314	6.8	9.4
11/2/78	6	4.0	4.0	3.9	3.8	4.0	284	16.5	16.6
	7	2.8	2.7	2.9	2.9	3.0	287	16.5	16.6
	8	2.8	3.0	3.2	3.1	3.3	313	16.6	16.9
	9	2.6	2.9	2.9	2.8	2.6	284	16.9	16.8
	10	2.2	2.4	2.6	2.4	2.6	256	16.8	16.9
	11	2.4	2.6	2.9	2.8	3.2	263	16.9	16.8
	12	4.3	4.4	4.5	4.3	4.3	260	16.7	16.7
	13	4.3	4.5	4.4	4.5	4.5	282	16.5	16.4
	14	4.3	4.4	4.4	4.6	4.4	282	16.4	16.3
	15	4.1	4.2	4.1	4.4	4.3	297	16.3	16.2
	16	3.9	4.0	4.2	4.3	4.5	299	16.2	16.1
	17	4.0	3.9	4.0	4.0	3.8	303	16.1	16.0
	18	3.0	3.6	3.8	4.0	4.2	292	16.0	16.0
	19	4.2	4.3	5.0	4.7	5.2	299	15.9	15.8
	20	2.9	3.2	3.7	3.9	3.8	299	15.7	15.7
	21	3.0	3.2	3.5	3.7	3.8	289	15.6	15.6
	22	2.8	2.9	3.3	3.3	3.3	304	15.5	15.5
	23	3.4	3.6	3.4	3.9	3.8	293	15.4	15.4
	24	3.8	4.0	4.0	3.8	4.2	305	15.4	15.3
	25	2.8	3.5	3.8	4.0	3.8	295	15.2	15.2
	26	2.4	2.4	2.6	2.8	3.2	289	15.0	15.0
	27	2.2	2.4	2.5	2.4	2.6	286	15.0	15.0

BUILDING C-15 WEATHER STATION

Date	Run no.	Wind direction, deg	Wind speed, m/s
11/1/78	1	320	3.4
	2	320	2.7
	3	320	3.6
	4	315	3.1
	5	320	2.7
11/2/79	6	230	1.8
	7	250	3.6
	8	280	2.7
	9	280	2.5
	10	250	2.7
	11	245	2.7
	12	240	1.8
	13	270	3.6
	14	270	3.4
	15	300	3.6
	16	280	3.6
	17	290	2.7
	18	280	3.1
	19	285	3.6
	20	290	2.7
	21	285	2.7
	22	290	2.9
	23	290	3.1
	24	290	2.7
	25	285	2.7
	26	280	2.7
	27	275	2.2
	28	270	2.5

1.2-m WEATHER STATION, VAN 1

Date	Run no.	Wind direction, deg	Wind speed, m/s	Relative humidity, percent	Temperature, °C
11/1/78	1	330	1.9	70	7.8
	2	330	1.9	70	7.8
	3	345	1.9	70	7.8
	4	345	1.9	70	7.8
	5	355	1.9	70	7.8
11/2/78	6	270	2.2	38	17.4
	7	285	2.5	38	17.9
	8	315	2.4	38	17.4
	9	315	2.4	38	17.4
	10	270	2.5	38	16.8
	11	300	2.5	38	16.8
	12	285	2.9	38	16.8
	13	290	3.1	39	16.2
	14	300	3.1	39	16.2
	15	315	3.4	40	15.7
	16	315	3.4	40	15.7
	17	315	3.5	40	15.7
	18	315	3.6	40	15.7
	19	315	3.6	40	15.7
	20	310	2.2	40	15.1
	21	310	2.2	40	15.1
	22	315	2.2	40	15.1
	23	315	2.2	40	14.6
	24	315	2.2	40	14.3
	25	320	2.2	40	13.4
	26	300	1.9	40	13.4
	27	300	1.9	40	13.4
	28	295	1.4	42	11.2

1.2-m WEATHER STATION, VAN 5

Date	Run no.	Wind direction, deg	Wind speed, m/s	Relative humidity, percent	Temperature, °C
11/1/78	1	320	3.2	97	6.2
	2	325	3.2	96	6.7
	3	325	3.2	96	6.7
	4	330	2.7	96	6.7
	5	330	2.7	96	6.7
11/2/78	6	270	2.5	82	16.8
	7	290	2.5	82	16.2
	8	270	2.5	82	16.2
	9	240	2.5	82	15.7
	10	240	2.5	82	15.7
	11	250	2.5	82	15.7
	12	260	2.5	82	15.7
	13	270	2.7	82	14.6
	14	280	2.7	82	14.6
	15	285	2.5	82	14.0
	16	285	2.5	82	13.4
	17	285	2.3	82	13.4
	18	275	2.3	82	13.4
	19	275	2.3	82	13.4
	20	270	2.3	82	13.4
	21	300	1.4	82	13.4
	22	285	1.4	82	13.4
	23	255	1.4	82	12.9
	24	265	1.4	82	12.3
	25	270	1.4	82	11.8
	26	255	1.4	82	11.2
	27	255	1.4	82	11.2
	28	255	1.3	82	10.1

10-m WEATHER STATION, VAN 3

Date	Run no.	Wind direction, deg	Wind speed, m/s	Barometric pressure, kPa	Temperature, oC	Relative humidity, percent
11/1/79	1	19.0	3.2	101.62	8.3	100.0
	2	25.0	2.7	101.62	8.3	99.0
	3	23.0	3.6	101.62	8.9	98.0
	4	31.0	3.6	101.62	9.4	95.0
	5	22.0	2.7	101.62	9.4	95.0
11/2/79	6	330.0	3.2	101.62	17.8	35.0
	7	344.0	1.4	101.90	17.8	35.0
	8	354.0	2.2	101.90	17.2	35.0
	9	4.0	1.4	101.90	17.2	35.0
	10	333.0	3.2	101.90	17.2	34.0
	11	359.0	1.8	101.90	17.2	34.0
	12	340.0	2.2	101.62	17.2	34.0
	13	342.0	2.7	101.79	16.7	36.0
	14	335.0	2.7	101.83	16.7	36.0
	15	360.0	2.7	101.83	16.1	37.0
	16	358.0	2.7	101.83	16.1	37.0
	17	356.0	2.2	101.83	16.1	38.0
	18	2.0	2.7	101.83	16.1	38.0
	19	6.0	2.7	101.79	15.6	39.0
	20	6.0	2.7	101.79	15.6	39.0
	21	2.0	2.2	101.83	15.6	39.0
	22	6.0	2.7	101.83	15.6	39.0
	23	2.0	2.2	101.79	15.6	39.0
	24	6.0	1.8	101.83	15.6	39.0
	25	6.0	2.2	101.79	15.0	39.0
	26	4.0	1.8	101.79	15.0	39.0
	27	359.0	1.4	101.79	14.4	39.0
	28	349.0	1.4	101.76	13.3	42.0

APPENDIX B

## N-159 WEATHER STATION

| Date	Run no.	Barometric pressure, kPa	Wind speed, m/s	Wind direction, deg	Temperature, °C	Dewpoint, °C
11/1/78	1	101.9	2.2	325	9.0	6.0
	2	102.1	2.2	325	9.0	6.1
	3	102.2	2.2	325	9.0	6.2
	4	102.2	2.2	325	9.5	6.2
	5	102.2	2.2	325	9.5	6.2
11/2/78	6	102.0	1.8	340	18.5	-15.5
	7	101.9	2.2	330	18.5	-15.4
	8	101.9	1.8	340	18.5	-15.2
	9	101.9	2.7	345	18.5	-15.1
	10	101.9	1.8	340	18.2	-15.1
	11	101.9	4.0	15	18.2	-15.1
	12	101.9	2.2	0	18.2	-15.1
	13	101.9	2.2	350	17.6	-15.0
	14	101.9	2.2	340	17.6	-15.1
	15	101.9	2.2	345	17.4	-15.1
	16	101.9	2.2	335	17.4	-15.1
	17	101.9	1.8	330	16.8	-15.1
	18	101.9	2.2	340	16.8	-15.1
	19	101.9	2.7	340	16.5	-15.1
	20	101.9	3.6	320	16.5	-15.2
	21	101.9	2.7	340	16.2	-15.2
	22	101.9	1.4	5	16.2	-15.2
	23	101.9	1.8	340	16.0	-15.3
	24	101.9	1.8	335	16.0	-15.4
	25	101.9	.9	350	15.7	-15.5
	26	101.9	.9	5	15.7	-15.5
	27	101.9	1.4	350	15.4	-15.6
	28	101.9	1.8	345	15.4	-15.6
	29	101.9	1.4	350	14.3	-16.0
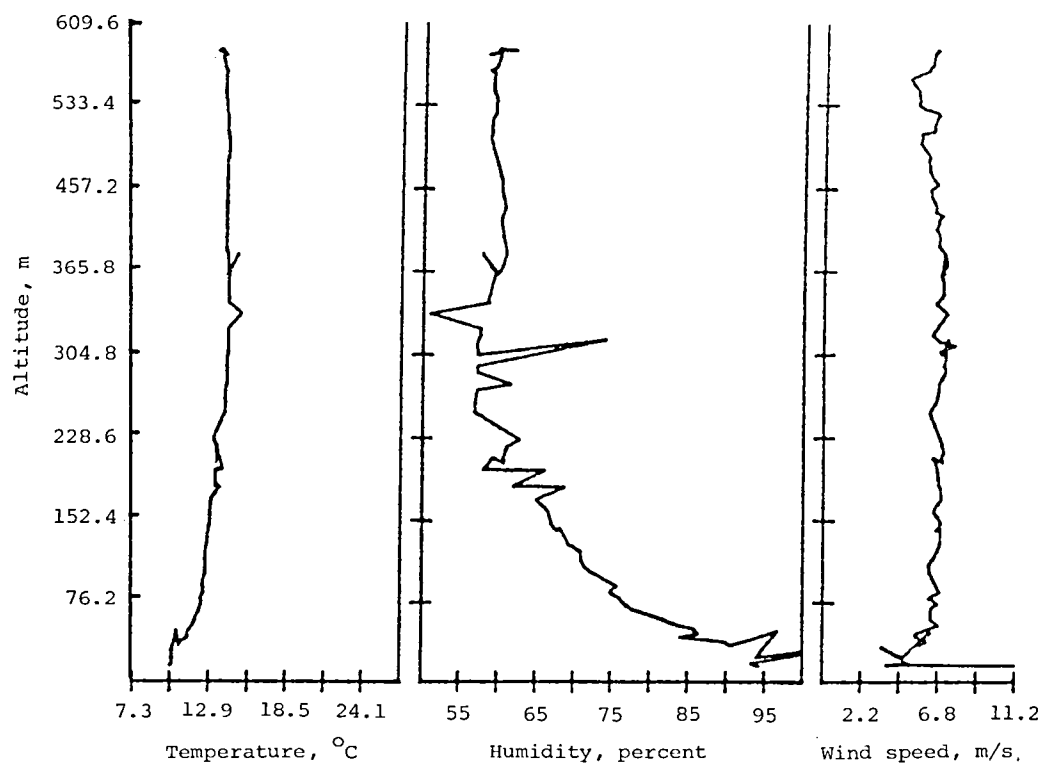
Date - 11/1/78; Ascent - #1; G.m.t. - Start - 11:45, End - 12:04
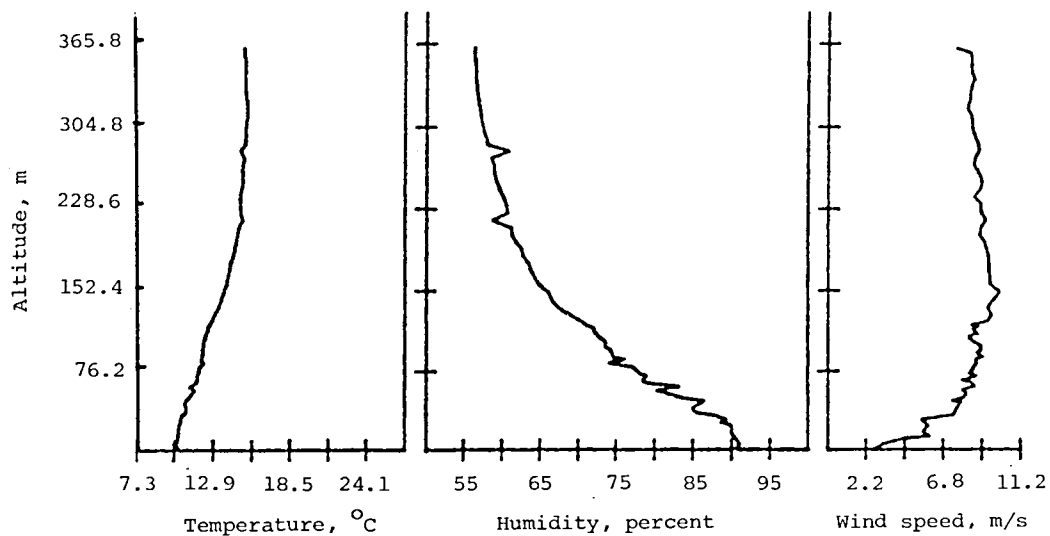
Date - 11/1/78; Descent - #1; G.m.t. - Start - 12:12, End - 12:33

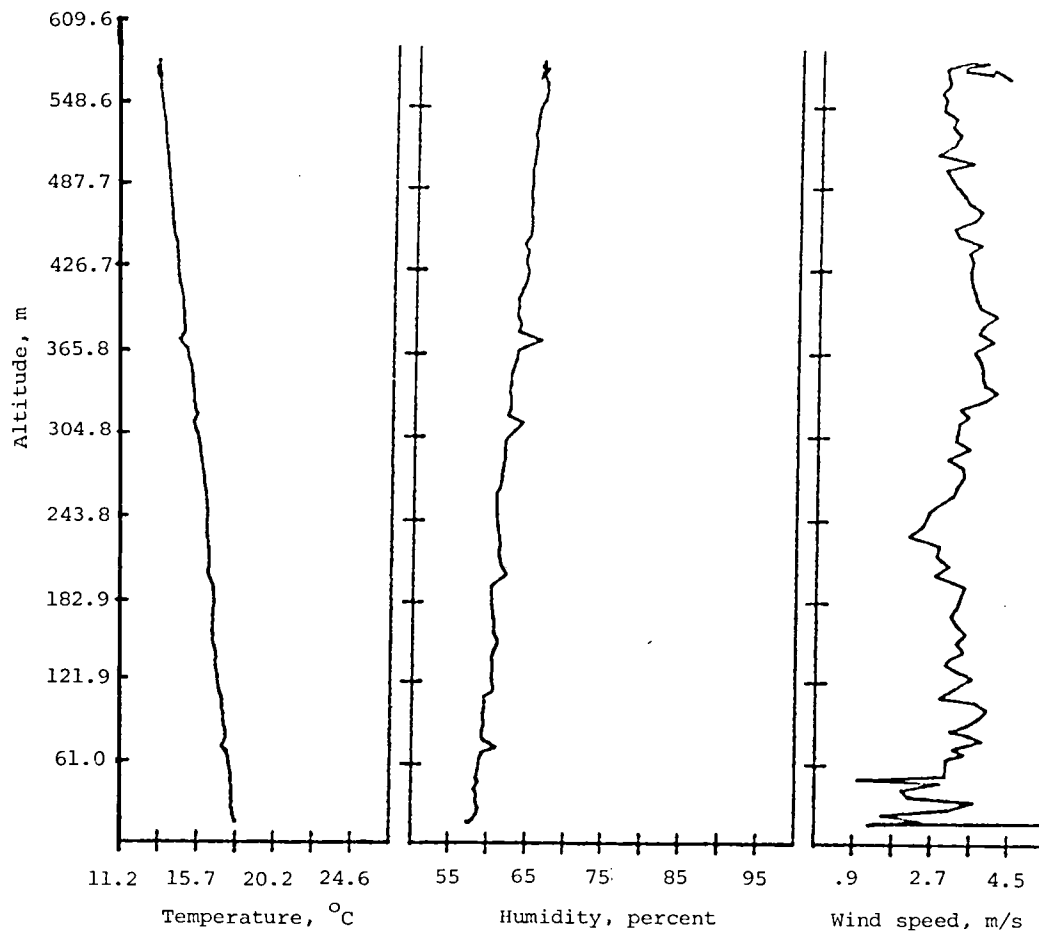Figure B1.- Profiles obtained by balloon station.
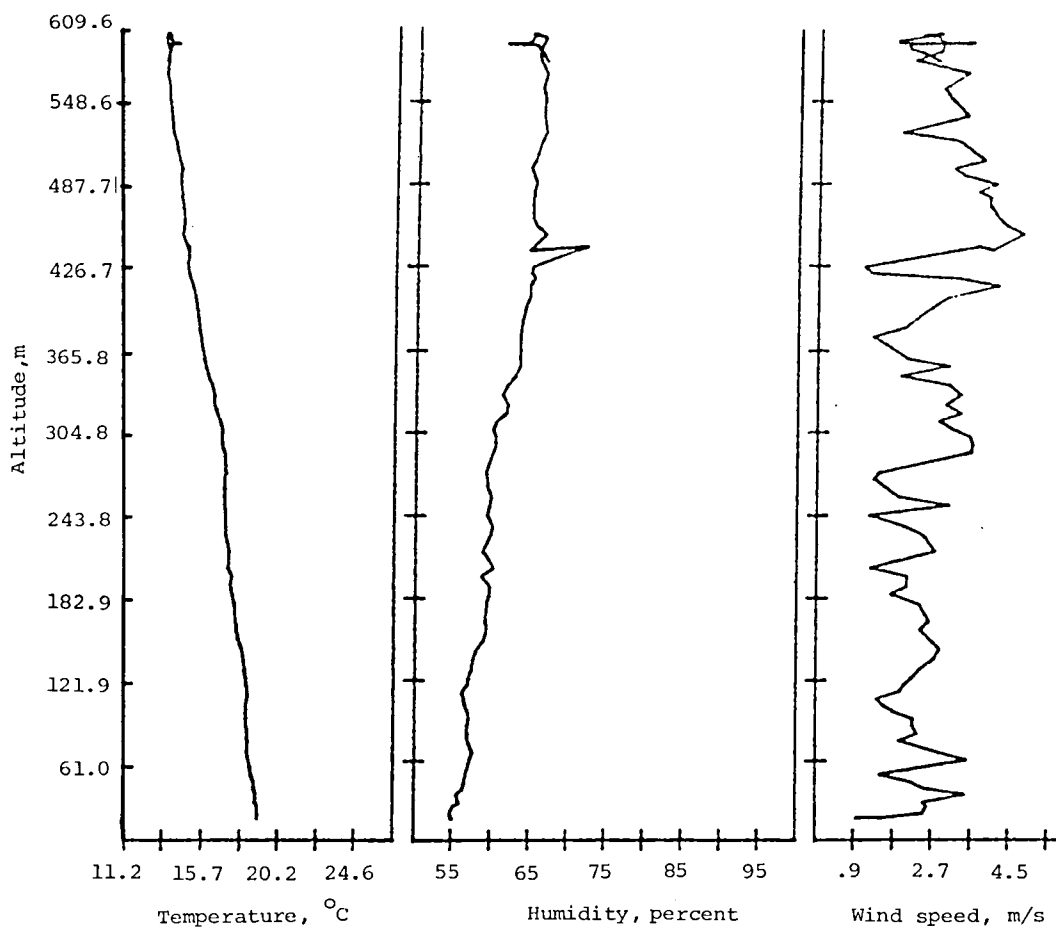
Date - 11/2/78; Ascent - #1 G.M.T. - Start - 19:06, End - 19:33
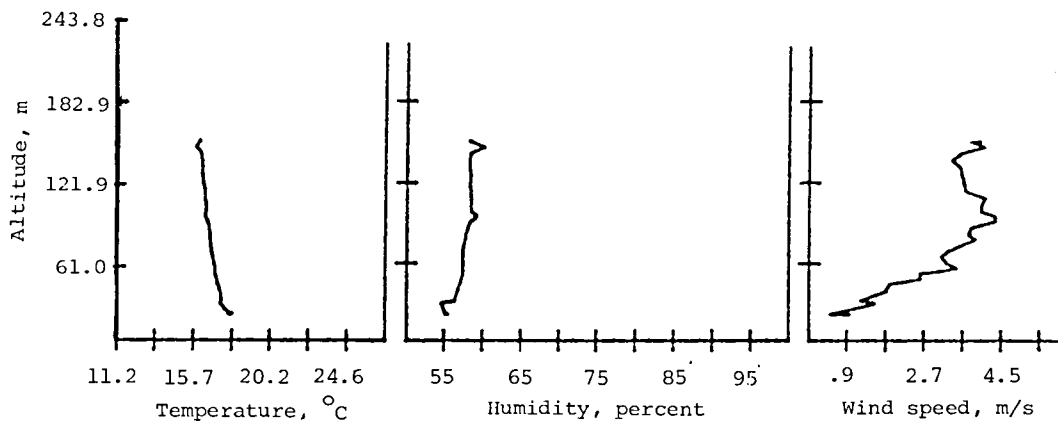
Date - 11/2/78; Descent - #1; G.m.t. - Start - 20:19, End - 20:23

Figure B1.- Continued.

Date - 11/2/78; Ascent - #2; G.m.t. - Start-20:41, End-20:58

Figure B1.- Continued.
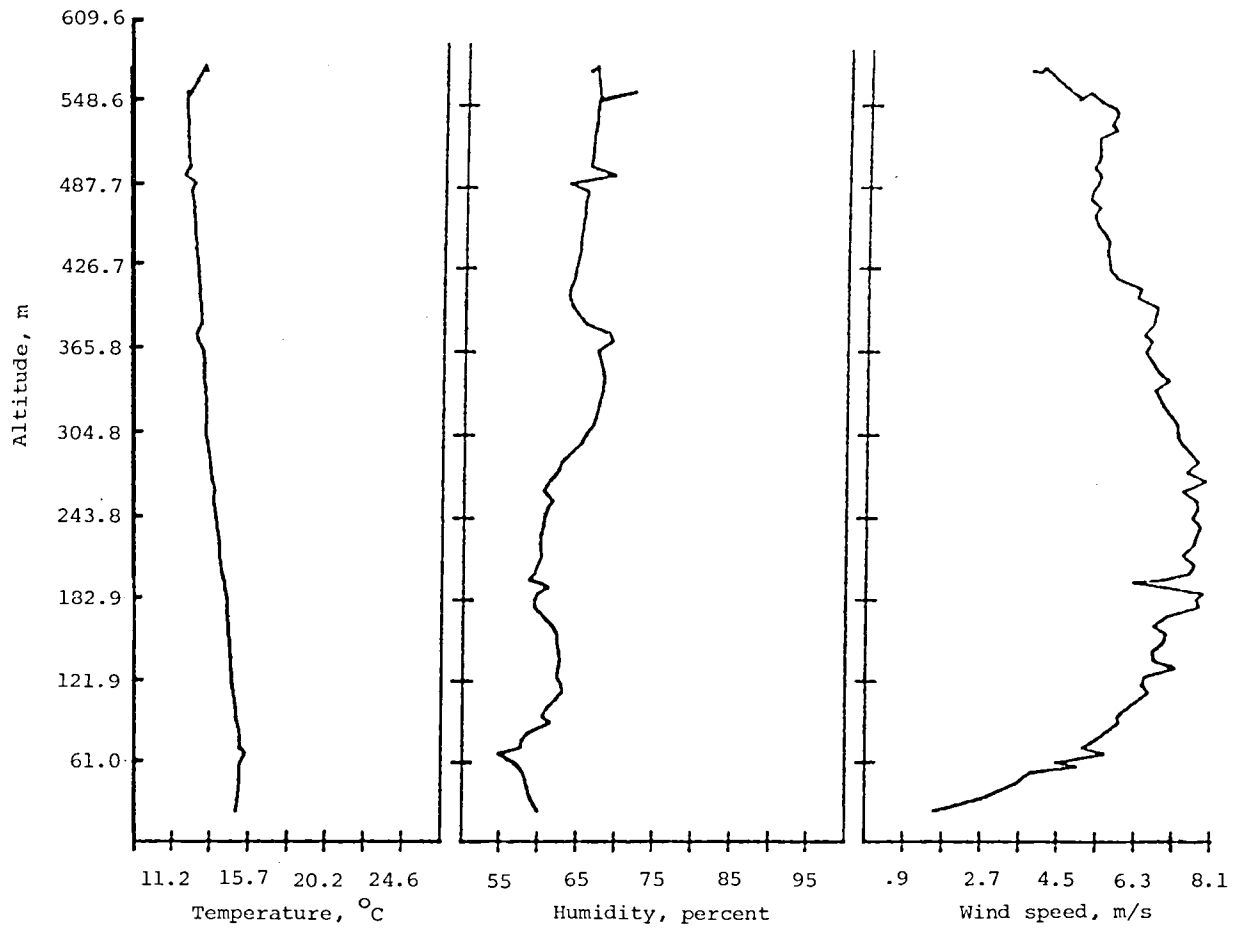
Date - 11/2/78; Descent - #2; G.m.t. - Start-21:36, End-21:50

Figure B1.- Concluded.

APPENDIX C

ACOUSTIC DATA

A 1/3-octave spectrum is tabulated in this section for each microphone for each run. The spectra listed are averages of the two 1/3-octave band spectra located on either side of the reception time, calculated using the 122.5° directivity angle criteria. The 1/3-octave bands from 10 Hz to 2 kHz are included along with the reception time, the elevation angle β, and the slant range of the overall sound pressure level (OSPL) associated with each spectrum. The data for a particular run and microphone are identified with the following nomenclature EGFR ##.M**, where ## is the run number and ** is the microphone number.

DIRECTIVITY ANGLE = 122.5 deg

1/3 OCTAVE BAND CENTER FREQUENCIES (kHz)

FILENAME	RECEIVE TIME	BETA (deg)	SR (m)	OSPL	0.10	0.13	0.16	0.20	0.25	0.32	0.40	0.50	0.63	0.79	1.0	1.3	1.6	2.0
EGFR01.M01	11:46:38.69	3.2	212.9	100.4	76.9	82.4	87.6	91.7	94.2	93.5	94.2	91.8	85.2	79.9	78.0	76.5	76.8	74.6
EGFR01.M02	11:46:38.70	2.8	215.9	99.5	74.2	82.4	85.4	88.4	90.7	89.6	90.0	89.3	88.7	87.7	87.4	88.8	86.5	84.5
EGFR01.M03	11:46:38.71	0.7	218.6	102.4	75.0	84.2	88.8	94.0	95.2	88.6	88.4	95.1	88.7	91.3	90.7	90.1	88.7	85.4
EGFR01.M04	11:46:39.38	1.4	434.0	89.2	70.6	68.4	68.5	68.3	68.8	69.9	76.4	79.9	80.5	81.8	81.4	80.2	74.9	75.1
EGFR01.M05	11:46:40.30	0.8	729.1	85.5	76.2	73.2	71.3	64.6	66.6	66.7	74.1	74.5	77.0	74.8	72.6	68.9	67.6	64.7
EGFR01.M06	11:46:40.46	0.7	885.1	86.0	65.7	64.4	64.4	68.5	68.2	70.0	71.6	74.8	75.9	78.9	79.2	75.3	71.5	70.6
EGFR01.M07	11:46:41.16	0.6	1110.7	88.0	73.2	80.0	80.6	78.1	69.7	65.8	74.6	78.5	77.9	78.5	71.4	72.7	70.6	68.9
EGFR01.M08	11:46:41.92	0.5	1352.3	82.3	65.4	68.1	68.4	66.0	62.1	69.2	70.2	74.9	76.0	72.9	70.6	66.3	64.5	63.3
EGFR01.M09	11:46:42.61	0.4	1572.2	84.6	64.3	64.9	70.3	66.1	61.7	66.0	73.6	76.4	80.5	77.0	73.0	69.5	65.8	63.0
EGFR01.M10	11:46:43.38	0.4	1816.5	79.3	68.6	62.2	67.6	63.5	65.6	73.2	72.0	69.1	67.1	64.5	60.8	57.1	55.6	53.0
EGFR01.M11	11:46:43.38	0.3	1819.6	77.3	65.6	56.5	62.0	59.4	58.0	63.5	67.1	68.8	70.3	70.4	65.3	60.2	58.2	56.0
EGFR01.M12	11:46:43.39	0.1	1822.6	84.0	65.2	60.4	64.6	67.9	70.5	74.6	75.6	76.2	74.1	75.0	73.3	71.8	67.6	62.1
EGFR01.M18	11:46:43.11	0.4	1401.6	86.3	68.0	62.0	72.4	74.0	82.0	77.5	74.1	68.5	68.7	71.2	68.8	69.2	66.6	65.4
EGFR01.M19	11:46:43.80	0.4	1621.5	82.3	66.6	67.7	72.3	71.4	75.2	72.1	66.6	66.3	66.8	71.1	68.5	66.8	64.5	61.8
EGFR01.M20	11:46:44.58	0.3	1868.9	81.8	63.4	60.7	70.6	71.4	76.1	74.8	68.1	68.3	67.4	67.5	66.1	64.9	60.3	56.3

DIRECTIVITY ANGLE = 122.5 deg

1/3 OCTAVE BAND CENTER FREQUENCIES (kHz)

FILENAME	RECEIVE TIME	BETA (deg)	SR (m)	OSPL	0.10	0.13	0.16	0.20	0.25	0.32	0.40	0.50	0.63	0.79	1.0	1.3	1.6	2.0
EGFR02.M01	11:54:28.21	3.1	216.7	99.4	79.0	77.8	84.1	91.7	91.8	93.1	93.3	89.7	84.3	79.5	75.6	75.1	75.1	73.9
EGFR02.M02	11:54:28.21	2.8	219.7	98.3	79.4	81.4	80.5	82.1	89.9	89.1	90.7	89.3	88.7	87.7	84.6	84.1	85.9	84.6
EGFR02.M03	11:54:28.22	0.7	222.4	103.2	75.2	77.9	88.5	92.9	95.2	90.8	90.8	97.5	90.9	93.4	90.4	91.9	89.7	86.7
EGFR02.M04	11:54:28.90	1.4	437.8	93.3	80.8	77.4	71.8	73.4	70.3	73.6	80.4	81.8	81.0	82.2	85.2	79.9	78.2	79.0
EGFR02.M05	11:54:29.82	0.8	732.9	87.5	74.5	79.5	73.8	73.0	69.1	69.7	72.1	75.0	78.5	81.1	76.3	75.1	70.6	71.3
EGFR02.M06	11:54:29.97	0.7	888.9	85.1	70.7	67.3	64.4	65.8	70.2	69.8	70.6	73.1	79.4	77.0	75.2	70.7	70.4	69.6
EGFR02.M07	11:54:30.67	0.5	1114.5	89.0	78.6	79.5	79.5	72.5	65.9	66.4	74.4	77.2	77.6	80.1	79.6	75.7	75.0	70.9
EGFR02.M08	11:54:31.43	0.4	1356.1	84.0	65.6	65.1	66.6	64.4	66.7	68.8	73.2	76.6	81.1	76.4	71.9	69.5	67.4	66.0
EGFR02.M09	11:54:32.12	0.4	1575.9	82.9	64.1	68.0	67.7	64.3	63.4	66.9	70.6	73.0	70.9	69.4	68.7	68.1	64.5	62.0
EGFR02.M10	11:54:32.89	0.4	1820.3	76.5	60.4	66.2	62.0	66.6	68.1	66.3	65.6	59.9	61.1	62.5	59.4	60.6	59.5	54.4
EGFR02.M11	11:54:32.90	0.3	1823.4	75.8	60.3	58.6	60.8	59.7	62.8	59.9	63.2	64.4	66.9	68.9	63.0	62.3	60.7	56.6
EGFR02.M12	11:54:32.91	0.1	1826.4	87.3	65.3	65.8	66.0	70.3	73.2	69.1	75.1	66.5	67.9	66.8	66.8	63.5	61.8	59.1
EGFR02.M13	11:54:29.02	2.7	249.8	97.5	78.4	74.2	77.3	81.4	89.8	91.2	89.0	84.0	86.2	86.8	87.2	83.9	82.6	80.9
EGFR02.M14	11:54:29.03	2.4	252.8	100.2	82.4	89.1	91.0	92.3	93.4	92.0	91.3	87.4	84.4	80.1	74.8	80.6	79.9	79.0
EGFR02.M15	11:54:29.03	0.6	255.6	105.4	81.0	84.5	91.2	94.8	96.1	98.5	96.5	94.1	92.6	94.0	91.1	89.0	90.4	90.5
EGFR02.M16	11:54:28.33	54.8	13.1	100.6	90.3	91.2	91.4	89.7	89.5	90.5	87.7	86.9	87.5	82.0	83.3	83.8	84.4	81.8
EGFR02.M17	11:54:28.33	54.5	13.1	111.3	100.5	101.0	103.1	99.7	94.9	96.2	101.2	105.2	102.9	98.2	96.1	98.7	98.3	97.2
EGFR02.M18	11:54:32.64	0.4	1405.4	91.6	73.0	76.8	81.5	84.3	86.0	86.1	76.3	73.3	76.0	72.3	71.2	70.9	66.4	61.6
EGFR02.M19	11:54:33.33	0.4	1625.3	84.3	70.4	67.8	68.0	74.6	74.3	72.7	69.2	70.2	77.1	74.0	72.0	67.5	63.2	61.1
EGFR02.M20	11:54:34.10	0.3	1872.7	82.3	68.3	67.8	62.1	66.4	75.2	74.9	75.0	70.2	67.2	68.2	67.2	64.3	60.1	57.3

DIRECTIVITY ANGLE = 122.5 deg

FILENAME	RECEIVE TIME	BETA (deg)	SR (m)	OSPL	0.10	0.13	0.16	0.20	0.25	0.32	0.40	0.50	0.63	0.79	1.0	1.3	1.6	2.0
										1/3 OCTAVE BAND CENTER FREQUENCIES (kHz)								
EGFR03.M01	11:58:55.15	3.2	214.2	100.6	78.6	77.2	85.2	91.0	94.0	94.4	92.9	89.4	83.8	78.2	75.9	71.2	74.7	74.9
EGFR03.M02	11:58:55.16	2.8	217.2	78.4	62.3	63.0	61.1	61.2	62.6	61.3	62.5	62.7	63.3	61.9	62.0	63.2	62.8	61.2
EGFR03.M03	11:58:55.16	0.7	219.9	103.9	78.1	83.1	88.9	94.1	96.1	87.0	93.8	95.7	88.8	93.2	92.9	91.2	91.4	88.6
EGFR03.M04	11:58:55.85	1.4	435.7	91.5	75.1	68.6	66.8	69.3	70.1	72.1	80.9	81.0	81.8	79.9	85.1	81.0	78.9	79.3
EGFR03.M05	11:58:56.79	0.8	731.4	81.6	62.9	67.6	70.6	70.2	71.2	67.5	69.8	70.6	68.6	69.8	71.9	70.3	71.2	64.8
EGFR03.M06	11:58:56.95	0.7	887.8	87.2	71.1	72.1	69.9	67.5	68.6	72.3	77.3	75.6	78.3	79.9	78.0	73.7	71.7	70.6
EGFR03.M07	11:58:57.66	0.6	1113.9	87.5	75.1	75.4	72.5	63.3	67.8	72.6	75.9	76.2	77.6	79.5	76.8	75.0	72.5	70.9
EGFR03.M08	11:58:58.43	0.5	1355.9	86.7	65.1	65.2	66.8	62.5	66.8	68.0	76.5	81.7	81.0	76.7	76.3	68.3	69.3	68.4
EGFR03.M09	11:58:59.13	0.4	1576.2	86.8	68.5	67.2	64.8	59.4	60.6	66.5	70.3	69.4	68.3	71.2	72.1	66.2	64.1	62.5
EGFR03.M10	11:58:59.91	0.4	1821.0	81.9	66.4	65.7	67.9	64.6	65.7	69.5	67.3	67.7	66.1	62.4	61.3	58.3	58.8	58.2
EGFR03.M11	11:58:59.91	0.3	1824.1	78.9	62.7	63.6	61.7	57.5	60.6	62.7	64.9	68.1	68.3	67.5	65.4	63.0	62.3	58.3
EGFR03.M12	11:58:59.93	0.1	1827.1	85.4	66.3	67.1	67.1	72.0	75.1	75.4	72.8	69.9	70.7	69.4	70.0	67.0	65.0	62.5
EGFR03.M13	11:58:55.95	2.8	247.2	-1520.9	60.9	821.0	485.1	-444.0	313.0	-108.1	399.1	-21.7	147.1	145.8	62.2	820.2	483.3	-24.1
EGFR03.M14	11:58:55.96	2.4	250.2	-91.4	-27.1	-110.7	57.2	476.7	-700.5	-448.9	309.9	58.3	563.8	229.2	-277.6	900.5	-530.5	307.8
EGFR03.M15	11:58:55.97	0.6	253.0	160.5	62.7	229.8	-526.7	398.6	-189.6	316.0	401.6	401.3	990.7	653.5	-20.1	821.8	-189.1	-107.9
EGFR03.M16	11:58:55.28	57.5	12.7	686.1	166.1	251.7	166.9	-688.6	-91.0	-347.0	166.0	80.4	167.1	-5.9	-5.7	81.0	165.8	-5.8
EGFR03.M17	11:58:55.28	57.4	12.7	-251.5	-86.6	-86.1	84.0	770.5	-257.4	-257.9	-0.4	-428.7	-0.5	84.7	-86.9	85.4	-86.1	-173.0
EGFR03.M18	11:58:59.63	0.4	1405.0	84.3	70.6	70.8	65.3	72.5	75.0	72.1	71.0	69.0	70.5	71.8	67.0	71.3	68.4	65.1
EGFR03.M19	11:59: 0.32	0.4	1625.5	83.4	69.0	70.7	71.3	72.4	76.0	70.7	66.5	69.1	68.0	68.4	70.0	72.3	68.7	64.0
EGFR03.M20	11:59: 1.11	0.3	1873.6	80.6	67.9	69.7	71.9	69.6	72.0	72.1	68.2	66.6	66.1	63.4	62.9	63.9	62.3	59.4

DIRECTIVITY ANGLE = 122.5 deg

1/3 OCTAVE BAND CENTER FREQUENCIES (kHz)

FILENAME	RECEIVE TIME	BETA (deg)	SR (m)	OSPL	0.10	0.13	0.16	0.20	0.25	0.32	0.40	0.50	0.63	0.79	1.0	1.3	1.6	2.0
EGFR04.M01	12: 2:48.28	3.6	203.6	99.3	82.6	81.7	81.9	89.7	89.5	94.1	93.0	91.5	84.0	79.6	75.1	75.4	73.2	70.6
EGFR04.M02	12: 2:48.29	3.3	206.6	99.0	75.1	81.0	83.3	85.5	87.9	91.1	90.3	89.7	86.9	84.7	84.3	87.6	90.4	87.2
EGFR04.M03	12: 2:48.30	1.0	209.3	102.3	71.3	83.0	87.0	91.7	92.7	90.7	89.0	95.5	88.4	90.8	90.4	90.1	89.3	84.5
EGFR04.M04	12: 2:49.03	1.6	426.9	90.4	70.7	69.9	67.9	68.1	66.2	69.0	75.6	81.2	82.8	81.6	83.0	82.4	76.8	73.0
EGFR04.M05	12: 2:50.04	0.9	725.2	87.5	71.2	80.0	77.3	76.8	75.9	72.6	74.7	74.0	78.3	78.4	75.2	72.8	71.6	69.6
EGFR04.M06	12: 2:50.23	0.8	883.5	82.3	59.1	63.7	61.1	63.6	66.7	68.1	70.7	75.1	76.9	73.1	70.8	72.7	69.7	66.4
EGFR04.M07	12: 2:50.99	0.6	1111.6	89.0	75.4	81.3	76.4	74.4	72.8	75.9	79.6	78.9	78.1	80.4	73.2	73.1	70.0	68.5
EGFR04.M08	12: 2:51.82	0.5	1355.8	85.8	69.4	62.0	68.6	70.3	67.7	71.8	79.4	79.1	76.0	74.6	72.6	72.9	68.4	64.7
EGFR04.M09	12: 2:52.56	0.4	1578.0	84.2	67.7	66.1	69.2	64.6	64.4	71.0	73.0	78.3	79.9	76.8	71.0	69.2	68.2	65.4
EGFR04.M10	12: 2:53.39	0.4	1825.0	79.8	64.8	66.6	72.0	66.5	69.3	69.4	69.6	61.3	61.1	62.5	60.6	60.3	60.1	57.3
EGFR04.M11	12: 2:53.40	0.4	1828.0	77.9	62.2	62.7	65.7	59.1	63.1	67.4	69.2	66.6	67.3	68.5	68.4	61.9	62.0	56.5
EGFR04.M12	12: 2:53.41	0.1	1831.1	90.5	67.8	69.1	72.7	74.2	75.0	76.9	76.6	72.4	74.5	72.8	71.5	68.9	66.0	63.5
EGFR04.M13	12: 2:49.07	3.0	235.5	101.8	82.0	81.1	74.1	84.4	90.9	93.6	96.8	89.5	90.8	89.9	91.0	88.5	88.3	83.4
EGFR04.M14	12: 2:49.08	2.7	238.6	101.2	85.7	89.1	90.5	92.9	93.0	90.5	94.7	91.9	86.5	84.6	77.8	81.6	85.3	88.5
EGFR04.M15	12: 2:49.09	0.8	241.3	95.8	81.6	81.2	83.2	86.7	85.0	84.8	83.9	84.3	85.3	81.8	83.8	84.6	85.5	84.1
EGFR04.M16	12: 2:48.52	35.5	19.2	97.3	90.5	89.0	86.7	89.1	90.8	88.5	83.2	82.1	82.7	82.3	81.4	81.1	81.1	80.4
EGFR04.M17	12: 2:48.53	35.8	19.1	95.6	86.9	87.1	88.3	88.8	88.2	88.4	86.0	86.2	86.4	85.9	84.9	84.9	85.1	84.3
EGFR04.M18	12: 2:53.11	0.4	1408.3	84.8	71.5	70.6	74.9	70.2	76.0	76.4	72.9	69.3	72.2	74.2	73.7	72.4	67.1	66.4
EGFR04.M19	12: 2:53.87	0.4	1631.2	84.4	69.7	71.3	74.0	78.6	75.6	69.8	70.2	67.0	68.2	67.4	68.2	68.5	66.1	65.9
EGFR04.M20	12: 2:54.73	0.3	1882.1	82.1	67.2	71.8	65.5	72.9	76.0	71.6	68.2	68.4	67.3	66.4	65.5	66.8	60.6	59.3

APPENDIX C

DIRECTIVITY ANGLE = 122.5 deg

1/3 OCTAVE BAND CENTER FREQUENCIES (kHz)

FILENAME	RECEIVE TIME	BETA (deg)	SR (m)	OSPL	0.10	0.13	0.16	0.20	0.25	0.32	0.40	0.50	0.63	0.79	1.0	1.3	1.6	2.0
EGFR05.M01	12: 6:59.82	3.2	220.3	100.1	79.5	80.8	84.7	85.8	91.9	96.1	94.2	89.7	84.3	79.1	75.9	74.3	75.6	73.1
EGFR05.M02	12: 6:59.83	2.9	223.2	99.5	80.0	80.8	83.7	83.4	90.4	91.9	93.4	91.2	89.9	85.9	84.6	83.8	83.8	82.3
EGFR05.M03	12: 6:59.84	0.8	225.9	103.3	74.2	85.8	90.8	90.5	95.4	91.8	93.2	97.3	90.7	93.6	91.0	92.6	89.5	84.6
EGFR05.M04	12: 7: 0.50	1.5	440.8	92.5	73.4	70.0	65.3	66.4	68.4	73.9	80.7	80.8	82.1	82.1	85.0	85.6	82.1	75.6
EGFR05.M05	12: 7: 1.40	0.9	735.1	83.0	70.2	70.3	70.3	70.3	70.0	69.8	70.0	73.1	72.4	74.5	75.4	71.7	69.7	68.9
EGFR05.M06	12: 7: 1.55	0.7	890.6	88.8	66.2	70.4	72.8	70.4	73.0	76.8	82.2	79.7	78.1	82.0	79.7	78.8	76.9	71.0
EGFR05.M07	12: 7: 2.24	0.6	1115.7	84.7	73.9	69.7	79.0	74.2	73.6	67.1	66.8	68.9	73.6	74.2	75.2	74.3	71.4	68.7
EGFR05.M08	12: 7: 2.98	0.5	1356.6	83.3	65.4	64.9	67.1	67.4	62.7	64.2	75.3	78.6	77.7	72.6	71.3	68.4	67.2	66.6
EGFR05.M09	12: 7: 3.66	0.4	1575.9	85.2	67.8	69.9	70.0	63.8	61.5	67.0	73.6	73.9	75.4	73.9	71.5	70.8	66.9	66.3
EGFR05.M10	12: 7: 4.41	0.4	1819.7	79.3	62.6	64.3	66.4	69.3	70.8	70.6	70.2	66.1	65.6	62.8	62.9	62.5	61.1	59.1
EGFR05.M11	12: 7: 4.41	0.4	1822.7	77.9	61.8	57.8	59.6	62.9	59.4	61.7	66.1	69.3	69.9	67.9	66.5	63.9	63.7	62.9
EGFR05.M12	12: 7: 4.43	0.1	1825.8	82.5	62.4	67.2	68.6	70.3	70.8	72.5	72.7	70.1	70.6	68.7	68.1	65.3	63.4	62.3
EGFR05.M13	12: 7: 0.61	2.8	253.6	97.4	77.5	75.5	84.2	84.5	86.4	89.9	91.1	89.3	88.1	87.1	86.7	87.7	82.8	80.4
EGFR05.M14	12: 7: 0.62	2.5	256.6	103.4	83.7	93.3	89.8	95.7	96.9	95.1	96.1	90.4	87.4	85.1	79.5	84.4	87.3	88.5
EGFR05.M15	12: 7: 0.62	0.7	259.3	106.5	85.0	88.1	95.2	97.6	93.7	97.0	98.4	98.2	94.6	94.4	93.2	94.2	90.3	89.3
EGFR05.M16	12: 6:59.91	47.0	15.4	107.4	100.5	98.6	100.0	97.6	96.0	94.0	88.6	88.6	91.5	92.6	91.9	92.1	91.0	89.4
EGFR05.M17	12: 6:59.92	46.6	15.5	96.5	87.2	87.8	88.8	88.3	88.4	88.7	87.2	86.8	88.8	86.2	85.6	86.6	85.8	84.3
EGFR05.M18	12: 7: 4.15	0.5	1406.3	90.5	75.4	78.8	81.7	79.3	85.2	82.7	76.6	68.4	72.1	73.5	74.0	70.0	68.5	67.1
EGFR05.M19	12: 7: 4.82	0.4	1625.6	87.0	73.0	77.3	80.3	76.5	74.4	72.2	67.4	72.9	74.8	75.2	74.2	72.8	72.4	66.5
EGFR05.M20	12: 7: 5.59	0.3	1872.4	79.2	66.0	71.0	72.1	66.2	68.0	70.1	64.3	65.7	63.4	64.7	61.3	61.0	56.9	56.3

DIRECTIVITY ANGLE = 122.5 deg

1/3 OCTAVE BAND CENTER FREQUENCIES (kHz)

FILENAME	RECEIVE TIME	BETA (deg)	SR (m)	OSPL	0.10	0.13	0.16	0.20	0.25	0.32	0.40	0.50	0.63	0.79	1.0	1.3	1.6	2.0
EGFR06.M01	19:37:38.44	3.4	219.6	93.6	80.5	80.3	83.2	89.2	84.9	86.3	87.3	82.3	77.6	74.8	68.3	67.8	66.5	64.9
EGFR06.M02	19:37:38.45	3.1	222.6	93.6	80.6	84.9	82.5	82.0	84.5	84.5	84.3	83.8	80.0	79.3	77.9	74.3	74.4	69.3
EGFR06.M03	19:37:38.45	1.0	225.2	103.1	78.6	76.5	82.1	87.3	94.3	96.4	98.0	94.6	87.5	90.7	85.6	87.0	86.8	85.1
EGFR06.M04	19:37:39.09	1.6	439.4	86.4	75.1	76.4	77.3	71.2	72.5	69.9	70.8	76.5	74.9	76.8	76.7	70.2	67.2	65.1
EGFR06.M05	19:37:39.98	0.9	732.9	72.3	61.3	61.5	61.9	55.7	52.7	51.6	55.2	53.5	56.8	56.2	54.2	54.9	54.2	50.3
EGFR06.M06	19:37:40.11	0.8	887.7	74.0	59.5	63.4	54.4	58.5	53.0	53.0	55.1	53.1	53.3	55.6	54.9	54.6	52.5	48.5
EGFR06.M07	19:37:40.78	0.6	1112.1	68.5	60.1	61.8	55.4	50.1	52.3	50.8	51.0	52.6	56.4	54.8	53.4	52.0	51.1	47.2
EGFR06.M08	19:37:41.51	0.5	1352.3	66.4	59.8	53.2	58.0	51.9	53.7	53.0	51.5	52.4	52.1	55.6	54.2	54.5	50.3	49.6
EGFR06.M09	19:37:42.17	0.4	1571.0	65.8	55.0	54.9	55.5	52.4	51.2	49.5	50.5	51.6	52.4	51.8	51.7	50.9	49.3	48.4
EGFR06.M10	19:37:42.84	0.5	1835.6	63.9	49.4	50.3	55.5	49.6	52.3	48.6	49.1	48.5	47.2	45.8	45.4	45.6	43.2	42.5
EGFR06.M11	19:37:42.86	0.5	1838.6	61.2	47.3	47.7	54.5	49.9	48.2	45.5	46.0	49.6	52.2	50.3	49.3	47.4	44.5	42.5
EGFR06.M12	19:37:42.87	0.2	1841.6	68.1	47.1	49.3	58.6	52.2	52.0	57.6	56.7	55.5	51.8	52.9	50.8	51.2	45.8	43.2
EGFR06.M13	19:37:39.23	3.0	253.2	98.9	80.0	83.9	87.7	87.9	82.4	78.4	85.3	92.7	92.6	88.3	87.5	87.1	85.2	78.3
EGFR06.M14	19:37:39.23	2.7	256.2	99.1	76.6	82.1	80.6	80.3	77.9	76.5	78.3	73.6	71.3	67.3	67.9	69.2	67.9	65.3
EGFR06.M15	19:37:39.24	0.9	258.9	96.7	80.2	80.8	83.6	88.4	86.7	87.7	87.3	86.4	85.3	84.4	82.6	78.6	76.4	72.4
EGFR06.M16	19:37:38.55	47.4	16.3	123.1	102.3	102.9	99.8	102.8	110.1	114.2	112.8	113.7	113.1	115.3	111.6	111.1	108.7	105.6
EGFR06.M17	19:37:38.56	47.1	16.4	123.0	102.0	102.0	100.5	102.1	110.9	113.9	112.7	115.4	113.3	115.7	111.8	111.0	108.6	107.1
EGFR06.M18	19:37:42.69	0.5	1402.4	70.3	53.1	52.6	53.1	52.5	54.1	57.1	56.2	55.5	55.3	53.1	51.5	49.6	49.1	47.3
EGFR06.M19	19:37:43.35	0.4	1621.0	65.3	54.6	50.8	57.1	56.6	53.5	54.6	54.1	52.1	53.1	52.0	50.9	49.0	48.3	47.2
EGFR06.M20	19:37:44.09	0.4	1867.1	64.4	50.0	47.8	57.9	51.2	54.2	53.3	50.4	51.5	48.4	47.2	46.4	44.7	43.1	42.3

DIRECTIVITY ANGLE = 122.5 deg

1/3 OCTAVE BAND CENTER FREQUENCIES (kHz)

FILENAME	RECEIVE TIME	BETA (deg)	SR (m)	OSPL	0.10	0.13	0.16	0.20	0.25	0.32	0.40	0.50	0.63	0.79	1.0	1.3	1.6	2.0
EGFR07.M01	19:42:48.59	1.8	215.1	93.5	82.2	85.4	88.5	84.1	82.7	79.6	79.2	75.5	71.1	65.6	62.1	60.7	60.3	59.4
EGFR07.M02	19:42:48.59	1.5	218.1	92.8	82.7	86.3	86.4	80.7	81.6	78.6	78.5	75.7	72.2	70.5	71.6	70.2	69.2	70.2
EGFR07.M03	19:42:48.60	-0.6	221.1	104.0	84.4	87.3	86.4	83.2	90.1	91.6	95.3	95.3	96.0	92.9	93.1	93.6	92.4	89.9
EGFR07.M04	19:42:49.27	0.7	435.9	83.8	74.9	79.2	77.7	69.3	64.1	59.1	59.3	57.1	62.7	61.4	59.7	60.8	58.9	57.6
EGFR07.M05	19:42:50.17	0.4	730.4	72.7	63.1	67.7	61.6	54.1	51.4	52.3	53.7	57.0	58.8	59.1	59.1	56.7	54.9	51.4
EGFR07.M06	19:42:50.32	0.4	886.0	71.6	64.7	65.0	60.2	52.5	53.6	53.7	54.6	54.8	56.7	58.4	56.0	56.5	54.6	51.5
EGFR07.M07	19:42:51.02	0.3	1111.2	70.9	60.3	63.9	55.9	53.0	54.3	52.5	54.1	53.2	57.5	55.7	54.6	54.0	51.7	47.5
EGFR07.M08	19:42:51.76	0.2	1352.2	67.7	58.2	50.5	48.3	48.7	46.1	47.9	50.7	55.4	56.9	57.6	58.5	56.5	52.2	49.9
EGFR07.M09	19:42:52.44	0.2	1571.6	68.8	58.2	52.3	53.8	49.6	49.5	52.1	53.5	55.1	54.2	55.8	54.2	52.0	50.8	45.9
EGFR07.M10	19:42:53.19	0.2	1815.5	76.8	55.6	53.2	53.4	51.8	49.3	56.1	55.4	52.4	50.1	48.7	48.0	46.4	43.9	40.0
EGFR07.M11	19:42:53.20	0.2	1818.6	67.6	51.1	47.6	44.7	48.9	46.6	50.0	51.3	52.4	56.1	56.5	54.6	52.9	49.8	45.4
EGFR07.M12	19:42:53.20	-0.1	1821.6	79.1	51.2	49.1	54.8	58.1	56.9	61.4	63.0	60.4	59.5	55.2	54.3	53.4	50.2	45.6
EGFR07.M13	19:42:49.36	1.6	248.4	100.9	79.1	86.8	89.4	87.5	90.1	92.8	94.1	94.4	89.1	84.4	87.0	89.2	85.8	80.7
EGFR07.M14	19:42:49.38	1.3	251.5	91.9	77.8	80.8	82.9	81.7	82.5	80.3	81.0	80.5	79.6	71.5	70.1	66.4	65.4	64.0
EGFR07.M15	19:42:49.38	-0.5	254.5	95.2	82.9	83.9	83.8	82.6	84.9	90.0	88.7	84.6	78.2	77.4	78.7	76.5	71.2	68.1
EGFR07.M16	19:43:9.34	****	1930.2	89.0	80.2	81.0	81.0	82.1	80.4	81.8	81.4	80.6	81.0	81.1	80.0	81.4	80.6	79.5
EGFR07.M17	19:43:9.34	****	1929.9	94.4	84.9	85.1	85.2	87.4	85.4	86.0	85.5	85.9	86.3	84.8	84.4	86.2	85.4	84.9
EGFR07.M18	19:42:52.91	0.2	1401.8	70.8	59.9	65.8	59.0	58.6	61.7	60.4	58.5	57.9	56.5	55.9	52.7	53.1	50.6	45.4
EGFR07.M19	19:42:53.59	0.2	1621.2	69.4	58.3	56.2	50.8	53.3	58.3	59.7	57.1	55.5	53.3	53.1	51.6	50.6	47.4	46.2
EGFR07.M20	19:42:54.36	0.2	1868.1	73.5	58.4	60.0	55.4	48.3	54.0	56.5	60.8	58.8	58.4	55.8	54.6	52.5	50.1	45.2

DIRECTIVITY ANGLE = 122.5 deg

1/3 OCTAVE BAND CENTER FREQUENCIES (kHz)

FILENAME	RECEIVE TIME	BETA (deg)	SR (m)	OSPL	0.10	0.13	0.16	0.20	0.25	0.32	0.40	0.50	0.63	0.79	1.0	1.3	1.6	2.0
EGFR08.M01	19:48:46.42	2.2	213.9	94.7	81.4	80.5	76.1	81.9	86.1	88.2	86.7	86.1	82.2	78.4	74.4	71.2	69.5	65.2
EGFR08.M02	19:48:46.44	1.9	216.9	96.6	82.0	80.5	75.2	80.8	84.4	84.0	85.8	87.1	86.1	85.8	86.2	86.3	86.0	85.0
EGFR08.M03	19:48:46.44	-0.2	219.8	100.3	82.0	81.4	75.5	85.9	89.6	95.1	95.1	92.5	83.0	86.7	84.3	84.1	83.0	78.8
EGFR08.M04	19:48:47.11	0.9	434.8	83.5	76.1	77.0	70.8	70.1	64.5	60.7	62.9	67.1	66.7	61.3	62.8	61.4	58.8	58.7
EGFR08.M05	19:48:48.02	0.6	729.6	80.6	52.7	58.9	58.5	55.6	47.0	50.4	53.3	57.0	59.8	59.6	59.5	54.6	55.1	51.8
EGFR08.M06	19:48:48.18	0.5	885.3	77.6	56.4	60.0	57.0	54.5	54.0	54.3	56.4	56.1	62.3	63.4	63.6	61.6	59.2	56.7
EGFR08.M07	19:48:48.88	0.4	1110.7	70.9	59.7	67.0	60.9	56.0	50.0	51.0	53.5	54.2	56.8	55.0	56.9	56.8	54.3	49.7
EGFR08.M08	19:48:49.63	0.3	1352.0	67.6	53.2	53.6	51.2	49.9	53.5	51.5	53.9	57.9	57.0	59.0	54.9	50.5	51.7	47.6
EGFR08.M09	19:48:50.30	0.3	1571.6	71.0	56.5	56.7	52.7	50.9	50.6	50.0	55.5	52.1	54.8	59.6	56.2	55.7	50.3	46.5
EGFR08.M10	19:48:51.06	0.3	1815.7	63.5	47.7	48.5	46.7	47.0	44.1	47.4	47.5	47.8	44.6	41.8	40.8	39.3	36.4	33.5
EGFR08.M11	19:48:51.07	0.2	1818.8	59.7	44.9	41.6	45.4	40.4	41.5	43.3	48.0	48.7	49.3	48.9	46.8	44.8	43.6	40.1
EGFR08.M12	19:48:51.08	-0.0	1821.8	73.5	55.6	53.8	51.3	55.3	60.0	65.7	67.0	62.2	62.0	61.7	56.5	53.8	49.4	46.5
EGFR08.M13	19:48:47.20	1.9	247.1	99.6	77.4	81.7	85.3	87.6	88.8	88.8	86.6	83.2	89.3	93.5	90.5	85.7	89.4	83.6
EGFR08.M14	19:48:47.20	1.6	250.1	92.8	79.6	77.6	78.6	77.1	77.0	78.6	80.1	82.2	82.5	77.9	76.8	74.9	74.1	72.0
EGFR08.M15	19:48:47.21	-0.2	253.1	94.1	85.6	84.1	85.2	84.3	84.6	87.3	84.3	83.5	78.3	77.5	72.7	72.5	71.0	67.6
EGFR08.M16	19:48:46.49	56.8	8.5	121.9	102.1	99.4	98.8	98.0	102.0	110.2	115.6	117.9	114.0	104.8	105.6	104.3	106.8	108.0
EGFR08.M17	19:48:46.49	56.5	8.6	121.8	103.2	101.1	99.7	98.1	105.2	110.7	115.4	118.1	112.0	105.9	105.6	104.4	106.4	107.2
EGFR08.M18	19:48:50.77	0.3	1401.5	72.8	60.0	63.1	57.1	59.3	62.1	66.1	63.2	58.5	56.2	57.8	53.7	49.3	47.0	43.8
EGFR08.M19	19:48:51.45	0.3	1621.1	66.9	54.1	55.8	52.8	55.4	55.2	59.5	56.1	54.8	53.5	52.2	50.8	48.0	44.7	40.9
EGFR08.M20	19:48:52.22	0.2	1868.2	67.9	51.5	57.3	52.0	50.7	53.0	54.0	53.4	51.3	52.3	51.1	47.1	45.6	42.1	39.4

DIRECTIVITY ANGLE = 122.5 deg

1/3 OCTAVE BAND CENTER FREQUENCIES (kHz)

FILENAME	RECEIVE TIME	BETA (deg)	SR (m)	OSPL	0.10	0.13	0.16	0.20	0.25	0.32	0.40	0.50	0.63	0.79	1.0	1.3	1.6	2.0
EGFR09.M01	19:52:39.03	1.5	214.9	94.6	82.0	84.5	82.1	82.9	81.4	82.8	86.8	86.3	80.3	73.5	69.9	66.9	64.3	61.3
EGFR09.M02	19:52:39.04	1.2	217.9	94.6	83.2	82.1	84.0	82.0	81.2	80.8	84.4	85.5	83.0	78.8	79.9	79.6	78.2	74.8
EGFR09.M03	19:52:39.05	-0.9	220.9	101.0	83.9	82.4	82.5	80.6	88.0	91.9	94.9	96.1	90.7	85.4	82.9	86.8	87.7	83.1
EGFR09.M04	19:52:39.72	0.6	436.1	82.9	75.6	74.9	74.6	72.3	64.5	59.8	59.3	64.3	62.2	64.6	65.6	62.2	59.7	61.2
EGFR09.M05	19:52:40.64	0.4	731.3	74.1	64.6	60.6	54.4	51.3	49.1	49.6	58.4	55.5	56.4	61.5	57.8	57.0	54.4	50.3
EGFR09.M06	19:52:40.80	0.3	887.3	74.4	65.0	65.9	56.9	51.3	52.5	50.5	54.9	56.5	57.6	58.3	57.5	55.2	52.4	49.7
EGFR09.M07	19:52:41.51	0.2	1113.0	76.7	57.4	64.2	50.5	56.4	53.7	53.8	56.4	55.3	53.5	54.9	52.4	52.3	50.4	47.4
EGFR09.M08	19:52:42.26	0.2	1354.5	69.6	53.8	47.4	44.7	48.0	49.6	48.2	49.8	54.6	53.7	52.1	51.0	48.2	47.7	43.3
EGFR09.M09	19:52:42.95	0.2	1574.4	81.5	53.1	44.9	46.1	48.3	45.7	48.2	48.0	47.4	49.8	47.3	46.0	44.2	43.2	39.8
EGFR09.M10	19:52:43.71	0.2	1818.7	72.3	48.2	40.6	45.9	47.9	46.3	50.3	48.1	44.1	45.6	42.3	40.3	39.5	35.6	34.0
EGFR09.M11	19:52:43.72	0.1	1821.8	62.0	49.1	42.2	39.2	36.8	42.3	44.2	46.9	49.1	47.3	48.5	46.6	42.6	39.9	36.1
EGFR09.M12	19:52:43.73	-0.1	1824.8	75.1	47.6	49.6	44.7	48.3	51.5	50.3	54.1	52.6	53.4	48.3	47.3	45.9	43.6	41.2
EGFR09.M13	19:52:39.80	1.3	248.1	98.5	80.1	75.8	78.3	75.4	80.6	86.0	89.2	90.3	90.0	88.7	88.9	88.8	87.0	85.0
EGFR09.M14	19:52:39.81	1.0	251.1	92.0	79.0	82.1	83.2	81.1	78.6	80.8	77.0	79.4	74.7	75.3	70.2	70.7	68.8	66.9
EGFR09.M15	19:52:39.83	-0.8	254.1	93.3	81.7	84.9	83.7	82.9	81.9	83.7	83.4	80.9	79.7	80.2	76.4	74.0	72.9	71.9
EGFR09.M16	19:52:39.06	52.6	5.5	111.4	103.4	103.1	103.3	103.8	101.4	99.7	94.5	97.6	98.0	96.3	95.8	95.1	95.7	96.6
EGFR09.M17	19:52:39.06	51.7	5.6	112.0	105.0	103.9	103.5	104.8	102.1	97.8	94.8	98.8	97.0	95.7	96.6	96.1	96.2	96.9
EGFR09.M18	19:52:42.60	0.4	1386.1	69.5	56.5	54.1	50.4	53.5	55.0	54.3	52.9	55.7	54.6	54.5	51.1	49.2	47.6	43.2
EGFR09.M19	19:52:44.10	0.2	1623.7	64.9	52.1	45.7	45.2	48.4	50.4	49.5	50.8	51.0	50.0	48.5	45.8	43.9	41.1	38.8
EGFR09.M20	19:52:44.88	0.1	1871.1	64.5	50.1	46.5	48.2	52.4	53.6	56.1	52.9	53.0	48.3	49.6	46.5	46.8	40.8	39.9

DIRECTIVITY ANGLE = 122.5 deg

FILENAME	RECEIVE TIME	BETA (deg)	SR (m)	OSPL	0.10	0.13	0.16	0.20	0.25	0.32	0.40	0.50	0.63	0.79	1.0	1.3	1.6	2.0
EGFR10.M01	19:56:24.78	4.9	217.3	100.8	79.6	82.3	87.8	88.9	92.7	95.4	95.0	89.9	88.9	83.6	79.2	76.9	76.3	75.1
EGFR10.M02	19:56:24.79	4.5	220.2	99.6	81.5	80.9	85.9	87.6	91.5	90.4	90.8	90.2	89.2	89.2	87.8	87.8	86.3	84.0
EGFR10.M03	19:56:24.79	2.4	222.6	101.6	71.7	81.3	88.6	91.1	94.0	90.2	92.4	94.2	89.7	90.6	86.7	88.9	87.3	84.9
EGFR10.M04	19:56:25.45	2.3	437.4	83.2	74.5	72.9	74.5	71.0	71.0	68.6	66.4	68.4	71.0	69.1	66.7	65.0	63.7	62.0
EGFR10.M05	19:56:26.35	1.4	731.5	74.7	62.6	61.7	57.4	55.0	52.0	50.7	54.1	56.1	55.4	57.2	56.9	55.7	52.4	50.0
EGFR10.M06	19:56:26.50	1.1	886.9	72.3	62.4	65.9	52.4	49.8	51.7	51.0	49.4	55.7	56.1	58.0	52.3	53.6	52.9	48.3
EGFR10.M07	19:56:27.19	0.9	1111.9	72.5	62.3	64.0	55.8	50.3	52.5	50.5	50.8	52.0	55.0	53.3	53.6	52.8	50.3	46.7
EGFR10.M08	19:56:27.93	0.7	1352.7	67.3	54.7	54.6	53.4	46.5	47.0	47.8	52.0	52.6	53.9	54.2	54.1	52.3	50.2	46.5
EGFR10.M09	19:56:28.60	0.6	1571.9	64.7	54.7	49.9	51.1	49.5	48.0	46.9	48.7	49.5	47.8	50.7	47.8	45.5	43.4	39.9
EGFR10.M10	19:56:29.35	0.6	1815.6	64.3	42.3	42.8	46.2	48.7	47.8	48.7	47.1	44.5	43.6	40.6	39.1	36.3	35.5	33.0
EGFR10.M11	19:56:29.36	0.5	1818.6	59.8	48.6	40.6	43.9	41.7	45.1	43.6	47.0	46.9	46.9	49.1	48.2	45.9	41.6	37.5
EGFR10.M12	19:56:29.37	0.3	1821.6	72.0	51.2	49.0	52.0	50.3	57.3	52.8	59.2	60.6	55.5	53.3	56.5	52.6	48.5	44.6
EGFR10.M13	19:56:25.55	4.3	250.6	99.9	79.3	81.0	80.3	80.6	89.1	92.5	94.2	85.8	91.1	87.2	88.9	87.6	86.7	81.5
EGFR10.M14	19:56:25.56	3.9	253.5	102.0	81.5	86.8	91.9	94.7	91.2	90.2	93.5	93.0	91.4	88.7	86.2	84.6	82.0	73.9
EGFR10.M15	19:56:25.56	2.1	256.0	99.1	81.2	82.7	84.4	86.2	87.7	90.6	92.0	93.0	89.8	87.5	85.0	86.3	84.6	81.5
EGFR10.M16	19:56:24.94	55.8	21.0	113.0	99.7	101.5	101.2	102.9	93.0	90.5	97.6	107.5	105.7	101.9	95.5	96.0	97.9	97.3
EGFR10.M17	19:56:24.94	55.6	21.1	113.3	100.4	100.9	102.2	102.6	91.4	92.8	99.4	109.6	105.5	99.7	96.4	95.9	98.8	97.8
EGFR10.M18	19:56:29.09	0.7	1402.4	72.4	59.6	56.4	54.4	53.8	58.7	58.2	56.7	53.2	51.8	54.5	50.2	48.8	45.9	43.0
EGFR10.M19	19:56:29.75	0.6	1621.6	70.8	50.5	51.2	45.4	47.9	52.0	58.8	54.5	51.3	48.9	48.0	45.3	43.3	40.2	37.9
EGFR10.M20	19:56:30.51	0.5	1968.3	62.2	54.6	48.1	49.1	47.4	50.4	51.6	49.2	49.0	48.9	47.3	45.0	43.3	41.5	38.9

DIRECTIVITY ANGLE = 122.5 deg

1/3 OCTAVE BAND CENTER FREQUENCIES (kHz)

FILENAME	RECEIVE TIME	BETA (deg)	SR (m)	OSPL	0.10	0.13	0.16	0.20	0.25	0.32	0.40	0.50	0.63	0.79	1.0	1.3	1.6	2.0
EGFR11.M01	20: 0: 2.70	5.8	211.0	99.3	79.4	80.7	85.6	89.7	90.9	93.9	93.2	89.3	84.5	80.7	77.2	74.9	73.1	70.6
EGFR11.M02	20: 0: 2.71	5.4	213.9	96.9	84.6	83.4	84.8	85.8	85.1	86.0	88.2	86.8	86.9	85.3	84.6	84.7	83.5	81.9
EGFR11.M03	20: 0: 2.72	3.2	216.1	98.8	71.7	79.8	81.8	85.9	91.6	88.1	91.1	91.0	88.3	87.4	86.2	85.1	85.0	82.5
EGFR11.M04	20: 0: 3.41	2.6	432.1	83.5	74.9	73.4	71.2	69.1	65.6	64.9	69.6	70.4	70.3	69.1	70.0	70.4	69.6	65.1
EGFR11.M05	20: 0: 4.35	1.6	728.0	75.1	62.4	64.1	54.9	54.6	51.4	50.5	55.2	54.3	58.0	54.6	54.0	53.2	51.7	52.0
EGFR11.M06	20: 0: 4.52	1.3	884.6	71.2	53.9	61.1	60.3	57.9	51.2	50.8	55.8	54.1	55.8	57.2	54.0	52.8	50.1	47.8
EGFR11.M07	20: 0: 5.25	1.0	1111.0	66.9	53.7	62.0	53.9	54.8	51.5	49.0	50.5	49.7	51.8	52.2	50.9	48.8	47.3	42.9
EGFR11.M08	20: 0: 6.02	0.8	1353.3	66.6	56.9	55.7	51.4	48.8	44.5	48.3	53.1	54.3	51.4	51.5	52.0	50.4	49.1	46.5
EGFR11.M09	20: 0: 6.72	0.7	1573.8	69.5	49.1	53.1	43.7	46.6	46.0	46.9	46.6	50.4	50.6	49.2	46.5	45.3	42.3	39.6
EGFR11.M10	20: 0: 7.50	0.7	1818.9	73.3	49.4	43.3	44.7	46.6	43.8	49.4	46.7	46.4	46.2	40.4	38.3	36.4	35.6	32.9
EGFR11.M11	20: 0: 7.51	0.6	1822.0	65.6	47.0	50.2	45.4	41.3	39.0	43.5	44.3	45.9	48.4	49.8	48.6	44.8	42.6	37.4
EGFR11.M12	20: 0: 7.52	2.4	1825.0	69.7	46.5	45.2	52.4	47.6	54.0	52.6	57.1	55.7	52.6	53.9	51.5	50.9	46.3	42.9
EGFR11.M13	20: 0: 3.48	5.0	243.7	81.0	57.6	57.9	57.3	58.1	57.3	59.3	58.9	56.8	56.6	56.2	56.2	56.8	56.4	54.9
EGFR11.M14	20: 0: 3.48	4.6	246.6	87.2	54.6	54.0	52.0	53.4	53.7	53.6	52.8	54.2	54.7	52.9	51.6	53.4	50.0	49.5
EGFR11.M15	20: 0: 3.49	2.8	248.9	67.8	61.1	57.5	56.3	56.8	57.4	57.3	58.4	58.7	58.4	57.1	56.3	57.3	56.3	54.8
EGFR11.M16	20: 0: 2.92	55.9	24.0	88.2	80.2	80.6	80.2	82.8	80.9	80.3	80.9	80.3	81.2	81.2	80.3	81.1	81.1	79.9
EGFR11.M17	20: 0: 2.92	56.0	24.0	90.1	80.4	80.3	81.7	84.8	80.9	82.7	81.3	81.0	81.8	80.7	80.1	80.8	80.7	79.8
EGFR11.M18	20: 0: 7.16	0.8	1402.2	70.6	54.7	59.2	55.1	56.5	60.3	55.4	54.8	54.7	53.7	52.1	49.8	47.8	44.2	42.2
EGFR11.M19	20: 0: 7.86	0.7	1622.7	69.0	47.5	52.8	48.9	52.4	53.1	54.5	56.3	54.1	53.2	49.6	48.8	46.4	43.3	39.5
EGFR11.M20	20: 0: 8.66	0.6	1870.9	64.5	53.2	53.3	48.5	53.4	50.2	52.5	54.1	52.7	51.2	49.2	47.9	44.6	42.4	39.5

DIRECTIVITY ANGLE = 122.5 deg

1/3 OCTAVE BAND CENTER FREQUENCIES (kHz)

FILENAME	RECEIVE TIME	BETA (deg)	SR (m)	OSPL	0.10	0.13	0.16	0.20	0.25	0.32	0.40	0.50	0.63	0.79	1.0	1.3	1.6	2.0
EGFR12.M01	20: 3:59.73	5.9	215.7	97.7	79.1	83.0	81.5	84.9	89.6	91.1	91.6	90.0	85.4	77.4	74.4	71.7	69.0	63.5
EGFR12.M02	20: 3:59.73	5.5	218.5	97.5	78.5	77.0	79.2	80.7	87.5	87.0	87.6	90.5	86.6	84.7	85.3	85.7	83.9	81.3
EGFR12.M03	20: 3:59.74	3.4	220.7	95.2	80.9	83.6	80.5	82.7	83.8	87.3	88.2	87.8	82.6	77.4	80.4	79.6	75.4	77.8
EGFR12.M04	20: 4: 0.41	2.8	435.7	82.9	74.9	74.0	75.6	71.7	69.0	65.1	67.5	69.6	68.6	70.5	67.9	65.9	62.8	60.5
EGFR12.M05	20: 4: 1.31	1.7	730.1	73.7	62.2	61.3	58.2	58.0	52.0	50.7	50.7	58.4	59.3	58.0	57.2	57.3	54.1	50.3
EGFR12.M06	20: 4: 1.47	1.4	885.7	72.5	62.1	62.6	61.3	55.7	48.6	51.0	50.8	53.7	56.6	58.6	60.7	56.6	55.4	49.7
EGFR12.M07	20: 4: 2.16	1.1	1110.9	72.3	66.3	67.5	58.7	55.9	53.4	49.9	52.9	53.0	52.2	54.7	55.8	53.3	50.1	48.0
EGFR12.M08	20: 4: 2.91	0.9	1352.0	67.1	60.4	56.7	52.9	51.8	50.1	48.2	51.2	53.9	53.9	55.5	54.0	50.5	47.8	44.2
EGFR12.M09	20: 4: 3.59	0.8	1571.5	66.2	55.3	53.1	49.1	51.8	50.0	45.3	47.1	48.1	53.5	52.4	51.4	48.6	45.8	41.8
EGFR12.M10	20: 4: 4.34	0.7	1815.4	70.9	54.7	53.0	57.6	51.8	51.1	48.9	50.5	46.2	48.6	42.0	41.8	39.2	35.4	33.5
EGFR12.M11	20: 4: 4.35	0.7	1818.4	66.2	48.7	43.4	46.5	46.8	51.2	45.0	47.5	49.2	49.1	50.4	50.8	45.9	42.0	36.6
EGFR12.M12	20: 4: 4.36	0.4	1821.4	76.8	52.2	48.9	59.2	59.0	56.0	60.9	60.7	62.0	55.0	56.8	53.9	50.9	47.2	43.0
EGFR12.M13	20: 4: 0.49	5.2	248.8	97.8	76.2	76.6	85.7	88.3	87.1	90.9	86.5	88.3	88.4	84.7	87.4	85.9	86.7	83.7
EGFR12.M14	20: 4: 0.50	4.8	251.7	101.4	82.8	84.3	88.7	89.2	89.0	91.8	92.0	93.3	90.1	89.8	85.6	81.4	77.9	78.5
EGFR12.M15	20: 4: 0.50	3.0	254.0	105.3	80.7	82.5	89.5	86.4	93.0	96.1	95.7	95.0	96.2	93.9	93.8	95.3	94.6	90.2
EGFR12.M16	20: 3:59.91	57.4	25.1	124.6	89.9	100.1	106.9	111.0	115.4	110.8	114.6	114.4	116.3	114.5	113.1	111.6	110.6	109.2
EGFR12.M17	20: 3:59.91	57.3	25.2	124.7	91.5	100.3	106.5	113.9	116.1	111.9	114.3	115.3	115.5	114.6	113.0	111.6	111.3	109.1
EGFR12.M18	20: 4: 4.04	0.9	1401.5	69.7	58.7	59.2	57.0	59.7	58.6	54.2	56.9	53.3	55.2	52.7	51.0	47.0	43.0	40.6
EGFR12.M19	20: 4: 4.72	0.7	1621.0	68.3	55.7	48.5	55.3	54.5	55.7	55.2	57.2	56.5	51.4	52.3	48.4	48.1	44.4	40.4
EGFR12.M20	20: 4: 5.48	0.6	1868.0	66.3	49.9	52.3	53.6	53.2	55.1	59.4	56.6	52.6	52.2	49.6	49.4	46.5	42.9	40.5

DIRECTIVITY ANGLE = 122.5 deg

1/3 OCTAVE BAND CENTER FREQUENCIES (kHz)

FILENAME	RECEIVE TIME	BETA (deg)	SR (m)	OSPL	0.10	0.13	0.16	0.20	0.25	0.32	0.40	0.50	0.63	0.79	1.0	1.3	1.6	2.0
EGFR13.M01	21: 2:30.64	5.5	204.9	97.0	84.7	81.4	83.7	87.3	88.0	89.6	90.8	88.3	84.2	81.6	78.0	73.2	72.7	71.0
EGFR13.M02	21: 2:30.65	5.1	207.8	101.1	82.3	84.1	83.0	85.5	88.5	88.0	88.8	90.9	89.4	90.4	91.1	89.3	90.0	89.5
EGFR13.M03	21: 2:30.66	2.9	210.1	103.3	75.9	78.1	87.6	90.5	92.8	94.5	91.3	95.7	93.2	92.7	90.8	90.9	89.5	87.0
EGFR13.M04	21: 2:31.38	2.5	428.0	87.6	75.4	77.2	72.6	68.5	66.8	63.1	69.7	72.9	74.0	72.4	73.0	71.8	75.4	76.1
EGFR13.M05	21: 2:32.37	1.5	726.3	75.6	62.3	65.1	57.7	58.4	62.3	59.7	63.0	65.4	68.9	68.1	66.2	61.5	64.7	63.4
EGFR13.M06	21: 2:32.68	1.2	884.7	81.1	66.7	59.4	57.8	62.5	64.5	51.2	64.9	69.6	72.3	72.9	73.6	71.7	65.9	62.7
EGFR13.M07	21: 2:33.36	0.9	1112.9	73.6	58.8	63.9	55.9	52.6	56.4	54.9	55.9	60.1	65.3	64.1	64.0	58.0	56.7	55.4
EGFR13.M08	21: 2:34.17	0.8	1357.3	72.2	55.6	52.8	54.2	52.6	55.8	56.5	58.6	61.6	61.7	62.2	62.9	62.7	60.8	55.3
EGFR13.M09	21: 2:34.91	0.7	1579.6	70.1	49.1	47.2	50.3	48.4	53.9	56.1	56.9	61.5	63.2	60.3	57.8	59.3	57.7	52.3
EGFR13.M10	21: 2:35.73	0.6	1826.8	68.0	51.5	46.6	46.6	49.7	49.4	45.6	45.7	48.5	49.2	43.6	43.2	41.8	39.9	38.8
EGFR13.M11	21: 2:35.73	0.6	1829.9	67.0	48.0	45.4	48.2	43.7	48.6	50.8	52.4	57.1	56.8	55.0	58.4	58.3	52.6	47.3
EGFR13.M12	21: 2:35.74	0.3	1832.9	73.5	45.3	47.6	48.0	53.4	54.6	55.9	56.0	53.7	57.3	55.8	53.1	49.1	46.1	41.6
EGFR13.M13	21: 2:31.35	4.8	236.9	97.9	76.7	78.6	83.5	85.6	89.5	91.5	85.8	87.0	88.5	87.3	89.4	88.0	86.0	79.4
EGFR13.M14	21: 2:31.36	4.4	239.8	99.8	82.3	83.8	88.4	90.8	92.9	90.7	90.0	90.3	89.3	88.8	85.4	84.6	79.8	75.1
EGFR13.M15	21: 2:31.37	2.5	242.3	100.9	80.7	84.6	89.7	92.4	93.6	92.3	91.2	89.1	89.9	90.1	88.9	85.9	84.1	80.8
EGFR13.M16	21: 2:30.84	46.3	25.6	107.1	94.6	98.2	95.1	97.9	91.7	89.7	89.0	94.1	100.0	100.6	92.9	88.1	91.0	89.1
EGFR13.M17	21: 2:30.84	46.6	25.5	105.0	97.8	96.9	96.5	96.9	94.4	91.1	84.9	88.1	94.2	95.7	92.3	88.2	86.3	88.6
EGFR13.M18	21: 2:35.23	0.8	1405.1	81.1	55.4	59.6	67.1	67.8	65.4	69.7	70.7	69.7	66.4	62.8	60.6	55.1	54.9	48.3
EGFR13.M19	21: 2:35.96	0.7	1627.4	76.2	53.4	50.6	57.9	63.4	64.9	65.4	64.6	63.3	57.8	55.7	56.2	51.5	49.6	43.3
EGFR13.M20	21: 2:36.80	0.6	1877.7	77.8	53.4	53.0	58.3	67.2	68.1	70.2	69.2	69.6	68.8	70.3	66.6	59.8	54.8	48.6

DIRECTIVITY ANGLE = 122.5 deg

1/3 OCTAVE BAND CENTER FREQUENCIES (kHz)

FILENAME	RECEIVE TIME	BETA (deg)	SR (m)	OSPL	0.10	0.13	0.16	0.20	0.25	0.32	0.40	0.50	0.63	0.79	1.0	1.3	1.6	2.0
EGFR14.M01	21: 6:19.69	5.5	217.1	102.6	87.3	87.4	86.7	93.6	94.2	95.6	96.9	93.2	89.2	83.8	80.3	77.7	73.5	71.1
EGFR14.M02	21: 6:19.70	5.1	220.0	102.7	87.0	86.9	86.2	90.5	92.7	93.5	94.4	92.4	92.9	92.1	90.6	89.6	89.2	88.7
EGFR14.M03	21: 6:19.70	3.0	222.3	104.1	86.6	91.3	89.5	86.5	87.8	93.0	97.0	97.7	91.6	93.7	90.0	93.9	91.2	87.4
EGFR14.M04	21: 6:20.36	2.6	437.1	89.0	83.0	84.5	77.4	76.3	72.5	68.4	71.8	74.9	71.9	71.5	70.8	74.3	72.5	74.5
EGFR14.M05	21: 6:21.27	1.5	731.3	78.8	66.8	66.7	64.9	60.4	63.5	56.9	63.2	63.6	63.7	63.2	64.9	66.5	65.1	62.3
EGFR14.M06	21: 6:21.41	1.3	886.7	77.6	66.8	64.6	61.5	55.8	57.3	57.2	66.3	61.0	62.2	64.8	64.6	64.3	63.4	61.3
EGFR14.M07	21: 6:22.10	1.0	1111.7	76.9	65.3	59.4	61.6	55.1	56.7	59.6	55.3	60.3	65.3	63.1	64.2	63.7	60.0	55.4
EGFR14.M08	21: 6:22.84	0.8	1352.7	80.4	66.4	64.8	52.8	54.9	59.6	61.6	66.2	68.3	65.0	71.3	65.8	70.4	65.5	62.4
EGFR14.M09	21: 6:23.52	0.7	1572.0	75.0	58.6	58.0	55.5	49.2	51.2	56.7	59.8	61.7	62.1	59.9	59.0	59.4	58.0	56.6
EGFR14.M10	21: 6:24.27	0.7	1815.7	64.6	52.3	50.4	51.1	54.0	50.9	52.5	53.4	52.0	50.1	46.1	42.5	44.7	41.6	38.6
EGFR14.M11	21: 6:24.27	0.6	1818.7	67.1	50.7	48.3	50.2	49.7	52.2	53.1	51.7	58.5	59.1	58.0	56.4	54.8	52.8	49.8
EGFR14.M12	21: 6:24.28	0.4	1821.7	75.7	48.6	47.6	57.4	57.1	60.1	55.5	60.4	65.6	65.1	62.9	61.7	57.8	53.8	48.4
EGFR14.M13	21: 6:20.47	4.7	250.3	104.9	81.0	72.4	85.3	92.1	96.2	98.6	90.1	95.2	92.6	97.7	94.8	92.2	91.9	87.4
EGFR14.M14	21: 6:20.48	4.4	253.3	105.9	87.0	90.9	93.2	91.9	95.0	96.2	97.5	99.2	95.7	93.3	86.6	89.8	91.6	90.5
EGFR14.M15	21: 6:20.48	2.6	255.6	109.7	88.5	91.1	94.0	93.6	95.0	96.9	99.3	101.4	100.2	101.4	99.3	97.9	96.9	95.3
EGFR14.M16	21: 6:19.88	56.4	23.4	117.5	101.7	104.5	98.5	91.8	102.5	109.7	111.2	109.3	102.4	107.4	104.5	106.9	102.6	100.4
EGFR14.M17	21: 6:19.88	56.3	23.5	103.6	95.0	98.0	94.8	94.5	94.7	89.4	89.4	88.6	88.0	90.2	93.0	92.6	90.3	86.3
EGFR14.M18	21: 6:24.01	0.8	1402.3	78.1	62.3	61.6	65.5	63.3	65.5	70.8	69.4	64.5	65.0	60.7	59.0	59.4	57.7	55.4
EGFR14.M19	21: 6:24.68	0.7	1621.6	71.8	62.0	58.0	58.8	57.7	60.3	61.4	62.8	59.9	59.6	56.1	56.2	53.6	50.7	48.6
EGFR14.M20	21: 6:25.45	0.6	1868.4	71.9	60.1	61.0	57.8	59.5	57.0	62.7	60.9	57.8	57.9	55.9	54.3	52.1	51.3	45.8

DIRECTIVITY ANGLE = 122.5 deg

1/3 OCTAVE BAND CENTER FREQUENCIES (kHz)

FILENAME	RECEIVE TIME	BETA (deg)	SR (m)	OSPL	0.10	0.13	0.16	0.20	0.25	0.32	0.40	0.50	0.63	0.79	1.0	1.3	1.6	2.0
EGFR15.M01	21: 9:53.99	5.2	205.3	100.6	81.1	82.2	88.2	91.3	91.7	93.8	93.8	92.0	87.4	80.9	77.4	76.7	73.4	71.7
EGFR15.M02	21: 9:54.00	4.8	208.3	102.2	83.5	83.9	85.7	88.2	90.0	89.0	94.0	92.7	90.2	90.1	92.0	90.6	90.0	88.5
EGFR15.M03	21: 9:54.31	2.6	210.6	104.7	73.8	85.3	90.8	95.4	96.2	92.1	91.5	97.0	95.4	93.1	90.6	93.6	94.3	88.9
EGFR15.M04	21: 9:54.71	2.3	427.2	88.5	75.2	76.7	77.0	67.5	66.1	64.9	69.9	74.9	76.1	74.9	79.2	81.7	79.5	72.1
EGFR15.M05	21: 9:55.66	1.4	723.7	78.9	67.3	65.6	67.1	60.6	56.8	55.1	61.9	66.1	71.4	68.3	65.8	67.5	66.4	64.0
EGFR15.M06	21: 9:55.85	1.1	880.9	77.1	68.3	63.8	63.8	65.2	58.3	59.0	60.6	60.8	66.6	68.0	65.2	64.7	66.3	62.6
EGFR15.M07	21: 9:56.59	0.9	1107.7	76.7	62.9	64.0	60.0	58.9	58.3	60.1	58.3	56.2	57.9	58.9	59.9	58.6	59.0	57.0
EGFR15.M08	21: 9:57.37	0.7	1350.6	78.6	65.9	57.9	53.9	52.6	57.5	56.9	61.5	61.5	62.6	66.4	66.3	66.2	63.7	59.4
EGFR15.M09	21: 9:58.09	0.6	1571.6	73.3	54.5	52.4	51.0	49.6	46.8	50.5	55.0	55.6	56.2	56.9	55.6	55.6	53.0	49.4
EGFR15.M10	21: 9:58.88	0.6	1817.3	66.5	53.0	51.8	48.7	52.4	51.7	55.4	55.7	54.3	52.1	53.1	49.8	47.5	46.4	43.6
EGFR15.M11	21: 9:58.89	0.5	1820.3	68.8	48.8	44.1	44.9	45.5	48.5	54.1	59.2	58.7	59.9	62.1	58.9	57.7	57.6	53.1
EGFR15.M12	21: 9:58.90	0.3	1823.3	71.1	43.3	48.0	54.9	54.2	58.3	54.6	54.7	59.7	59.2	55.6	55.8	52.3	50.2	46.3
EGFR15.M13	21: 9:54.77	4.5	238.1	103.8	83.6	80.8	78.9	81.1	88.6	97.5	97.9	93.1	90.0	94.3	90.4	93.0	93.2	88.7
EGFR15.M14	21: 9:54.77	4.2	241.1	106.6	87.1	87.5	88.0	95.7	97.8	98.9	97.5	97.3	97.2	96.4	95.1	93.5	93.3	89.7
EGFR15.M15	21: 9:54.78	2.3	243.6	108.1	86.2	88.0	88.8	96.2	98.4	99.7	98.4	97.5	98.0	96.5	97.3	96.6	97.0	95.2
EGFR15.M16	21: 9:54.23	48.5	23.5	112.9	98.1	99.8	98.8	97.7	94.9	92.3	102.9	104.4	107.5	101.9	98.6	100.2	96.2	95.7
EGFR15.M17	21: 9:54.23	48.8	23.4	106.4	94.9	103.1	93.4	91.8	91.8	88.4	88.9	88.0	87.5	87.3	85.8	86.7	87.0	85.5
EGFR15.M18	21: 9:58.56	0.7	1402.1	78.8	58.2	56.8	61.0	64.8	67.8	66.8	68.2	66.0	62.3	61.9	56.8	57.8	54.9	49.1
EGFR15.M19	21: 9:59.29	0.6	1623.6	65.8	54.5	56.5	53.5	52.3	54.6	54.9	55.8	53.7	53.5	51.6	50.5	48.8	47.0	43.3
EGFR15.M20	21:10: 0.10	0.5	1872.9	71.2	50.9	52.3	57.3	62.3	62.1	62.2	62.3	63.0	61.0	60.0	61.4	58.4	52.5	50.0

DIRECTIVITY ANGLE = 122.5 deg

										1/3 OCTAVE BAND CENTER FREQUENCIES (kHz)								
FILENAME	RECEIVE TIME	BETA (deg)	SR (m)	OSPL	0.10	0.13	0.16	0.20	0.25	0.32	0.40	0.50	0.63	0.79	1.0	1.3	1.6	2.0
EGFR16.M01	21:13:55.13	10.6	205.0	98.3	86.3	89.5	88.7	90.3	89.0	90.6	87.2	85.5	82.1	83.1	83.1	81.3	81.4	79.5
EGFR16.M02	21:13:55.13	10.1	207.7	98.0	82.7	88.6	85.1	89.8	84.6	79.0	82.1	88.0	89.5	91.6	88.7	82.2	83.4	87.4
EGFR16.M03	21:13:55.13	7.8	209.0	102.9	80.4	84.8	88.0	89.6	90.2	93.4	94.2	93.4	93.5	92.7	93.0	89.7	88.0	85.1
EGFR16.M04	21:13:55.84	4.9	425.5	89.5	75.5	75.9	71.4	74.8	74.0	72.1	76.3	79.4	79.8	79.3	81.7	81.9	77.6	74.7
EGFR16.M05	21:13:56.81	2.9	722.3	81.0	63.2	65.5	63.5	62.1	61.6	63.6	64.1	70.2	68.2	67.5	72.8	72.2	73.4	70.8
EGFR16.M06	21:13:57.01	2.4	880.0	77.9	62.6	67.4	64.9	61.6	61.1	66.1	68.1	69.4	66.8	67.8	65.2	69.6	62.7	61.6
EGFR16.M07	21:13:57.76	1.9	1107.4	75.6	60.4	63.3	60.9	64.5	56.9	51.2	58.3	62.7	59.0	58.8	60.9	62.6	63.8	59.3
EGFR16.M08	21:13:58.55	1.5	1350.9	77.5	60.6	59.9	57.3	56.7	57.7	60.0	64.9	66.7	63.0	67.3	71.0	67.9	69.0	64.2
EGFR16.M09	21:13:59.29	1.3	1572.6	70.6	51.4	52.9	51.5	50.0	48.2	52.8	59.6	62.2	64.9	60.1	58.7	60.0	61.1	56.3
EGFR16.M10	21:14:0.09	1.2	1819.0	64.9	55.1	49.3	50.0	51.6	51.5	57.6	55.1	53.3	51.5	47.6	44.4	42.8	41.7	39.7
EGFR16.M11	21:14:0.10	1.1	1822.1	68.0	48.2	50.3	43.2	45.4	47.8	47.5	49.6	55.4	56.3	57.7	55.1	54.8	51.9	46.2
EGFR16.M12	21:14:0.11	0.9	1825.0	70.5	45.7	45.5	48.1	56.0	59.1	53.7	61.2	63.5	57.7	51.2	52.1	50.0	51.8	46.7
EGFR16.M13	21:13:55.87	9.3	236.8	97.5	73.2	84.0	88.4	88.8	84.6	90.7	90.8	87.1	84.6	84.1	83.5	82.3	79.0	76.8
EGFR16.M14	21:13:55.88	8.9	239.6	98.4	83.0	87.3	89.4	89.0	89.2	90.0	91.2	89.3	84.8	77.0	79.9	84.1	85.1	82.7
EGFR16.M15	21:13:55.88	6.9	241.2	101.5	83.5	87.0	89.3	89.9	91.4	92.1	93.2	90.8	91.0	88.9	88.3	87.5	86.8	85.5
EGFR16.M16	21:13:55.54	53.1	46.6	100.1	93.6	90.3	90.7	89.0	88.1	83.4	81.8	84.9	91.6	87.1	84.8	83.9	86.1	83.2
EGFR16.M17	21:13:55.54	53.2	46.6	98.2	89.7	89.0	91.7	92.0	90.9	88.1	87.5	85.8	86.3	85.7	87.5	87.7	86.2	84.8
EGFR16.M18	21:13:59.66	1.5	1399.0	78.0	63.7	60.8	59.9	63.7	62.0	66.7	65.1	70.0	68.4	69.1	67.5	66.3	64.0	56.2
EGFR16.M19	21:14:0.38	1.3	1620.8	68.4	59.4	57.1	57.1	54.3	58.7	60.5	59.3	58.8	55.7	54.7	51.6	49.5	47.0	42.7
EGFR16.M20	21:14:2.14	1.2	1912.1	78.0	57.7	58.5	55.6	56.2	58.0	63.1	59.9	59.5	54.4	52.8	54.6	50.6	48.8	44.3

DIRECTIVITY ANGLE = 122.5 deg

1/3 OCTAVE BAND CENTER FREQUENCIES (kHz)

FILENAME	RECEIVE TIME	BETA (deg)	SR (m)	OSPL	0.10	0.13	0.16	0.20	0.25	0.32	0.40	0.50	0.63	0.79	1.0	1.3	1.6	2.0
EGFR17.M01	21:17:36.15	10.6	214.1	99.4	86.2	88.2	90.1	91.6	94.6	91.5	90.1	86.4	84.0	80.8	81.3	79.0	79.1	80.3
EGFR17.M02	21:17:36.16	10.1	216.8	99.1	82.3	85.8	88.7	88.3	90.2	84.8	81.5	87.2	90.2	90.1	87.9	88.3	83.7	78.5
EGFR17.M03	21:17:36.15	7.9	218.1	100.5	82.4	85.9	91.2	87.6	86.5	92.6	90.8	92.5	91.5	91.4	88.7	86.5	84.6	82.2
EGFR17.M04	21:17:36.82	5.0	433.0	90.3	74.4	73.5	72.0	72.3	73.0	71.0	75.4	79.1	80.3	80.9	82.5	80.5	77.2	71.0
EGFR17.M05	21:17:37.74	3.0	727.6	81.7	62.8	64.7	63.7	56.7	53.3	56.8	62.3	64.3	68.0	68.5	66.7	66.0	61.2	54.9
EGFR17.M06	21:17:37.91	2.5	883.6	75.6	61.8	63.0	61.5	53.4	50.8	56.4	63.0	64.6	64.8	64.9	62.6	64.7	64.8	62.7
EGFR17.M07	21:17:38.62	2.0	1109.3	77.1	68.4	64.8	65.4	63.8	63.6	63.8	60.1	59.9	59.1	61.6	63.2	63.2	58.5	55.0
EGFR17.M08	21:17:39.38	1.6	1351.0	78.5	67.0	68.5	59.6	59.0	55.0	54.1	60.8	64.8	61.6	60.3	63.2	61.3	65.2	61.4
EGFR17.M09	21:17:40.07	1.4	1571.1	71.8	56.3	57.5	56.0	52.5	51.3	52.4	57.4	59.1	56.8	57.5	55.0	55.8	54.1	49.8
EGFR17.M10	21:17:40.84	1.2	1815.7	68.7	52.7	51.9	50.9	51.7	49.4	52.9	52.8	48.7	46.1	46.1	43.4	43.0	41.9	39.7
EGFR17.M11	21:17:40.85	1.2	1818.7	64.4	53.2	46.7	47.4	47.9	45.3	49.0	51.4	52.5	50.0	53.9	53.3	52.7	50.7	46.7
EGFR17.M12	21:17:40.86	0.9	1821.6	71.3	40.7	47.5	51.0	55.1	57.8	53.7	60.2	62.7	62.7	57.3	54.2	52.1	49.4	44.1
EGFR17.M13	21:17:36.90	9.1	246.5	101.2	78.7	88.6	87.8	83.7	87.0	94.7	93.1	92.4	92.3	92.1	90.7	88.5	85.2	80.9
EGFR17.M14	21:17:36.91	8.7	249.2	99.9	83.5	89.2	87.4	89.5	88.2	90.4	87.9	78.8	86.3	90.7	92.4	86.2	84.8	84.6
EGFR17.M15	21:17:36.90	6.9	250.7	104.4	82.8	90.1	89.0	92.2	91.1	98.4	97.9	96.1	95.1	94.4	92.3	91.6	90.7	88.1
EGFR17.M16	21:17:36.50	56.9	45.2	118.3	94.2	95.7	88.7	96.0	109.0	114.0	110.0	105.3	108.4	104.2	104.3	103.6	103.9	101.7
EGFR17.M17	21:17:36.50	56.9	45.1	100.5	91.1	96.6	92.1	92.6	92.6	85.5	82.2	83.4	87.7	88.4	83.3	83.0	86.1	82.5
EGFR17.M18	21:17:40.50	1.5	1400.2	79.0	62.3	64.8	62.6	71.0	72.6	71.1	69.1	63.9	62.4	58.1	57.0	59.4	56.9	53.5
EGFR17.M19	21:17:41.19	1.3	1620.2	75.8	60.0	63.0	62.4	64.6	61.4	62.6	67.6	68.4	67.9	61.9	58.5	58.3	55.5	51.0
EGFR17.M20	21:17:41.98	1.2	1867.9	70.5	49.1	50.1	54.9	56.7	62.1	62.7	63.8	63.9	56.6	53.4	49.5	50.2	45.6	43.0

DIRECTIVITY ANGLE = 122.5 deg

1/3 OCTAVE BAND CENTER FREQUENCIES (kHz)

FILENAME	RECEIVE TIME	BETA (deg)	SR (m)	OSPL	0.10	0.13	0.16	0.20	0.25	0.32	0.40	0.50	0.63	0.79	1.0	1.3	1.6	2.0
EGFR18.M01	21:20:58.28	10.1	216.1	99.4	84.5	86.9	91.1	91.4	92.9	90.2	91.2	86.0	84.2	77.8	78.7	79.0	78.5	78.0
EGFR18.M02	21:20:58.29	9.6	218.9	100.5	86.0	87.7	87.7	88.8	91.7	88.6	84.7	84.9	91.1	90.6	90.4	88.2	86.7	81.7
EGFR18.M03	21:20:58.29	7.5	220.2	103.9	80.8	85.1	89.4	90.5	86.7	96.8	94.1	97.8	94.9	93.5	91.2	92.7	88.7	87.1
EGFR18.M04	21:20:58.96	4.8	435.3	94.3	74.7	74.6	74.3	73.7	74.3	72.3	79.3	83.8	84.3	86.4	86.9	86.3	80.7	72.4
EGFR18.M05	21:20:59.89	2.9	730.0	87.5	71.4	67.0	65.9	62.1	62.5	64.1	69.9	75.4	75.6	80.6	81.9	79.4	75.9	70.2
EGFR18.M06	21:21:0.06	2.4	886.2	85.2	62.2	65.8	66.2	61.5	65.3	65.0	72.6	72.0	76.2	77.4	74.0	72.8	70.0	67.8
EGFR18.M07	21:21:0.77	1.9	1112.0	76.7	62.1	64.4	62.5	63.0	64.0	62.6	61.9	63.4	65.1	65.3	65.6	66.7	60.5	57.8
EGFR18.M08	21:21:1.53	1.6	1353.8	83.1	65.0	71.3	64.5	60.8	56.1	56.2	58.8	64.3	66.4	65.8	68.6	66.5	65.3	59.6
EGFR18.M09	21:21:2.23	1.3	1573.9	75.3	54.6	58.2	56.6	52.6	54.4	54.9	57.2	60.3	61.2	60.0	61.2	57.3	54.5	50.8
EGFR18.M10	21:21:2.99	1.2	1818.6	68.3	52.6	53.8	53.5	50.9	51.6	50.0	53.3	50.1	45.9	46.3	45.9	45.9	41.8	39.8
EGFR18.M11	21:21:3.00	1.2	1821.6	66.9	50.5	50.7	49.6	44.8	43.4	46.4	49.6	54.6	53.8	53.0	51.7	52.6	49.9	45.2
EGFR18.M12	21:21:3.01	0.9	1824.5	71.7	44.1	50.5	56.0	50.6	57.0	60.9	64.7	63.5	62.2	56.9	55.4	55.8	46.7	45.3
EGFR18.M13	21:20:59.02	8.7	248.5	101.0	78.6	82.6	89.1	91.6	85.6	94.6	90.9	91.3	90.4	91.8	88.3	87.5	85.1	82.4
EGFR18.M14	21:20:59.04	8.3	251.3	100.6	85.4	89.0	87.4	92.2	92.0	91.8	91.7	90.0	82.6	76.9	84.7	89.0	87.4	84.1
EGFR18.M15	21:20:59.03	6.4	252.8	100.4	80.6	79.8	84.8	89.1	88.3	91.3	90.7	90.9	91.1	91.4	89.9	89.7	87.6	89.1
EGFR18.M16	21:20:58.60	57.0	43.0	112.1	94.4	97.5	92.6	86.9	97.3	105.0	106.7	103.7	102.5	104.2	99.6	99.0	97.3	96.7
EGFR18.M17	21:20:58.60	57.1	43.0	107.6	88.9	98.3	93.0	88.4	83.8	90.9	100.6	102.6	100.0	91.6	92.0	90.6	95.2	91.7
EGFR18.M18	21:21:2.65	1.5	1402.8	75.7	58.8	65.6	63.9	63.0	61.2	59.3	61.2	64.2	62.2	63.6	63.2	57.5	54.4	52.5
EGFR18.M19	21:21:3.34	1.3	1623.0	70.6	56.3	60.7	54.1	57.0	61.3	63.4	64.3	60.1	57.4	57.5	53.6	52.8	49.0	46.1
EGFR18.M20	21:21:4.12	1.1	1870.7	73.2	64.4	61.2	58.8	66.3	63.0	64.0	58.8	58.5	61.2	59.4	54.2	50.3	50.8	46.6

DIRECTIVITY ANGLE = 122.5 deg

1/3 OCTAVE BAND CENTER FREQUENCIES (kHz)

FILENAME	RECEIVE TIME	BETA (deg)	SR (m)	OSPL	0.10	0.13	0.16	0.20	0.25	0.32	0.40	0.50	0.63	0.79	1.0	1.3	1.6	2.0
EGFR19.M01	21:25:58.45	18.7	219.8	100.6	88.2	85.5	89.5	88.9	88.6	89.4	91.4	90.6	91.7	91.3	89.3	88.9	88.3	86.4
EGFR19.M02	21:25:58.45	18.1	222.1	101.1	85.3	84.4	83.2	77.8	81.7	89.8	93.8	94.2	91.7	89.1	91.6	91.1	85.9	85.3
EGFR19.M03	21:25:58.43	16.0	221.8	103.4	86.3	82.2	91.1	87.5	93.6	94.8	95.5	94.9	93.2	95.1	91.6	90.7	88.3	84.4
EGFR19.M04	21:25:59.09	9.2	433.4	91.1	78.2	77.1	77.1	71.4	71.8	76.1	81.0	84.8	84.3	83.6	78.3	72.9	74.5	70.7
EGFR19.M05	21:26: 0.00	5.5	726.5	80.8	67.7	70.5	64.3	64.7	65.6	61.7	62.9	66.9	71.5	72.9	69.0	69.2	61.4	60.1
EGFR19.M06	21:26: 0.19	4.5	882.5	84.8	64.2	68.4	64.4	63.5	63.7	59.8	62.6	65.4	68.9	69.6	68.7	67.8	64.6	60.1
EGFR19.M07	21:26: 0.90	3.6	1108.2	80.0	66.7	68.2	71.2	70.6	72.5	66.3	67.6	68.6	69.7	71.1	64.2	65.4	67.1	60.1
EGFR19.M08	21:26: 1.67	2.9	1350.2	78.9	63.1	63.6	63.7	62.9	62.4	58.8	64.0	64.9	67.2	69.1	69.0	68.1	67.5	59.6
EGFR19.M09	21:26: 2.37	2.5	1570.5	73.6	58.4	54.0	55.0	53.4	57.5	56.3	61.4	62.7	61.2	62.7	59.9	59.7	57.0	51.9
EGFR19.M10	21:26: 3.15	2.2	1815.6	69.1	59.5	54.4	56.8	57.7	56.9	57.5	57.6	50.0	51.8	48.9	48.9	48.3	46.5	39.7
EGFR19.M11	21:26: 3.16	2.2	1818.6	66.9	59.1	53.0	55.0	48.8	51.6	51.4	53.4	53.4	58.0	56.7	55.3	52.9	51.0	44.6
EGFR19.M12	21:26: 3.16	1.9	1821.3	75.5	51.4	51.4	56.6	56.6	55.8	61.8	57.8	55.6	56.6	53.7	51.9	50.4	45.4	40.4
EGFR19.M13	21:25:59.16	16.4	250.6	102.1	77.4	84.3	90.3	88.2	93.5	92.2	92.1	93.8	92.8	92.9	92.0	92.5	89.2	85.6
EGFR19.M14	21:25:59.17	15.9	253.0	100.0	78.8	84.1	88.5	89.0	90.2	88.5	85.0	85.4	90.2	93.9	90.9	81.2	85.2	80.5
EGFR19.M15	21:25:59.16	14.0	253.1	96.7	72.3	80.0	79.4	78.8	85.5	86.1	88.2	90.1	89.6	87.6	85.5	84.8	83.3	79.2
EGFR19.M16	21:25:59.05	56.9	82.9	112.7	85.0	82.3	89.1	100.9	103.7	104.4	99.1	104.7	103.7	103.6	99.6	99.7	97.4	97.3
EGFR19.M17	21:25:59.05	57.0	82.9	107.6	96.0	91.2	81.8	86.9	94.1	100.5	101.2	94.0	100.3	96.9	92.8	88.9	90.4	92.1
EGFR19.M18	21:26: 2.77	2.8	1398.9	81.4	60.0	67.5	73.4	71.2	76.8	74.0	64.7	67.3	64.4	63.5	60.1	57.9	54.6	50.9
EGFR19.M19	21:26: 3.47	2.5	1619.3	81.1	61.8	64.4	69.8	68.4	71.8	69.6	65.2	64.1	62.9	61.3	60.7	57.5	55.7	51.2
EGFR19.M20	21:26: 4.26	2.1	1867.4	73.0	58.7	63.0	66.1	59.9	62.8	65.4	59.4	61.7	57.9	58.8	55.4	48.9	47.9	45.6

APPENDIX C

DIRECTIVITY ANGLE = 122.5 deg

1/3 OCTAVE BAND CENTER FREQUENCIES (kHz)

FILENAME	RECEIVE TIME	BETA (deg)	SR (m)	OSPL	0.10	0.13	0.16	0.20	0.25	0.32	0.40	0.50	0.63	0.79	1.0	1.3	1.6	2.0
EGFR20.M01	21:29:40.24	21.9	228.6	100.6	85.6	86.9	90.1	88.4	90.2	87.0	88.5	90.6	92.1	90.0	86.2	86.1	85.2	86.5
EGFR20.M02	21:29:40.24	21.4	230.8	99.3	84.5	85.4	83.3	78.6	81.9	86.4	92.6	94.0	93.8	84.3	85.6	85.6	81.8	84.1
EGFR20.M03	21:29:40.22	19.4	229.7	102.4	83.0	79.0	89.4	88.4	92.6	90.9	93.1	96.0	93.2	91.9	90.6	91.1	87.3	85.7
EGFR20.M04	21:29:40.84	11.1	438.3	89.3	75.9	78.9	75.3	72.8	72.5	75.6	79.1	83.3	82.8	80.8	76.0	73.3	70.9	69.5
EGFR20.M05	21:29:41.73	6.6	729.5	82.1	67.6	66.1	66.8	63.5	65.4	69.8	69.5	70.5	74.4	70.8	67.5	67.6	65.4	59.8
EGFR20.M06	21:29:41.91	5.4	884.7	81.7	62.7	65.5	64.1	66.3	64.0	66.4	66.4	67.2	69.3	69.0	71.1	69.5	66.0	59.1
EGFR20.M07	21:29:42.61	4.3	1109.7	82.2	69.9	68.8	71.7	68.3	69.7	69.5	70.2	67.8	71.1	71.8	69.8	72.0	68.7	64.6
EGFR20.M08	21:29:43.37	3.6	1350.9	86.1	64.5	62.5	59.2	61.6	62.3	71.6	76.2	77.5	79.3	79.2	77.1	75.7	69.4	59.0
EGFR20.M09	21:29:44.05	3.1	1570.7	69.8	58.0	56.9	52.8	51.1	50.4	53.4	55.8	57.9	58.9	57.8	55.5	55.5	53.7	49.6
EGFR20.M10	21:29:44.83	2.7	1815.2	66.4	57.2	56.3	58.9	55.8	51.2	54.2	49.3	50.8	50.7	51.7	48.2	47.9	45.9	40.6
EGFR20.M11	21:29:44.84	2.7	1818.2	65.9	53.4	52.4	54.4	50.6	45.8	48.3	49.3	53.0	57.9	58.7	56.8	56.6	51.6	45.9
EGFR20.M12	21:29:44.84	2.4	1820.9	70.7	44.0	48.8	58.3	59.0	57.9	63.7	65.3	62.2	57.0	55.8	54.2	54.5	51.2	42.6
EGFR20.M13	21:29:40.95	19.4	258.9	102.3	81.4	80.9	91.3	88.9	92.9	92.2	93.1	93.2	93.3	92.0	91.3	90.0	86.6	83.1
EGFR20.M14	21:29:40.96	18.9	261.2	102.7	84.6	87.7	85.7	86.0	80.6	85.4	93.2	97.5	96.6	90.0	91.9	90.9	87.4	85.0
EGFR20.M15	21:29:40.94	17.1	260.7	95.8	75.6	79.5	80.4	83.4	83.9	85.2	86.8	87.1	86.6	87.8	85.6	83.9	82.1	80.7
EGFR20.M16	21:29:40.94	57.7	100.5	107.1	82.2	87.1	83.2	82.9	93.2	101.0	101.2	97.1	96.0	95.9	91.9	92.1	91.7	90.4
EGFR20.M17	21:29:40.94	57.7	100.4	107.0	84.5	87.2	82.8	83.1	93.0	101.5	102.1	96.6	96.4	97.1	93.6	91.0	91.6	90.1
EGFR20.M18	21:29:44.47	3.5	1399.9	85.9	67.5	70.7	71.1	75.7	76.2	77.0	77.5	75.2	75.0	68.9	65.1	62.1	59.7	56.9
EGFR20.M19	21:29:45.16	3.0	1619.8	80.0	66.2	67.7	68.9	72.0	74.3	74.7	68.5	66.5	64.7	60.1	59.2	58.8	55.7	49.3
EGFR20.M20	21:29:45.93	2.6	1867.3	78.7	64.7	67.2	68.2	70.0	73.1	72.3	65.9	62.9	65.9	62.6	54.4	52.9	50.0	47.7

DIRECTIVITY ANGLE = 122.5 deg

1/3 OCTAVE BAND CENTER FREQUENCIES (kHz)

FILENAME	RECEIVE TIME	BETA (deg)	SR (m)	OSPL	0.10	0.13	0.16	0.20	0.25	0.32	0.40	0.50	0.63	0.79	1.0	1.3	1.6	2.0
EGFR21.M01	21:33:13.89	20.4	219.5	100.8	81.0	85.3	90.5	90.9	88.9	88.2	92.4	92.0	92.3	91.1	86.9	84.2	85.8	83.8
EGFR21.M02	21:33:13.89	19.9	221.8	99.9	82.3	80.8	84.6	81.1	83.4	87.6	95.5	95.5	92.9	84.5	86.3	84.2	82.8	82.5
EGFR21.M03	21:33:13.87	17.8	221.0	103.4	83.0	78.9	90.8	88.6	92.5	92.8	94.1	93.9	94.6	95.9	92.7	91.7	88.5	86.6
EGFR21.M04	21:33:14.55	13.0	432.8	96.5	75.8	77.1	80.9	76.3	76.1	81.4	87.7	91.0	89.9	87.9	83.7	82.2	81.4	78.4
EGFR21.M05	21:33:15.51	6.0	727.2	83.4	63.8	66.5	67.4	66.3	65.9	63.0	67.1	70.3	69.2	66.0	66.0	67.0	72.4	66.0
EGFR21.M06	21:33:15.71	4.9	884.5	85.9	66.9	65.1	69.1	66.3	68.5	69.4	71.6	76.0	79.1	78.8	79.0	76.1	72.7	67.1
EGFR21.M07	21:33:16.46	3.9	1111.6	79.0	66.2	68.8	69.6	66.8	67.5	59.3	62.6	65.6	66.8	69.9	69.4	67.5	66.0	60.0
EGFR21.M08	21:33:17.27	3.2	1355.0	87.7	64.8	65.3	67.9	64.1	69.8	70.7	73.2	77.8	79.6	81.1	80.1	78.7	74.3	65.8
EGFR21.M09	21:33:17.99	2.7	1576.8	71.8	58.5	56.8	56.6	52.1	55.7	57.9	60.3	61.9	62.8	61.9	61.8	57.3	55.1	49.0
EGFR21.M10	21:33:18.81	2.4	1823.4	65.3	52.4	52.5	51.9	55.3	51.8	51.8	50.7	51.5	49.8	46.8	45.9	43.8	41.9	38.7
EGFR21.M11	21:33:18.82	2.4	1826.4	64.8	51.9	49.4	51.2	48.5	48.5	48.8	50.9	54.1	56.4	57.5	54.6	51.7	50.6	44.5
EGFR21.M12	21:33:18.83	2.1	1829.1	73.8	52.2	52.3	60.6	61.8	63.3	59.6	61.3	63.6	60.8	61.3	58.1	57.3	52.7	47.2
EGFR21.M13	21:33:14.62	17.9	249.3	102.2	78.2	79.6	89.6	85.5	92.9	92.3	92.5	95.1	95.6	93.7	89.8	89.0	88.6	86.0
EGFR21.M14	21:33:14.62	17.5	251.7	100.0	84.4	83.4	84.8	80.9	77.9	87.4	92.4	94.8	92.1	86.1	92.8	84.3	86.4	82.2
EGFR21.M15	21:33:14.60	15.6	251.5	94.9	75.5	78.4	79.6	84.5	83.6	86.6	85.2	85.9	86.0	85.7	83.4	79.8	78.4	74.6
EGFR21.M16	21:33:14.55	56.2	91.1	111.0	87.1	82.8	85.1	94.3	101.6	104.1	98.3	101.8	104.6	99.9	97.5	98.7	98.4	94.7
EGFR21.M17	21:33:14.55	56.2	91.0	98.8	90.0	87.0	86.8	84.2	76.1	81.4	90.1	94.0	91.9	83.3	83.3	81.1	86.3	82.0
EGFR21.M18	21:33:18.38	3.1	1402.9	80.5	68.1	69.3	72.1	70.3	67.1	68.1	68.6	70.6	70.4	63.6	60.8	60.6	58.1	52.5
EGFR21.M19	21:33:19.10	2.7	1624.7	81.4	64.0	68.9	72.2	71.9	74.1	75.9	75.6	66.5	64.1	63.4	58.0	58.6	58.0	51.6
EGFR21.M20	21:33:19.93	2.3	1874.3	77.4	62.3	65.0	67.6	71.9	70.6	69.6	66.3	62.7	59.4	60.0	56.9	55.0	50.3	46.1

DIRECTIVITY ANGLE = 122.5 deg

1/3 OCTAVE BAND CENTER FREQUENCIES (kHz)

FILENAME	RECEIVE TIME	BETA (deg)	SR (m)	OSPL	0.10	0.13	0.16	0.20	0.25	0.32	0.40	0.50	0.63	0.79	1.0	1.3	1.6	2.0
EGFR22.M01	21:36:49.55	34.7	264.3	99.3	78.1	83.8	88.0	87.3	88.8	89.6	89.4	88.9	91.0	87.4	85.6	83.2	82.7	82.2
EGFR22.M02	21:36:49.55	34.1	265.7	98.5	78.2	76.8	78.3	85.1	91.0	94.2	92.1	85.1	90.1	83.5	83.3	80.5	79.8	77.9
EGFR22.M03	21:36:49.52	32.6	262.0	101.0	78.6	89.9	89.1	91.1	90.9	91.7	92.0	92.5	93.1	89.0	86.5	86.4	83.4	80.2
EGFR22.M04	21:36:50.02	19.1	454.7	93.8	73.1	75.6	72.0	76.0	78.5	85.5	87.7	85.6	78.4	84.6	82.0	79.7	78.3	76.4
EGFR22.M05	21:36:50.88	11.6	738.5	83.1	67.6	69.3	67.4	64.3	67.3	74.2	77.0	75.4	71.6	69.0	67.9	68.5	66.9	62.0
EGFR22.M06	21:36:51.08	9.6	892.7	86.3	68.7	70.8	71.9	67.5	69.0	74.5	78.2	79.9	77.5	73.2	69.8	70.7	63.9	65.3
EGFR22.M07	21:36:51.79	7.7	1117.0	82.3	62.0	70.3	68.4	65.3	59.4	66.1	69.4	72.8	76.4	75.1	68.3	62.8	66.4	58.3
EGFR22.M08	21:36:52.58	6.3	1358.4	77.9	62.0	63.3	65.2	64.3	68.6	67.2	67.1	71.4	71.1	69.8	66.6	61.9	57.0	53.6
EGFR22.M09	21:36:53.29	5.4	1578.7	74.4	58.1	60.1	60.0	57.3	53.9	55.5	58.7	62.2	60.8	62.9	58.4	55.7	51.2	47.8
EGFR22.M10	21:36:54.05	5.0	1838.9	69.8	58.6	60.5	62.1	61.9	59.7	57.6	55.7	56.0	57.7	55.3	49.5	49.2	46.1	41.7
EGFR22.M11	21:36:54.06	5.0	1841.9	68.9	57.4	56.2	57.0	55.6	54.0	51.2	54.9	57.4	60.3	62.7	57.6	56.0	49.1	42.7
EGFR22.M12	21:36:54.07	4.7	1844.1	75.2	58.5	62.1	65.5	67.2	65.5	66.0	64.7	61.4	59.2	59.9	57.8	57.7	52.8	46.4
EGFR22.M13	21:36:50.22	31.4	289.7	100.4	78.9	79.8	86.0	86.8	91.1	90.1	90.4	94.0	90.0	89.3	88.7	88.4	86.2	84.8
EGFR22.M14	21:36:50.23	31.0	291.3	99.5	69.9	69.5	82.9	90.2	93.0	91.5	86.3	92.5	87.3	89.1	86.4	85.5	83.4	81.5
EGFR22.M15	21:36:50.18	29.5	288.2	92.4	71.7	77.6	81.5	81.5	80.4	83.6	83.4	82.6	83.0	81.8	79.2	78.0	76.6	75.7
EGFR22.M16	21:36:50.53	57.7	178.3	107.5	73.8	84.7	94.0	95.6	97.5	93.3	100.3	95.0	100.7	98.7	96.4	96.2	95.1	92.0
EGFR22.M17	21:36:50.53	57.7	178.3	104.5	84.4	77.8	84.6	93.2	95.0	96.6	90.8	99.8	94.7	93.8	91.0	90.2	87.4	87.4
EGFR22.M18	21:36:53.64	6.1	1406.2	79.1	65.8	70.1	70.8	69.3	68.5	65.8	67.1	63.5	63.0	62.7	62.0	59.1	57.5	50.8
EGFR22.M19	21:36:54.36	5.3	1626.6	77.3	63.2	61.7	62.1	66.1	67.8	70.4	70.2	66.4	59.7	57.6	58.5	55.2	55.9	47.2
EGFR22.M20	21:36:55.17	4.6	1875.1	78.8	63.3	63.0	65.5	69.3	70.0	70.9	70.2	69.5	63.4	62.6	64.6	60.3	54.4	49.4

DIRECTIVITY ANGLE = 122.5 deg

1/3 OCTAVE BAND CENTER FREQUENCIES (kHz)

FILENAME	RECEIVE TIME	BETA (deg)	SR (m)	OSPL	0.10	0.13	0.16	0.20	0.25	0.32	0.40	0.50	0.63	0.79	1.0	1.3	1.6	2.0
EGFR23.M01	21:40:12.57	33.0	256.7	99.7	82.7	86.3	88.6	88.3	89.7	91.6	92.2	91.7	91.2	86.9	85.6	84.0	82.2	81.9
EGFR23.M02	21:40:12.56	32.5	258.2	99.9	82.9	78.1	75.6	81.3	89.1	94.6	91.5	88.0	91.2	88.7	86.6	83.1	81.9	79.3
EGFR23.M03	21:40:12.52	30.9	254.8	101.0	78.5	88.0	88.2	89.0	89.6	93.6	93.7	94.1	91.7	88.6	86.5	83.6	82.9	81.2
EGFR23.M04	21:40:13.08	17.9	451.5	94.1	72.0	73.5	70.6	70.9	76.8	85.9	89.3	85.4	79.8	84.0	77.3	79.3	75.6	73.7
EGFR23.M05	21:40:13.99	10.8	738.5	83.0	70.0	66.7	66.1	65.0	69.3	71.2	75.1	78.5	74.4	71.1	71.4	72.4	65.0	61.6
EGFR23.M06	21:40:14.20	8.9	894.4	88.4	70.7	69.5	73.0	68.0	73.4	79.4	82.8	81.3	79.2	73.2	73.4	75.7	70.1	67.0
EGFR23.M07	21:40:14.95	7.1	1120.2	80.2	68.9	71.7	72.2	69.3	59.9	65.9	71.8	69.7	69.9	67.6	65.1	59.1	56.3	53.3
EGFR23.M08	21:40:15.77	5.8	1363.1	81.5	63.4	61.1	62.0	60.2	62.0	70.4	74.1	75.9	75.7	74.7	71.3	64.7	63.0	61.4
EGFR23.M09	21:40:16.51	5.0	1584.8	73.6	62.8	63.5	63.9	59.9	62.5	62.6	64.0	62.6	65.5	64.9	60.6	57.4	55.4	47.8
EGFR23.M10	21:40:17.34	4.4	1831.6	69.9	57.2	62.3	60.9	61.2	59.8	59.1	58.5	56.3	56.8	57.3	52.8	50.4	45.2	41.5
EGFR23.M11	21:40:17.35	4.3	1834.6	68.5	57.9	58.7	57.0	55.8	55.3	53.2	55.9	57.9	60.4	61.2	56.7	51.0	46.4	42.5
EGFR23.M12	21:40:17.36	4.1	1836.9	75.2	57.3	66.1	67.9	67.1	64.3	66.9	65.5	61.8	59.9	61.2	57.0	53.3	50.6	44.4
EGFR23.M13	21:40:13.26	29.8	282.0	101.8	81.9	84.6	91.1	86.6	87.1	92.3	93.1	94.4	91.1	90.1	90.0	87.9	86.2	80.5
EGFR23.M14	21:40:13.26	29.3	283.7	99.3	74.1	67.9	81.9	88.5	95.5	90.5	84.0	90.4	89.0	89.0	85.3	83.6	80.2	80.0
EGFR23.M15	21:40:13.22	27.8	281.0	93.2	76.9	76.9	77.2	80.0	82.5	87.2	85.9	84.6	84.7	82.5	79.9	79.6	77.1	72.8
EGFR23.M16	21:40:13.53	57.0	166.0	108.8	72.3	84.2	92.2	95.5	99.0	93.2	103.3	99.3	101.7	99.8	96.5	95.1	94.4	89.9
EGFR23.M17	21:40:13.53	57.1	166.0	108.1	72.7	82.4	86.3	97.5	99.0	91.8	99.4	98.7	100.0	98.0	95.6	93.9	94.3	91.8
EGFR23.M18	21:40:16.86	5.7	1410.2	81.8	66.7	71.0	76.6	72.2	74.0	74.9	74.4	72.0	61.1	60.0	61.9	67.5	59.5	54.6
EGFR23.M19	21:40:17.62	4.9	1632.0	78.6	58.6	65.8	72.0	72.5	71.0	67.2	66.3	67.4	66.3	56.7	58.4	62.3	57.4	49.6
EGFR23.M20	21:40:18.46	4.2	1881.9	83.2	71.0	74.7	77.8	74.5	71.0	72.1	75.5	69.2	63.5	63.5	62.0	59.7	57.5	51.2

DIRECTIVITY ANGLE = 122.5 deg

1/3 OCTAVE BAND CENTER FREQUENCIES (kHz)

FILENAME	RECEIVE TIME	BETA (deg)	SR (m)	OSPL	0.10	0.13	0.16	0.20	0.25	0.32	0.40	0.50	0.63	0.79	1.0	1.3	1.6	2.0
EGFR24.M01	21:43:27.49	32.9	270.2	102.6	81.4	81.4	89.8	89.8	92.3	93.9	95.5	91.9	91.9	91.3	90.1	90.7	88.9	89.1
EGFR24.M02	21:43:27.48	32.4	271.6	99.9	79.6	75.6	73.3	85.6	91.8	94.1	94.6	88.5	89.6	86.2	86.0	84.9	82.2	80.9
EGFR24.M03	21:43:27.44	30.8	268.3	100.3	79.6	86.8	84.3	88.4	88.7	94.8	93.1	91.7	90.4	88.6	85.6	86.7	83.9	81.5
EGFR24.M04	21:43:27.94	18.3	461.9	94.6	76.7	75.9	72.7	69.8	78.8	90.4	88.5	86.9	81.3	85.3	78.3	81.5	75.2	73.2
EGFR24.M05	21:43:28.75	11.3	744.2	87.3	66.2	67.5	71.8	66.7	69.8	74.0	78.2	82.7	82.3	77.4	73.3	73.7	69.1	63.9
EGFR24.M06	21:43:28.90	9.3	896.7	86.8	62.3	68.7	68.5	66.6	66.8	75.4	80.9	78.7	80.7	76.9	74.1	77.1	73.1	67.5
EGFR24.M07	21:43:29.58	7.4	1119.1	79.6	67.7	72.2	67.9	66.1	60.9	62.5	66.3	71.2	70.5	70.6	62.9	58.7	58.4	51.3
EGFR24.M28	21:43:30.31	6.1	1358.5	78.4	61.6	66.1	64.5	61.1	60.6	65.5	66.8	71.4	71.9	72.5	67.3	62.2	64.6	57.5
EGFR24.M09	21:43:30.98	5.3	1576.9	73.0	61.7	61.8	59.0	59.7	57.7	57.7	59.9	64.0	63.5	66.6	62.8	60.5	54.9	49.4
EGFR24.M10	21:43:31.74	4.6	1820.3	76.0	61.0	63.4	63.8	62.9	65.0	68.1	67.4	66.4	66.2	65.8	64.7	60.2	53.9	45.8
EGFR24.M11	21:43:31.75	4.6	1823.2	78.4	56.5	60.7	58.6	55.3	57.3	59.7	69.1	69.6	73.1	72.8	67.4	60.1	57.2	49.7
EGFR24.M12	21:43:31.76	4.3	1825.5	79.4	60.1	67.7	68.0	69.4	65.0	70.8	75.1	66.5	67.8	62.2	60.1	55.9	52.2	49.9
EGFR24.M13	21:43:28.16	29.7	296.9	99.0	85.4	84.5	86.1	89.3	88.9	88.6	91.5	90.3	88.7	87.1	87.4	86.7	84.9	81.0
EGFR24.M14	21:43:28.15	29.3	298.6	99.7	80.3	76.4	70.9	82.9	90.0	91.8	92.6	83.7	90.0	86.1	89.8	89.4	86.8	85.4
EGFR24.M15	21:43:28.11	27.8	295.8	103.3	85.5	85.9	91.2	92.0	93.6	97.5	95.9	94.2	91.7	94.4	93.0	91.5	90.2	88.4
EGFR24.M16	21:43:28.38	58.2	172.8	104.0	78.1	72.8	81.0	91.2	96.0	99.1	94.8	92.4	97.5	90.1	90.9	89.9	87.9	87.3
EGFR24.M17	21:43:28.38	58.2	172.8	98.4	82.6	83.5	75.5	74.2	74.7	87.1	93.1	93.6	85.3	90.3	83.3	82.4	77.9	79.4
EGFR24.M18	21:43:31.38	6.0	1407.5	84.8	68.3	70.1	74.1	79.0	77.3	76.1	74.6	75.1	73.2	65.6	61.5	59.1	61.6	54.3
EGFR24.M19	21:43:32.05	5.2	1626.1	78.7	63.3	64.1	66.3	66.5	70.6	70.9	72.7	68.7	66.6	59.1	56.7	54.5	51.9	45.5
EGFR24.M20	21:43:32.81	4.5	1872.4	82.4	69.6	70.7	75.5	72.4	75.0	74.6	71.5	68.2	67.6	63.3	64.9	68.3	62.7	53.3

DIRECTIVITY ANGLE = 122.5 deg

1/3 OCTAVE BAND CENTER FREQUENCIES (kHz)

FILENAME	RECEIVE TIME	BETA (deg)	SR (m)	OSPL	0.10	0.13	0.16	0.20	0.25	0.32	0.40	0.50	0.63	0.79	1.0	1.3	1.6	2.0
EGFR25.M01	21:48:19.00	1.9	283.2	79.3	68.3	74.0	67.5	67.3	67.5	64.3	57.7	57.3	54.8	53.4	53.8	51.8	53.4	51.0
EGFR25.M02	21:48:19.02	1.6	286.3	76.1	64.8	65.8	66.2	62.7	56.9	55.0	56.7	57.5	56.0	57.9	55.5	54.8	54.4	52.2
EGFR25.M03	21:48:19.02	0.1	289.3	95.2	80.2	80.5	79.9	81.1	80.3	83.5	85.3	86.5	84.8	82.7	85.1	85.8	85.3	80.2
EGFR25.M04	21:48:19.81	0.9	510.1	80.5	70.5	65.4	67.4	68.0	62.9	63.4	64.2	70.2	67.9	64.3	62.6	65.6	68.1	61.2
EGFR25.M05	21:48:20.98	0.6	812.9	96.3	78.1	80.6	76.5	70.4	73.0	73.3	80.2	85.0	87.6	88.9	89.3	89.3	83.9	76.1
EGFR25.M06	21:48:21.20	0.5	974.6	96.4	77.1	81.0	76.1	69.7	71.5	74.0	80.8	84.9	88.0	88.8	89.9	88.6	79.2	70.7
EGFR25.M07	21:48:22.02	0.4	1206.1	70.7	56.1	63.6	54.1	51.6	50.5	45.4	48.8	53.3	53.8	56.6	57.7	55.2	50.7	47.5
EGFR25.M08	21:48:22.91	0.3	1454.0	68.7	47.4	45.9	44.8	46.0	43.7	50.8	55.5	62.2	58.5	58.4	58.4	63.4	57.9	46.3
EGFR25.M09	21:48:19.68	0.3	1513.8	69.7	53.8	48.0	46.5	45.3	43.1	44.7	49.7	54.1	56.8	57.4	55.7	55.8	50.2	43.7
EGFR25.M10	21:48:19.55	0.3	1731.9	68.1	46.8	41.3	46.6	50.5	46.2	54.8	60.1	55.8	54.8	51.8	48.7	50.0	42.8	39.4
EGFR25.M11	21:48:19.54	0.3	1734.6	67.1	46.2	42.0	43.1	42.3	48.2	51.7	52.5	53.4	59.4	62.1	55.9	50.7	44.7	41.4
EGFR25.M12	21:48:19.55	0.0	1737.4	73.4	44.9	45.3	45.7	54.7	55.7	61.4	66.0	64.5	68.0	60.5	58.5	55.5	47.0	44.2
EGFR25.M13	21:48:19.70	1.7	314.0	91.8	72.3	71.1	73.9	75.9	81.8	81.1	82.8	82.0	83.5	82.8	79.5	80.5	79.1	74.4
EGFR25.M14	21:48:19.71	1.5	317.1	88.3	78.1	79.4	77.8	76.6	75.1	77.1	72.3	73.6	70.6	71.4	70.7	73.2	73.4	71.6
EGFR25.M15	21:48:19.72	0.0	320.1	86.8	76.1	74.7	73.9	75.1	76.8	76.7	77.4	73.9	69.7	68.9	69.1	71.3	72.7	67.3
EGFR25.M16	21:48:18.80	7.5	62.0	98.0	85.0	84.0	82.6	84.6	85.6	87.0	92.9	89.9	86.8	84.0	85.1	84.1	81.8	81.1
EGFR25.M17	21:48:18.80	7.5	62.2	98.1	88.9	87.9	85.5	86.9	87.6	87.9	89.5	92.1	91.6	87.7	85.7	86.1	86.1	84.9
EGFR25.M18	21:48:23.95	0.3	1499.7	67.6	53.1	49.5	51.9	55.5	53.6	54.7	54.5	57.6	56.3	52.3	51.4	46.2	45.4	41.1
EGFR25.M19	21:48:24.77	0.3	1725.3	73.1	49.8	48.4	47.3	54.5	64.1	63.6	61.2	62.0	64.4	58.8	56.0	50.8	46.7	45.2
EGFR25.M20	21:48:25.67	0.2	1979.1	67.9	46.0	51.6	53.0	54.2	63.2	58.4	56.0	57.1	53.0	46.5	46.8	43.6	42.2	37.6

DIRECTIVITY ANGLE = 122.5 deg

1/3 OCTAVE BAND CENTER FREQUENCIES (kHz)

FILENAME	RECEIVE TIME	BETA (deg)	SR (m)	OSPL	0.10	0.13	0.16	0.20	0.25	0.32	0.40	0.50	0.63	0.79	1.0	1.3	1.6	2.0
EGFR26.M01	21:52:21.06	2.8	213.8	95.1	86.5	82.1	81.2	82.6	81.9	84.7	87.5	83.2	79.3	74.4	73.9	73.9	72.1	71.0
EGFR26.M02	21:52:21.08	2.4	216.8	97.0	86.9	83.0	80.8	81.1	80.0	81.3	84.2	82.8	84.0	83.3	85.3	84.3	85.6	84.9
EGFR26.M03	21:52:21.09	0.3	219.6	100.6	84.7	79.6	82.3	87.2	90.8	93.6	95.2	91.3	84.5	89.8	84.2	88.2	85.0	80.5
EGFR26.M04	21:52:21.77	1.2	435.3	85.5	79.2	78.2	70.0	62.5	57.1	59.1	68.9	67.3	72.8	77.0	76.2	75.2	74.4	69.5
EGFR26.M05	21:52:22.70	0.7	730.9	78.1	55.5	59.8	50.1	50.5	52.5	56.2	64.0	67.5	71.8	74.0	68.9	69.2	60.5	56.7
EGFR26.M06	21:52:22.87	0.6	887.3	78.9	55.6	61.6	54.1	52.6	50.5	56.9	64.0	67.6	69.7	73.8	71.8	69.5	65.2	58.6
EGFR26.M07	21:52:23.59	0.5	1113.3	72.8	61.7	59.7	55.4	52.8	54.1	52.6	52.1	54.8	59.6	64.2	64.4	57.5	59.1	52.1
EGFR26.M08	21:52:24.35	0.4	1355.3	70.3	49.6	53.4	45.9	47.6	45.2	49.7	56.8	59.9	63.3	64.9	60.6	58.7	52.7	45.1
EGFR26.M09	21:52:25.05	0.3	1575.6	66.1	47.8	54.4	48.9	48.4	43.4	48.9	52.7	53.7	56.0	58.8	56.5	56.3	52.6	45.7
EGFR26.M10	21:52:25.82	0.3	1820.3	63.9	45.0	50.6	48.1	51.8	48.6	50.3	54.0	48.9	49.6	50.5	45.2	48.3	43.1	38.2
EGFR26.M11	21:52:25.83	0.3	1823.4	65.2	44.6	48.6	44.5	43.1	41.6	44.4	52.6	52.4	54.8	60.7	54.7	56.9	47.1	36.9
EGFR26.M12	21:52:25.84	0.0	1826.5	72.8	46.0	54.7	59.5	59.1	59.3	60.4	63.1	64.0	64.5	66.0	57.0	52.3	48.1	44.7
EGFR26.M13	21:52:21.84	2.4	246.8	97.6	80.4	79.0	79.3	84.2	84.7	86.6	89.7	90.1	87.5	86.2	83.2	87.8	82.2	81.7
EGFR26.M14	21:52:21.85	2.1	249.8	100.1	80.4	84.2	86.9	87.8	91.9	93.8	92.1	90.5	87.3	87.1	82.1	77.7	74.7	80.0
EGFR26.M15	21:52:21.86	0.3	252.6	102.1	79.4	87.9	90.1	88.0	90.9	95.1	94.2	92.3	89.2	89.3	90.6	89.5	90.5	88.2
EGFR26.M16	21:52:21.16	57.6	11.1	126.6	98.4	105.2	104.6	108.7	115.6	121.3	118.9	115.4	114.9	112.3	111.4	113.3	111.7	110.0
EGFR26.M17	21:52:21.16	57.6	11.1	102.5	94.9	92.9	94.4	95.0	92.9	90.2	89.1	88.8	89.9	88.0	88.5	88.1	86.9	86.3
EGFR26.M18	21:52:25.50	0.4	1404.4	76.8	64.3	67.6	68.6	63.3	66.3	67.6	69.1	66.4	62.7	62.3	57.0	55.4	58.1	51.8
EGFR26.M19	21:52:26.20	0.3	1624.6	73.2	62.8	62.0	61.0	60.4	60.6	64.9	63.0	63.6	63.6	62.3	53.4	52.6	51.6	47.5
EGFR26.M20	21:52:26.98	0.3	1872.5	70.5	60.5	54.5	54.4	57.5	60.6	60.1	62.0	62.6	61.4	56.0	51.6	50.3	48.0	41.9

APPENDIX C

DIRECTIVITY ANGLE = 122.5 deg

1/3 OCTAVE BAND CENTER FREQUENCIES (kHz)

FILENAME	RECEIVE TIME	BETA (deg)	SR (m)	OSPL	0.10	0.13	0.16	0.20	0.25	0.32	0.40	0.50	0.63	0.79	1.0	1.3	1.6	2.0
EGFR27.M01	21:55:43.57	6.3	215.5	98.7	78.2	83.0	87.0	91.0	93.5	93.9	90.8	85.3	79.0	75.8	76.4	74.9	76.0	76.8
EGFR27.M02	21:55:43.58	5.9	218.3	97.3	81.7	82.1	82.9	89.3	89.4	88.9	85.0	82.2	83.2	83.4	85.9	85.6	83.8	79.7
EGFR27.M03	21:55:43.58	3.8	220.5	102.3	80.6	80.7	79.5	89.9	95.6	97.0	95.0	88.3	92.2	88.5	86.1	86.6	86.7	84.0
EGFR27.M04	21:55:44.24	3.0	435.4	91.6	74.0	70.7	67.9	66.7	68.9	68.7	75.9	82.0	83.7	82.1	84.1	83.9	81.6	75.4
EGFR27.M05	21:55:45.14	1.8	729.7	77.0	56.1	60.9	59.9	56.4	56.4	58.8	66.9	69.1	70.3	68.2	68.4	68.7	61.4	56.6
EGFR27.M06	21:55:45.31	1.4	885.2	76.2	59.2	59.8	58.9	57.4	55.8	57.9	65.1	65.3	69.4	63.9	66.2	68.3	62.1	55.1
EGFR27.M07	21:55:46.01	1.2	1110.4	70.5	58.6	63.9	52.7	51.4	50.2	50.8	52.7	53.8	56.9	63.1	55.0	56.2	52.4	46.4
EGFR27.M08	21:55:46.75	1.0	1351.4	71.6	52.0	49.8	45.0	44.7	47.8	54.7	58.4	59.4	61.7	64.8	65.6	60.7	52.2	47.4
EGFR27.M09	21:55:47.43	0.8	1570.9	67.9	52.2	49.0	47.6	50.2	51.2	47.8	53.6	53.6	56.7	58.2	56.1	54.0	49.5	44.5
EGFR27.M10	21:55:48.18	0.7	1814.8	61.0	47.0	44.3	49.7	51.4	52.7	49.2	48.0	42.3	42.4	42.4	43.0	42.0	40.8	35.7
EGFR27.M11	21:55:48.19	0.7	1817.8	61.3	46.9	41.0	43.9	43.8	46.3	42.5	44.4	46.6	49.1	50.2	51.8	49.7	45.1	37.9
EGFR27.M12	21:55:48.20	0.5	1820.8	74.8	42.3	51.7	53.7	55.1	54.6	60.6	67.2	68.2	64.4	59.7	58.1	56.3	49.6	44.0
EGFR27.M13	21:55:44.32	5.5	248.6	100.3	64.1	74.4	84.0	90.0	90.1	84.7	93.2	89.3	90.2	88.3	88.0	87.0	86.2	81.2
EGFR27.M14	21:55:44.33	5.2	251.5	100.6	80.8	84.2	85.6	92.9	91.9	92.5	94.5	90.0	82.8	79.2	86.4	90.1	89.3	82.0
EGFR27.M15	21:55:44.32	3.3	253.7	105.1	81.2	84.6	86.8	92.2	94.0	95.8	98.5	95.3	94.1	95.2	92.8	91.9	92.2	90.0
EGFR27.M16	21:55:43.75	57.5	26.9	121.8	100.2	96.5	93.0	105.0	112.0	115.5	112.7	109.8	112.6	107.2	109.3	109.4	107.6	106.9
EGFR27.M17	21:55:43.76	57.5	26.9	108.2	96.6	99.5	98.0	96.8	95.0	89.1	95.9	102.0	103.7	99.0	92.1	95.3	92.0	92.7
EGFR27.M18	21:55:47.85	0.9	1401.0	63.5	48.5	43.6	45.6	44.4	44.0	44.7	47.5	45.7	45.3	43.7	43.2	43.4	41.6	42.3
EGFR27.M19	21:55:48.53	0.8	1620.4	61.6	48.2	44.5	45.9	43.3	42.9	44.3	43.7	40.5	42.4	40.6	39.2	39.8	39.0	38.0
EGFR27.M20	21:55:49.28	0.7	1867.3	59.8	47.9	46.5	42.9	42.3	43.5	42.3	44.9	45.6	43.6	41.7	41.4	42.1	39.3	39.1

DIRECTIVITY ANGLE = 122.5 deg

1/3 OCTAVE BAND CENTER FREQUENCIES (kHz)

FILENAME	RECEIVE TIME	BETA (deg)	SR (m)	OSPL	0.10	0.13	0.16	0.20	0.25	0.32	0.40	0.50	0.63	0.79	1.0	1.3	1.6	2.0
EGFR28.M01	22:22:30.00	0.1	755.6	84.0	77.6	75.0	71.9	69.3	66.9	65.0	68.2	65.7	67.3	68.0	64.5	58.3	55.6	55.8
EGFR28.M02	22:22:30.00	0.0	758.6	85.4	77.7	74.3	70.8	68.0	65.7	61.1	65.8	66.4	72.4	75.6	74.1	69.2	67.2	65.4
EGFR28.M03	22:22:30.00	-0.6	761.7	88.0	72.9	68.5	73.8	76.8	76.9	75.5	76.9	75.5	78.7	79.3	75.2	72.7	67.8	65.4
EGFR28.M04	22:22:30.00	0.0	974.5	83.1	75.0	71.7	62.0	59.7	57.7	55.1	58.9	67.6	71.1	72.7	72.4	70.3	63.8	53.7
EGFR28.M05	22:22:48.00	0.0	1266.6	73.5	61.8	55.2	46.2	45.8	44.7	47.0	52.1	55.1	58.4	56.4	51.6	45.5	43.9	39.8
EGFR28.M06	22:22:48.00	0.0	1438.2	73.5	61.7	55.4	45.5	45.6	44.5	47.3	52.3	54.6	58.4	56.3	51.6	45.4	43.8	39.7
EGFR28.M07	22:22:48.00	0.0	1661.5	71.9	58.0	63.4	48.6	46.6	45.5	41.2	46.3	48.7	52.4	51.6	48.3	39.6	38.3	35.4
EGFR28.M08	22:22:38.00	0.0	1900.6	72.2	56.8	54.5	47.3	44.3	42.6	44.2	47.4	52.7	55.4	53.5	53.9	46.3	41.6	38.8
EGFR28.M09	22:22:30.00	0.0	2118.3	73.3	57.8	55.3	49.3	50.6	44.5	47.6	52.3	54.8	58.4	57.2	56.1	47.3	40.3	37.0
EGFR28.M10	22:22:30.00	0.0	2360.3	71.1	54.5	52.6	52.1	52.6	52.0	51.7	55.7	56.7	56.5	49.5	49.2	45.7	40.6	34.4
EGFR28.M11	22:22:30.00	0.0	2363.3	65.9	47.1	44.7	41.3	39.3	42.5	42.1	49.8	56.6	58.0	51.3	48.9	40.7	36.1	30.2
EGFR28.M12	22:22:30.00	-0.2	2366.4	62.1	41.8	47.5	50.5	49.7	53.7	51.3	50.5	51.9	47.5	44.5	43.7	38.4	30.7	26.8
EGFR28.M13	22:22:29.00	0.1	753.7	96.8	85.7	88.2	89.5	86.7	83.5	83.1	83.8	86.2	88.0	82.6	80.8	79.0	75.9	67.7
EGFR28.M14	22:22:29.00	0.0	756.7	101.6	86.5	90.1	91.7	91.9	92.7	94.4	93.3	92.7	88.2	83.5	75.7	73.1	71.3	65.5
EGFR28.M15	22:22:29.00	-0.6	759.8	102.5	86.6	90.9	92.3	92.7	93.5	95.7	94.5	93.5	89.5	85.0	76.0	77.5	76.7	68.4
EGFR28.M16	22:22:29.00	0.0	513.0	105.7	89.6	91.6	92.7	95.1	97.5	97.1	97.2	97.5	96.0	93.8	88.0	84.8	81.9	75.1
EGFR28.M17	22:22:29.00	0.0	510.0	105.5	89.8	91.3	92.7	95.2	97.3	96.4	97.4	97.3	96.0	93.5	88.4	84.7	81.7	75.3
EGFR28.M18	22:22:35.00	0.0	1899.0	96.8	78.9	84.2	89.8	91.0	90.0	86.0	87.7	79.9	73.1	65.9	60.5	59.2	58.5	57.1
EGFR28.M19	22:22:35.00	0.0	2116.8	94.0	78.4	83.5	88.4	89.8	86.4	80.1	79.2	67.9	62.3	60.3	55.9	54.3	53.6	51.5
EGFR28.M20	22:22:35.00	0.0	2362.0	92.5	77.5	84.1	87.9	87.9	82.4	74.5	71.8	62.2	57.3	57.8	56.6	55.5	53.0	51.9

REFERENCES

1. Putnam, Terrill W.: Review of Aircraft Noise Propagation. NASA TM X-56033, 1975.

2. Franken, Peter A.; and Bishop, Dwight E.: The Propagation of Sound From Aircraft Ground Operations. NASA CR-767, 1967.

3. Galloway, William J.: Community Noise Exposure Resulting From Aircraft Operations: Technical Review. AMRL-TR-73-106, U.S. Air Force, Nov. 1974. (Available from DTIC as AD A004 822.)

4. Pao, S. Paul; Wenzel, Alan R.; and Oncley, Paul B.: Prediction of Ground Effects on Aircraft Noise. NASA TP-1104, 1978.

5. Delany, M. E.; and Bazley, E. N.: Acoustical Properties of Fibrous Absorbent Materials. Appl. Acoust., vol. 3, no. 2, Apr. 1970, pp. 105-116.

6. Parkin, P. H.; and Scholes, W. E.: The Horizontal Propagation of Sound From a Jet Engine Close to the Ground, at Radlett. J. Sound. Vib., vol. 1, no. 1, Jan. 1964, pp. 1-13.

7. Parkin, P. H.; and Scholes, W. E.: The Horizontal Propagation of Sound From a Jet Engine Close to the Ground, at Hatfield. J. Sound Vib., vol. 2, no. 4, Oct. 1965, pp. 353-374.

8. Zorumski, William E.: Prediction of Aircraft Sideline Noise Attenuation. NASA TM-78717, 1978.

9. Benson, R. W.; and Karplus, H. B.: Sound Propagation Near the Earth's Surface as Influenced by Weather Conditions. WADC Tech. Rep. 57-353, Pt. I, U.S. Air Force, Mar. 1958. (Available from DTIC as AD 130 793.)

10. Burkhard, M. D.; Karplus, H. B.; and Sabine, H. J.: Sound Propagation Near the Earth's Surface as Influenced by Weather Conditions. WADC Tech. Rep. 57-353, Pt. II, U.S. Air Force, Dec. 1960. (Available from DTIC as AD 254 670.)

11. Sabine, H. J.; Raelson, V. J.; and Burkhard, M. D.: Sound Propagation Near the Earth's Surface as Influenced by Weather Conditions. WADC Tech. Rep. 57-353, Pt. III, U.S. Air Force, Jan. 1961. (Available from DTIC as AD 254 671.)

12. Sabine, H. J.: Sound Propagation Near the Earth's Surface as Influenced by Weather Conditions. WADC Tech. Rep. 57-353, Pt. IV, U.S. Air Force, Jan. 1961. (Available from DTIC as AD 254 672.)

13. Walker, David Q.: An Analysis of Aircraft Flyover Noise. AMRL-TR-78-8, U.S. Air Force, Apr. 1978. (Available from DTIC as AD A058 522.)

14. Mashita, Eric M.; and Bauer, Andrew B.: Lateral Noise-Attenuation Results From Flyovers of Three Transport Aircraft. AIAA Paper 79-0651, Mar. 1979.

15. Willshire, William L., Jr.; and Hilton, David A.: Ground Effects on Aircraft Noise. NASA TM-80185, 1979.

16. Hilton, David A.; and Henderson, Herbert R.: An Acoustic Range for the Measurement of the Noise Signature of Aircraft During Flyby Operations. Noise Contr. Eng., vol. 10, no. 3, May-June 1978, pp. 120-128.

17. Sentell, Ronald J.; Storey, Richard W.; Chang, James J. C.; and Jacobson, Stephen J.: Tethered Balloon-Based Measurements of Meteorological Variables and Aerosols. NASA TM X-73999, 1976.

18. Method for the Calculation of the Absorption of Sound by the Atmosphere. ANSI S1.26-1978 (ASA 23-1978), American Natl. Stand. Inst., Inc., June 23, 1978.

19. Chien, C. F.; and Soroka, W. W.: Sound Propagation Along an Impedance Plane. J. Sound & Vib., vol. 43, no. 1, Nov. 8, 1975, pp. 9-20.

20. Thomasson, Sven-Ingvar: Reflection of Waves From a Point Source by an Impedance Boundary. J. Acoust. Soc. America, vol. 59, no. 4, Apr. 1976, pp. 780-785.

21. Cooper, G. J.: B. Ae. Estimates for Aircraft Lateral Noise Attenuation. Acoustic Rep. 605, Weybridge-Bristol Div., British Aerosp. Aircr. Group (Weybridge, England), Dec. 20, 1979.

TABLE I.- T-38A ENGINE PARAMETERS

[Standard day]

Inlet Information:
```
Inlet area, m²  . . . . . . . . . . . . . . . . . . . . . . . . . . . . . . . . . 0.47
Stage 1 rotor diameter, m  . . . . . . . . . . . . . . . . . . . . . . . . . . . 0.4
Mass flow, kg/sec  . . . . . . . . . . . . . . . . . . . . . . . . . . . 19.91
Temperature rise (8 stages), K . . . . . . . . . . . . . . . . . . . . . 503.7
Number of rotor blades (stage 1) . . . . . . . . . . . . . . . . . . . . . 31
Number of inlet guide vanes  . . . . . . . . . . . . . . . . . . . . . . . 15
With/without guide vanes . . . . . . . . . . . . . . . . . . . . 15 with vanes
Design tip Mach number . . . . . . . . . . . . . . . . . . . . . . . . . . 1.0
Rotor-stator separation, cm  . . . . . . . . . . . . . . . . . . 0.38 to 0.61
Rotation speed (rpm/60), rps  . . . . . . . . . . . . . . . . . . . . . 275
```

Core information:
```
Mass flow rate (station 4), kg/sec . . . . . . . . . . . . . . . . . . . 19.60
Combustor inlet total pressure, N/cm²  . . . . . . . . . . . . . . . . . 67.48
Combustor inlet total temperature, K   . . . . . . . . . . . . . . . . . 536.7
Combustor outlet total temperature, K  . . . . . . . . . . . . . . . . . 1186.7
Turbine outlet total temperature, K  . . . . . . . . . . . . . . . . . . 958.3
Design value of drop in total temperature across the
   turbine stages (T4-T5), K  . . . . . . . . . . . . . . . . . . . . . 215.6
```

	Mil. power	Max. power
Jet information:		
Jet exit diameter, m	0.31	0.39
Jet density, kg/m³	0.785	0.368
Jet total temperature, K	958.3	1955.5
Jet exit velocity, m/sec	562.1	794.9
Nozzle pressure ratio	2.14	2.01
Mass flow, kg/sec	20.28	21.00
Ratio of specific heats	1.322	1.262

TABLE II.- NOMINAL AIRCRAFT OPERATING CONDITIONS

Date	Run no.	Altitude, m	Power setting, percent		Time, G.m.t.
			Engine 1	Engine 2	
11/1/79	1	9	Idle	100	11 46 38
	2	9			11 54 13
	3	10			11 58 37
	4	10			12 02 32
	5	10			12 06 47
11/2/79	6	12			19 37 32
	7	12			19 42 45
	8	12			19 48 43
	9	12			19 52 32
	10	18			19 56 13
	11	18			19 59 50
	12	18			20 03 50
	13	18			21 02 23
	14	18		Full burner	21 05 58
	15	18		Full burner	21 09 40
	16	36		100	21 13 48
	17	36			21 17 28
	18	36			21 19 58
	19	73			21 25 49
	20	73			21 29 34
	21	73			21 33 05
	22	146			21 36 39
	23	146			21 40 05
	24	146			21 43 18
	25	9			21 48 00
	26	9			21 51 58
	27	18			21 55 37
	28	Static	Off		

TABLE III.- COORDINATES OF MICROPHONE POSITIONS

Microphone number	X, m	Y, m	Z, m
1	-243.69	53.34	0.00
2	-246.74	53.34	1.20
3	-249.78	53.34	9.14
4	-462.99	53.34	1.20
5	-755.45	53.34	1.20
6	-926.01	79.25	1.20
7	-1149.61	79.25	1.20
8	-1388.97	79.25	1.20
9	-1606.81	79.25	1.20
10	-1848.92	79.25	.00
11	-1851.96	79.25	1.20
12	-1855.01	79.25	9.14
13	-243.69	.00	.00
14	-246.74	.00	1.20
15	-249.78	.00	9.14
16	.00	.30	1.20
17	.00	.00	1.20
18	-1388.97	.00	1.20
19	-1606.81	.00	1.20
20	-1851.96	.00	1.20

TABLE IV.- SAMPLE WEATHER DATA FOR RUN 27

Height and location of weather station	Wind speed, m/sec	Wind direction, deg	Temperature, °C	Atmospheric pressure, kPa	Humidity, percent	Dew point, °C
1.2 m, van 1	1.8	300	13.3			
1.2 m, van 5	1.4	270	12.2			
10 m, van 3	1.4	359	14.0	101.8	39.0	
10 m, N-159	1.8	285	15.0	101.9		-18
10 m, C-15	2.7	285				
3 m, triangle area	2.2	296	15.0			
6 m, triangle area	2.4	288				
9 m, triangle area	2.5	275				
12 m, triangle area	2.4	275				
15 m, triangle area	2.6	295	15.0			
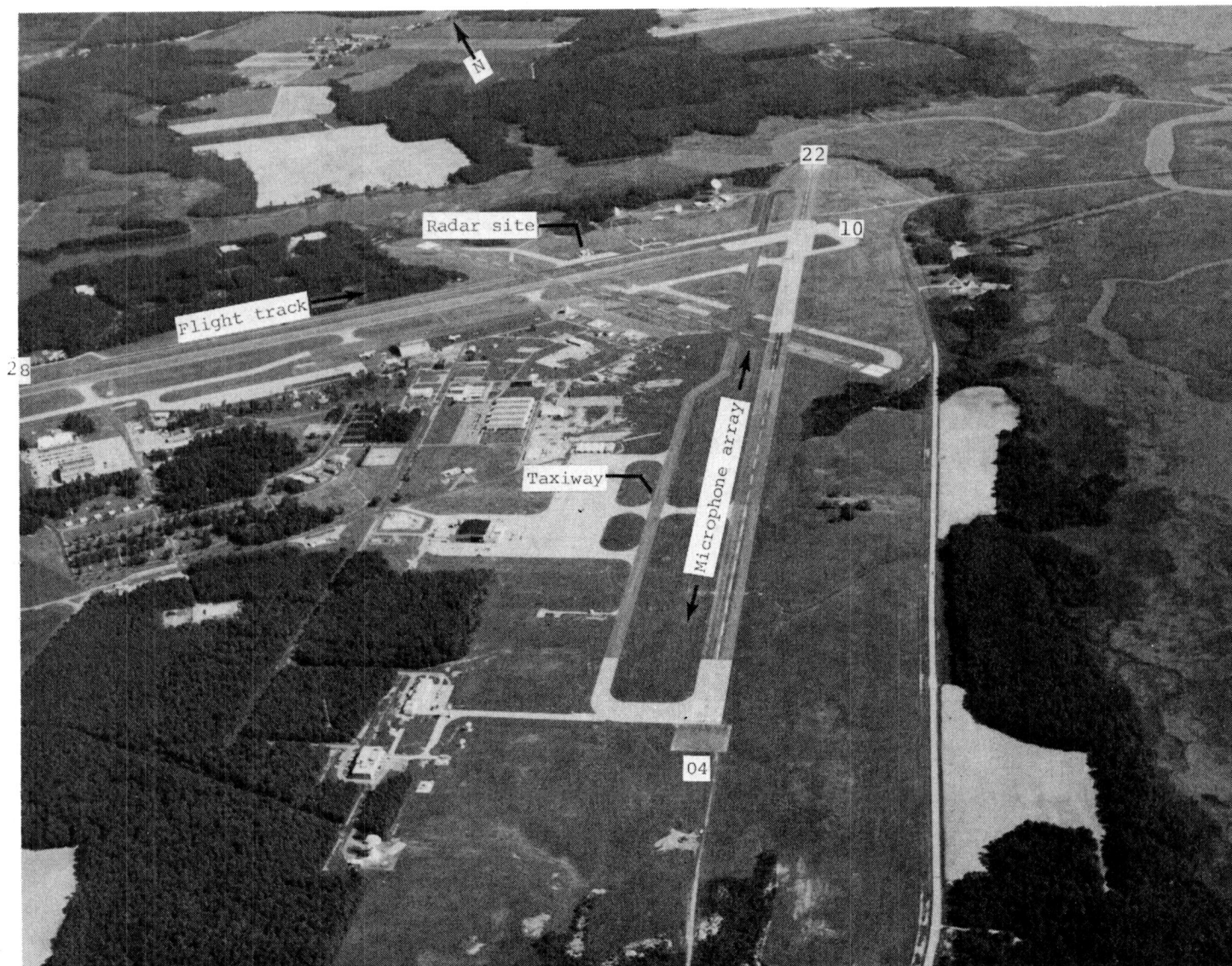
Figure 1.- Experimental site.

Main laser reflector

Secondary laser
reflector
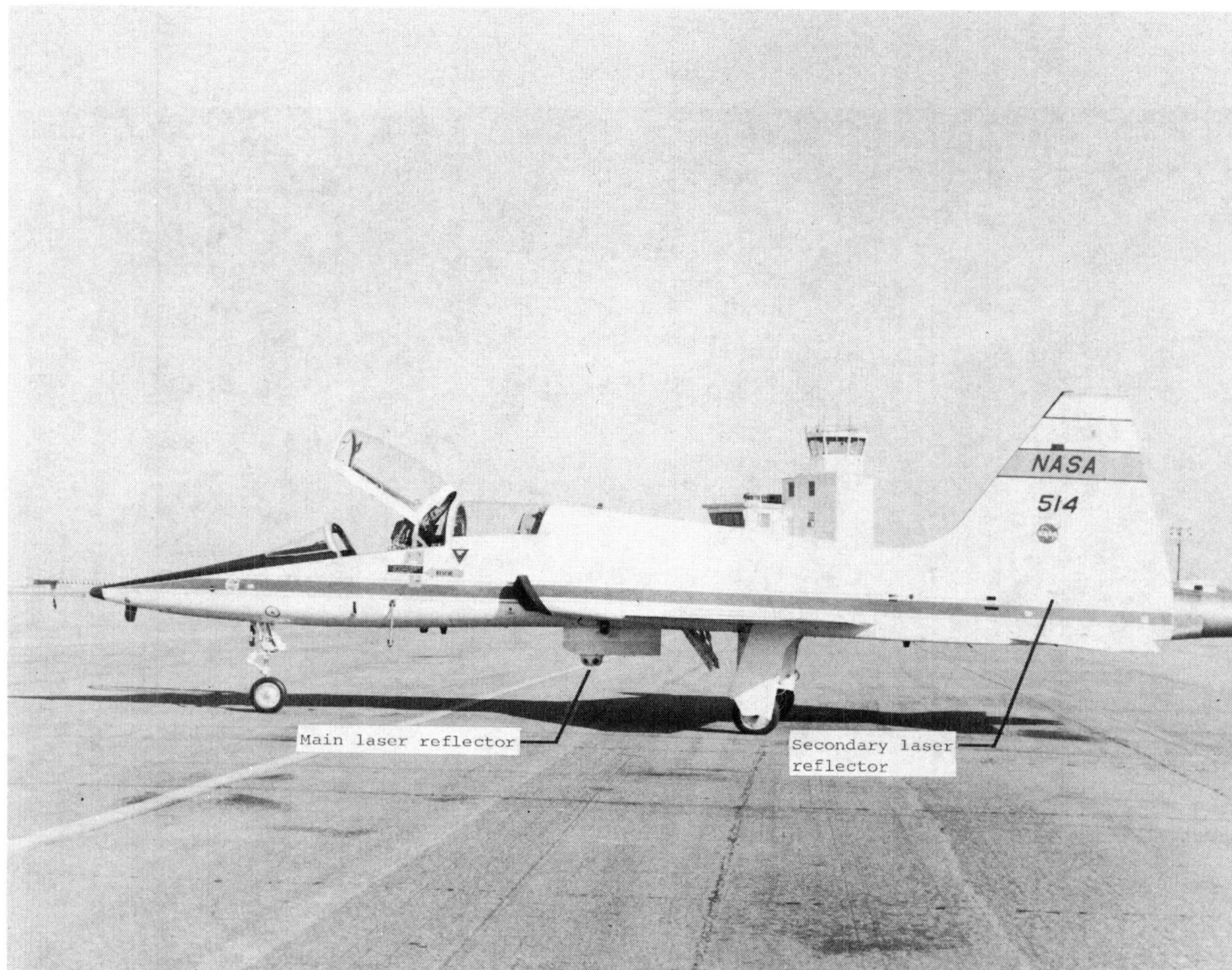
(a) Side view.

Figure 2.- Noise source.

Secondary laser reflector

Speed brake

Main gear door
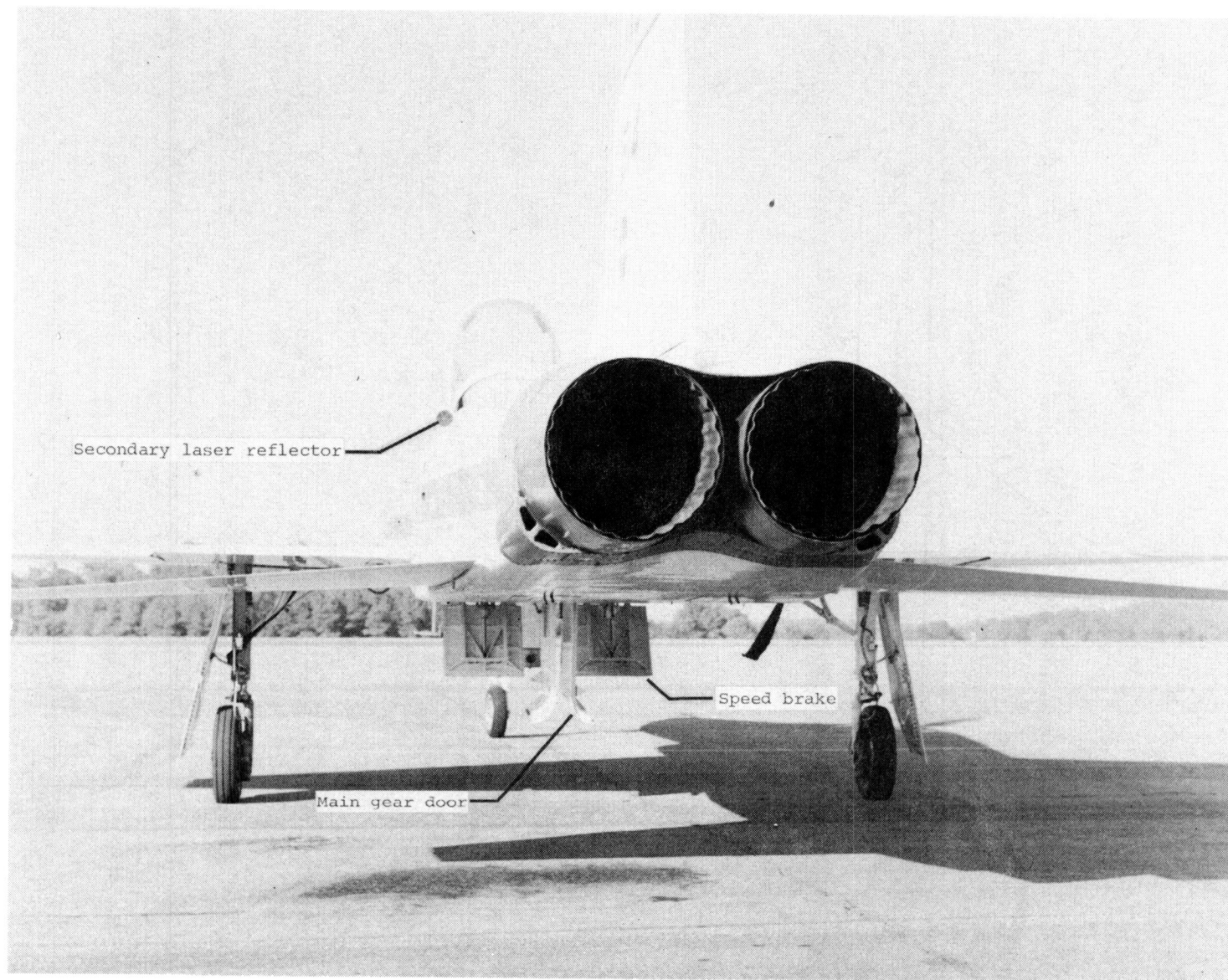
(b) Rear view.

Figure 2.- Concluded.
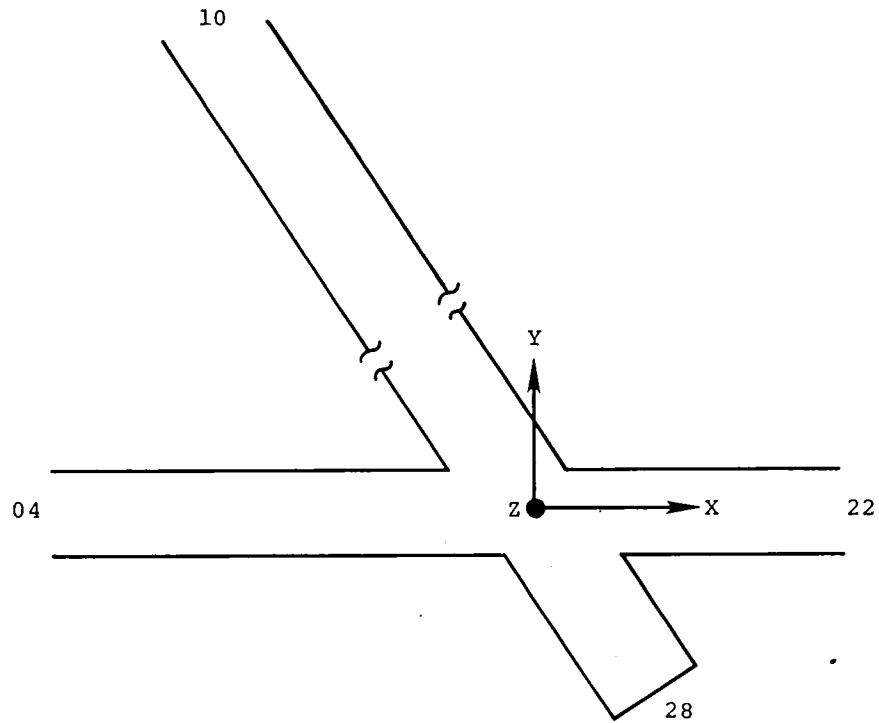
Figure 3.- Data reduction coordinates.
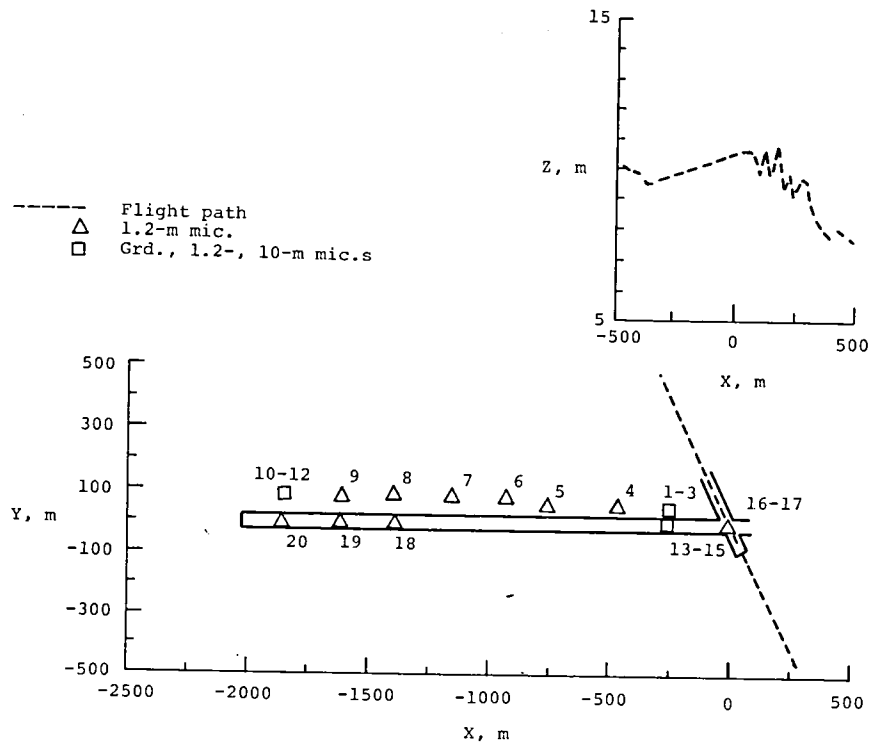
Figure 4.- Flight track for run 26.
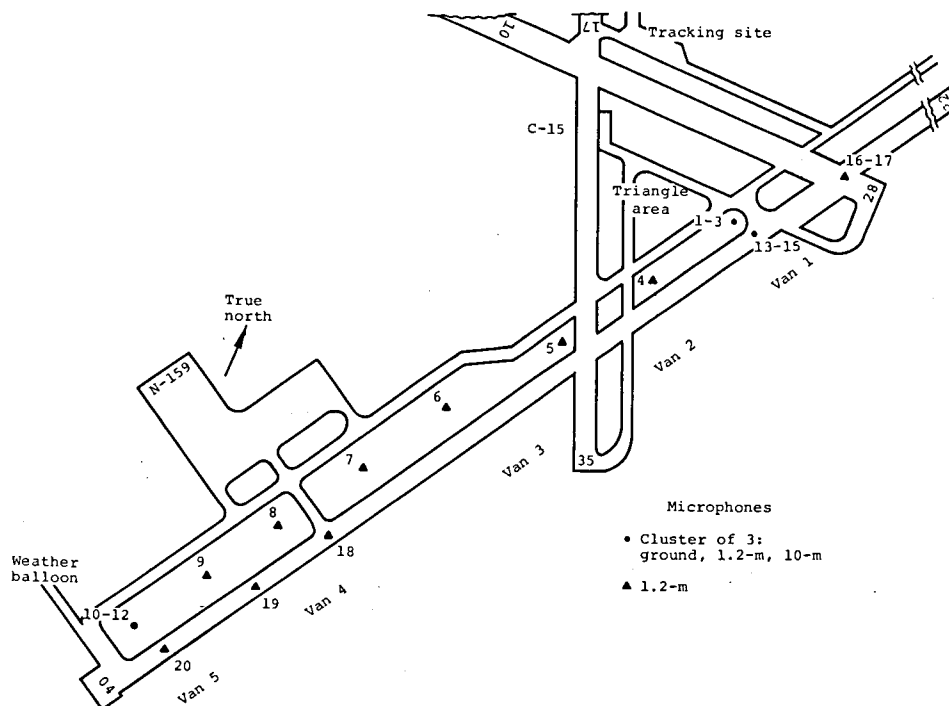
Figure 5.- Diagram of experimental site.
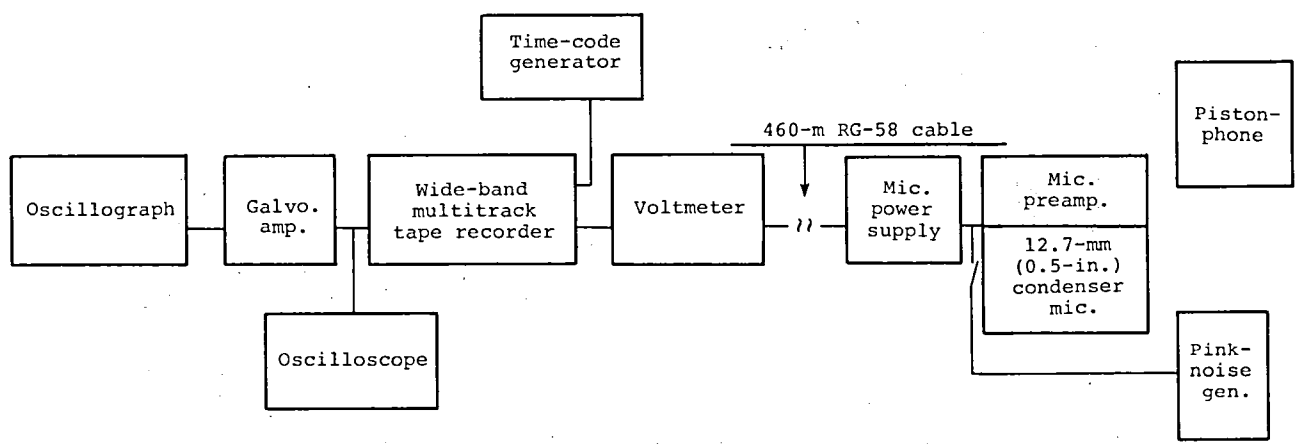
Figure 6.- Block diagram of acoustic instrumentation.
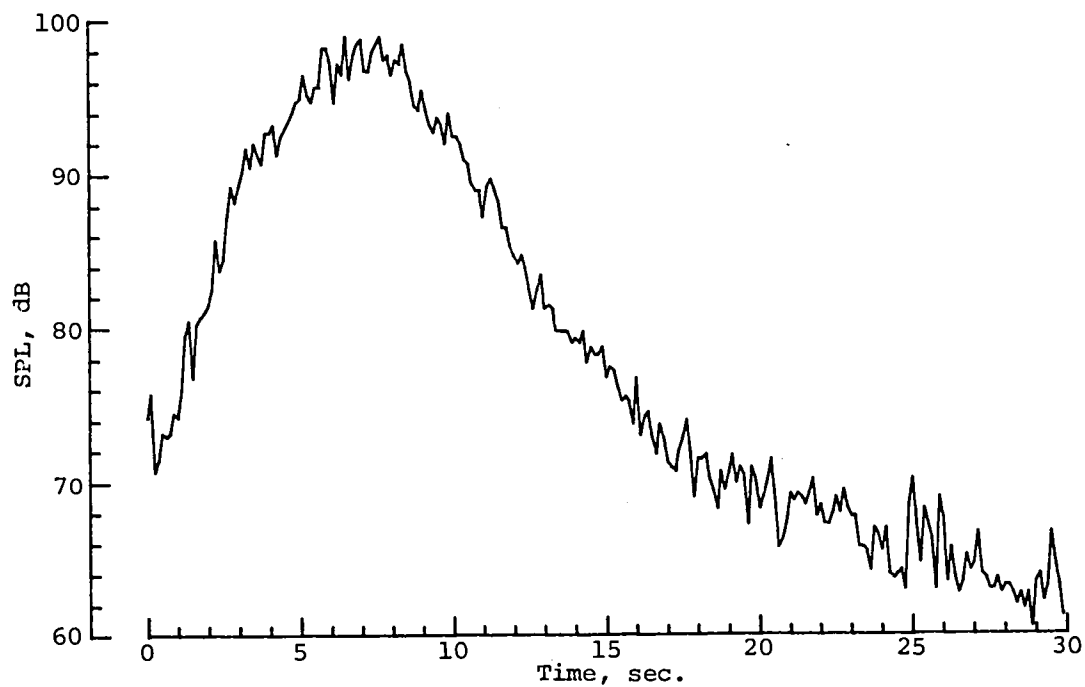
(a) Microphone 2.
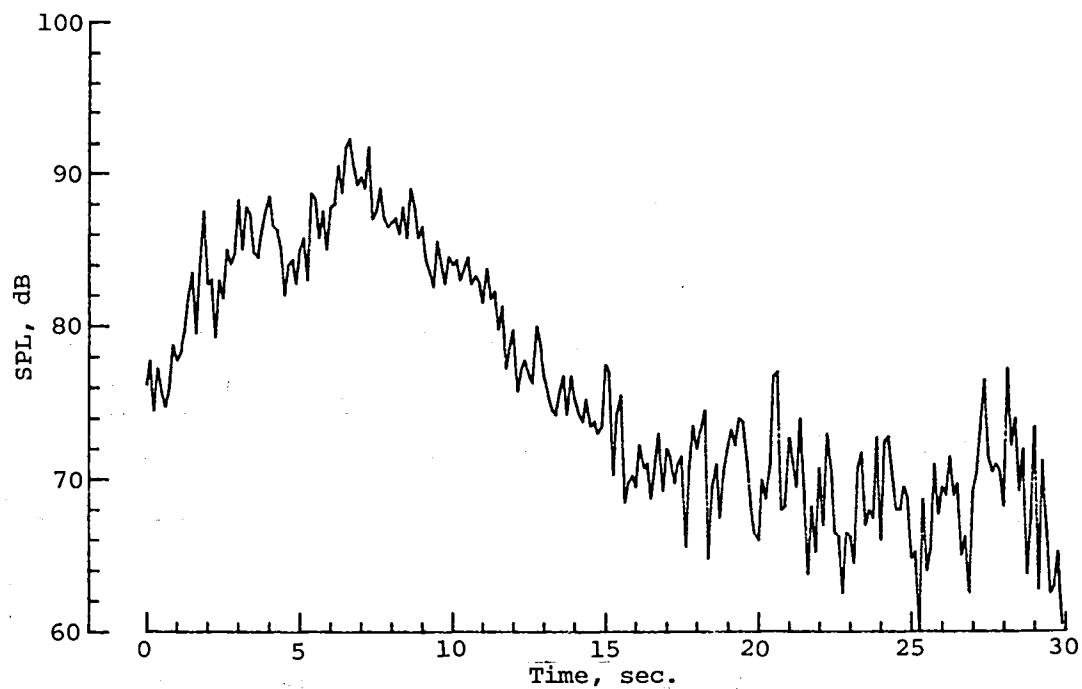
(b) Microphone 4.

Figure 7.- Time histories for run 27.
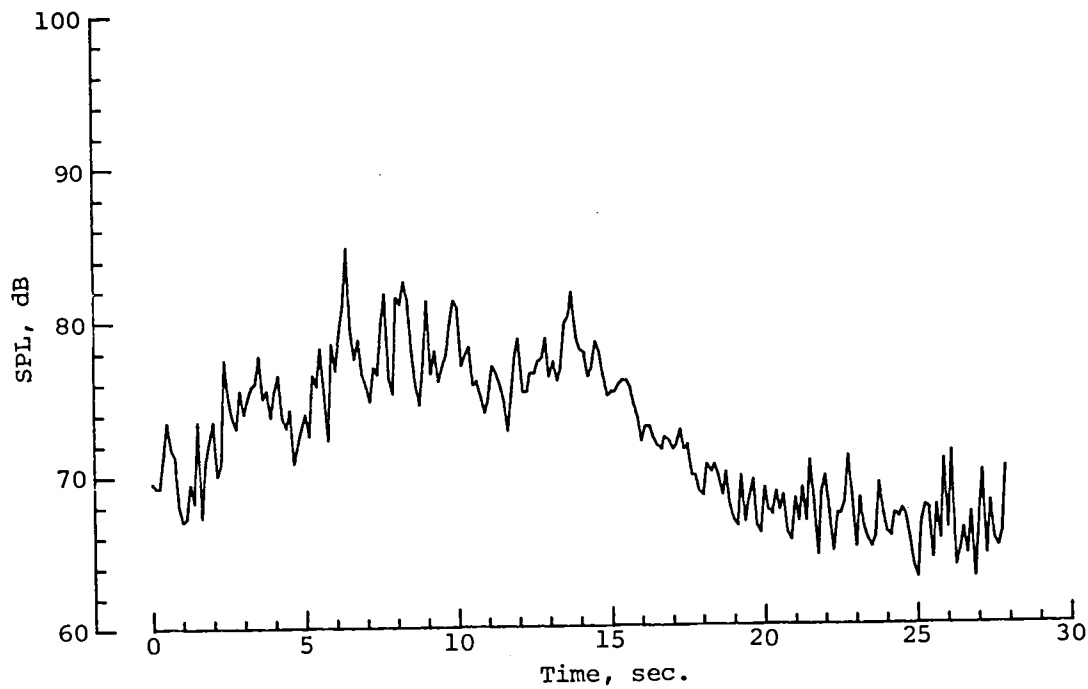
(c) Microphone 6.
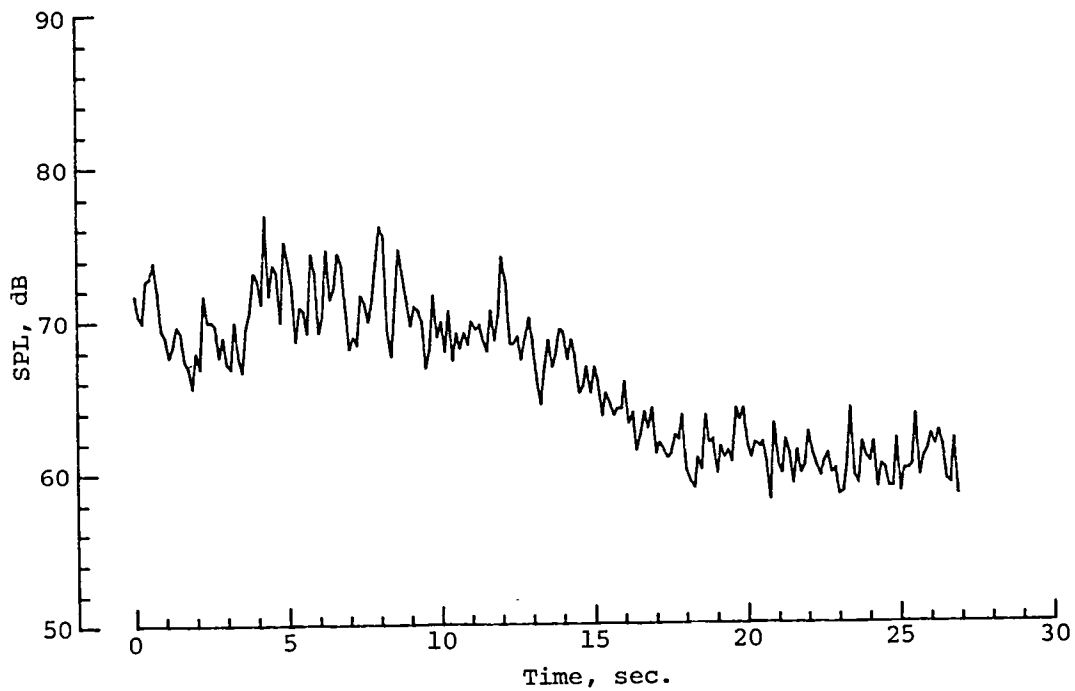
(d) Microphone 8.

Figure 7.- Concluded.
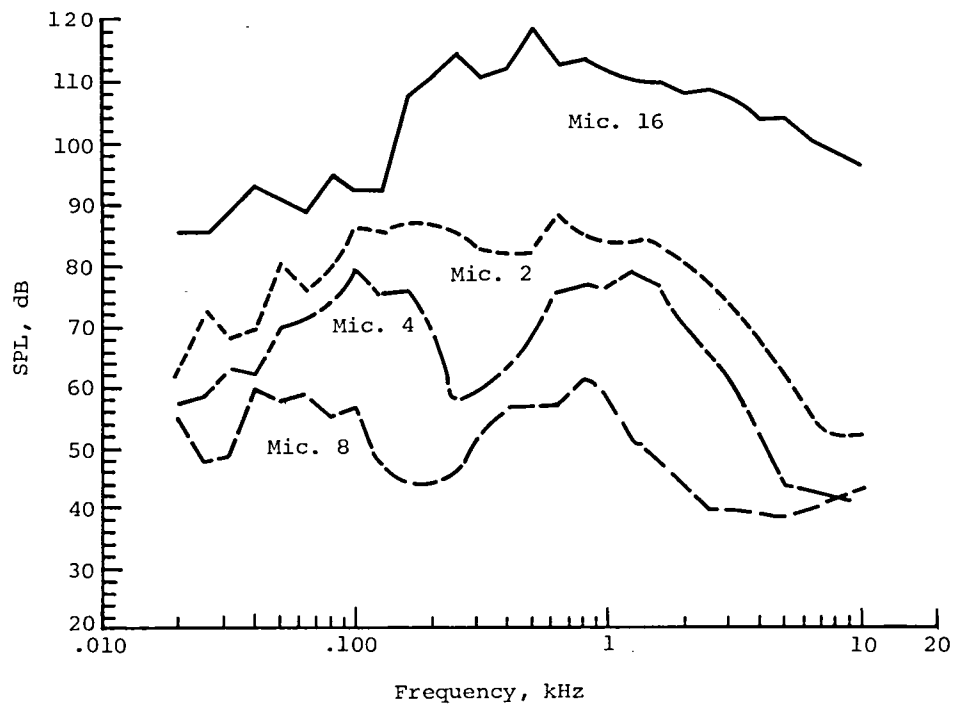
Figure 8.- Maximum overall spectra for run 27.
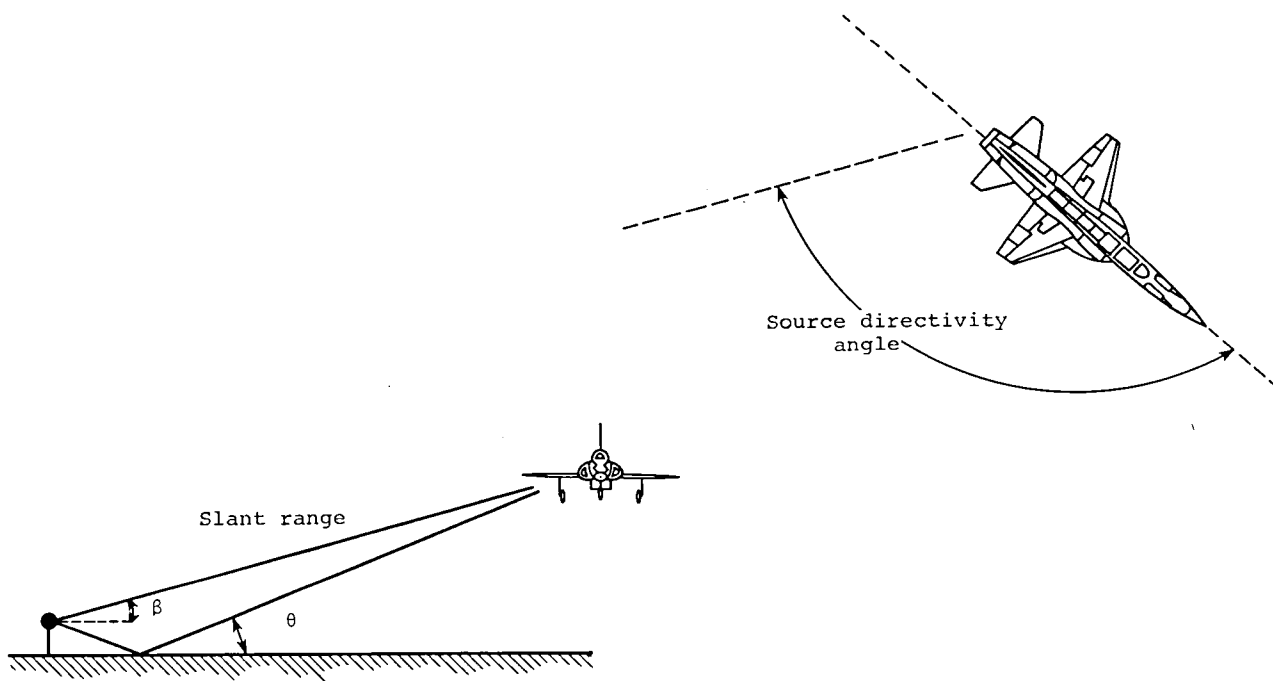
Figure 9.- Source-microphone geometry.
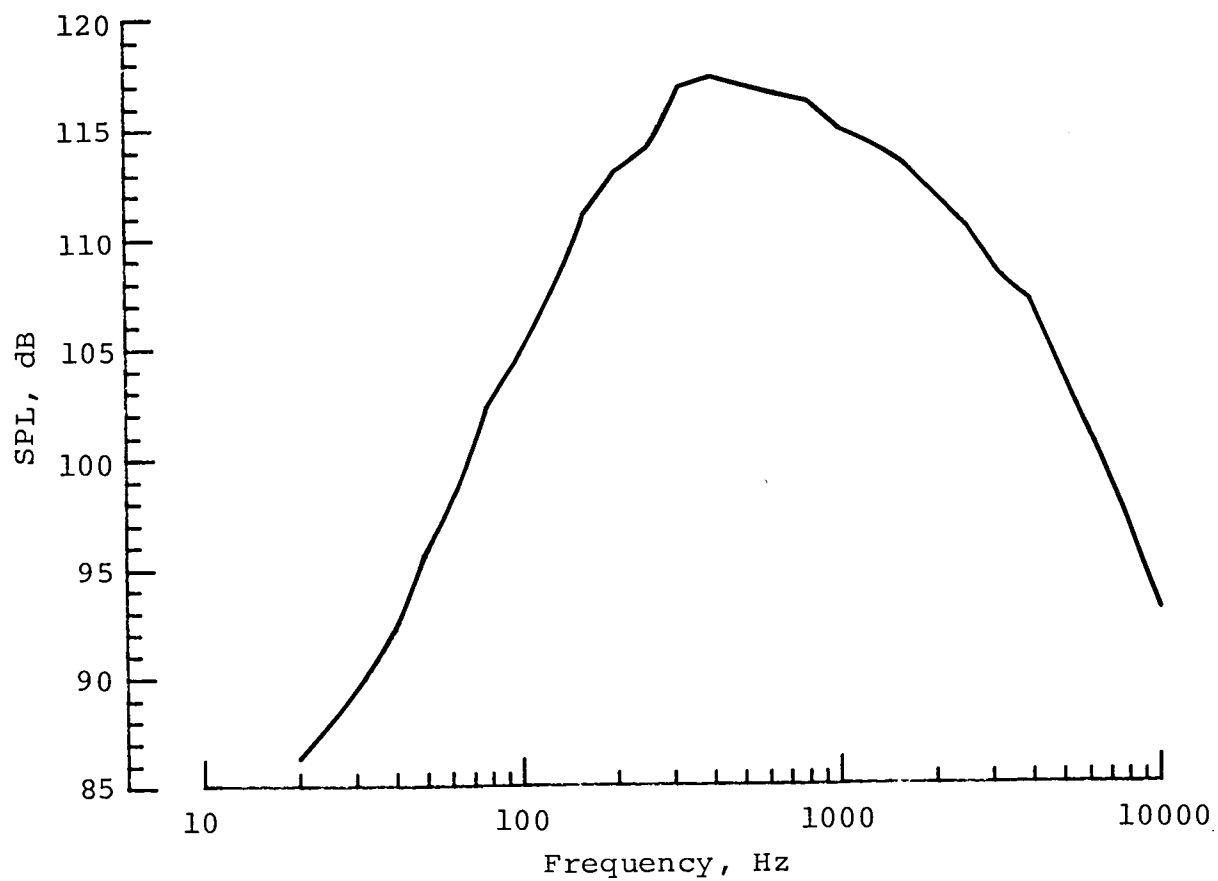
Figure 10.- Reference spectrum for near/far comparison method.

Mic. 4
SR 462 m
β   18.3 deg

Mic. 6
SR 897 m
β   9.3 deg
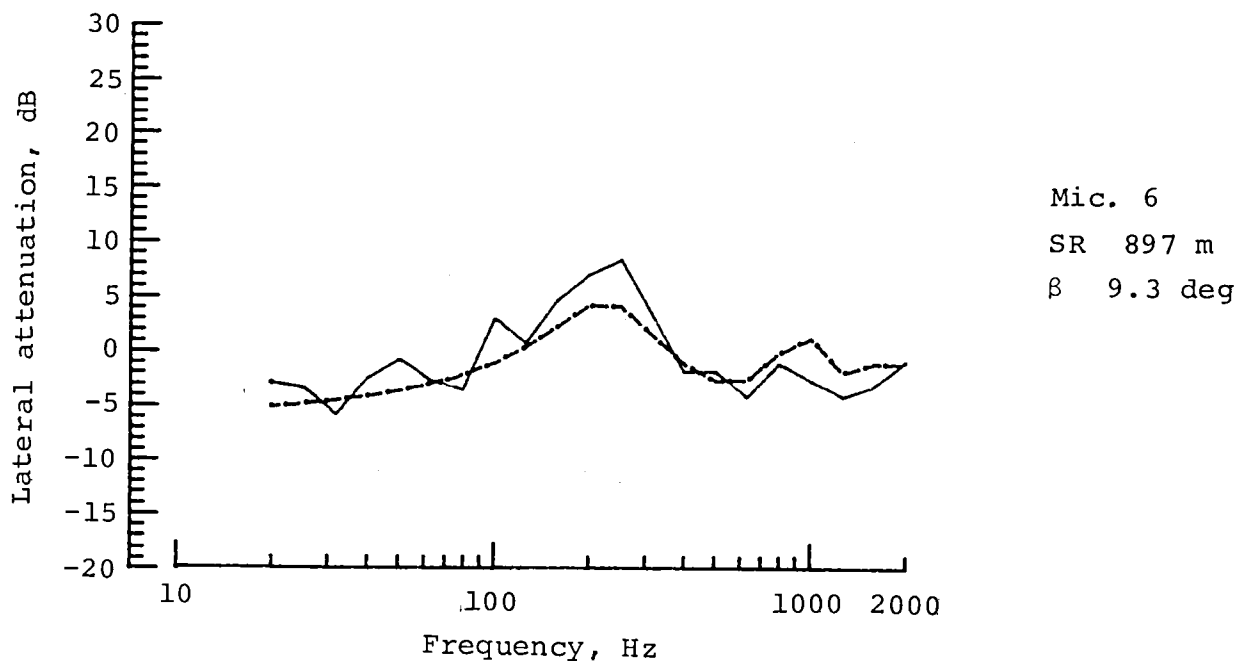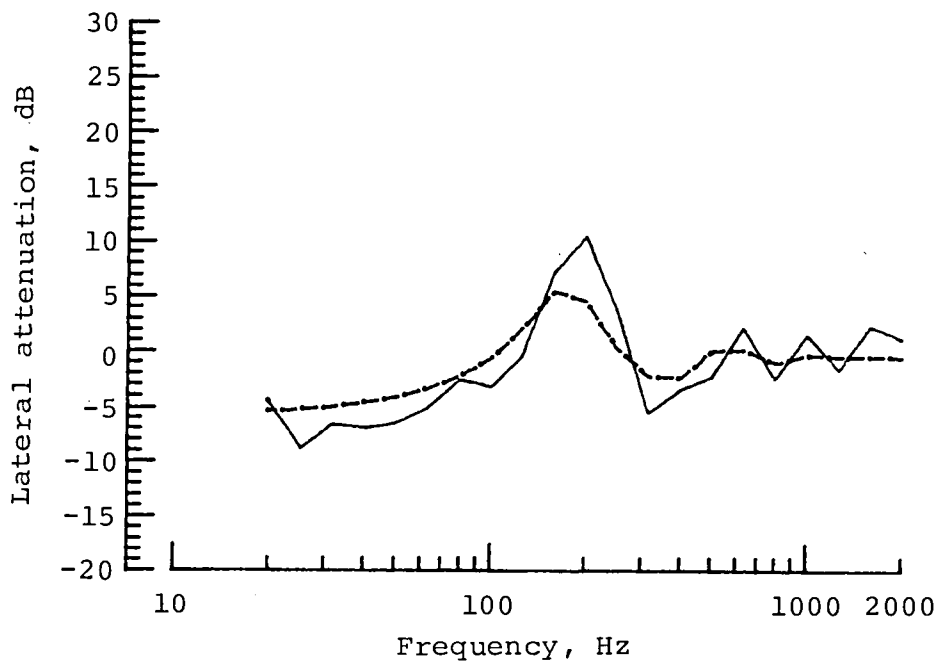
(a) Run 24; altitude, 160 m.

Figure 11.- Near/far results. Solid curve, measured results; dashed
curve, predicted results.

Mic. 8
SR 1358 m
β 6.1 deg

Mic. 11
SR 1823 m
β 4.6 deg

(a) Concluded.

Figure 11.- Continued.

Mic. 4
SR 433 m
β 10.0 deg

Mic. 6
SR 885 m
β 4.9 deg
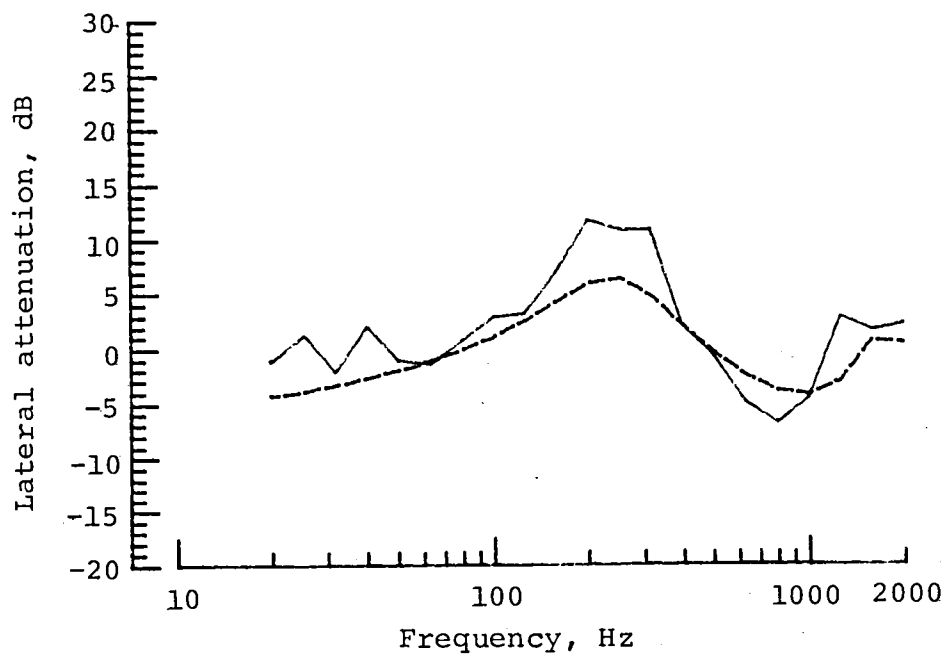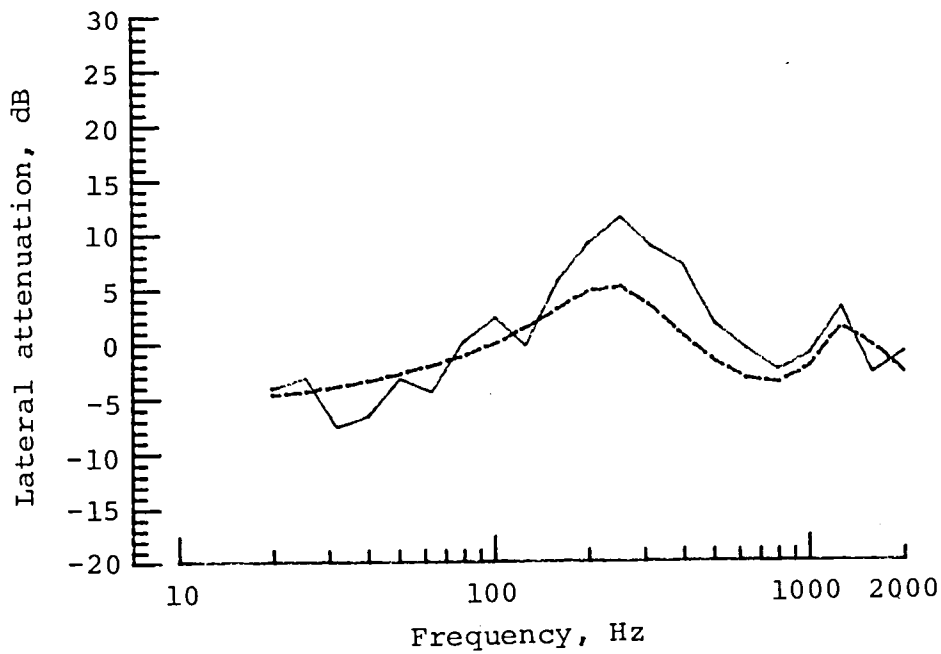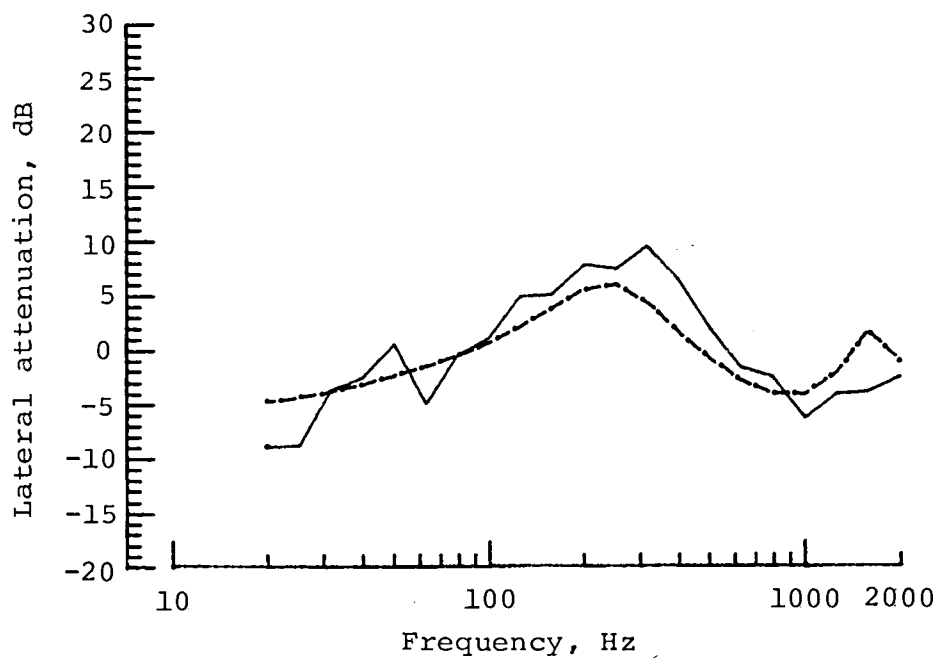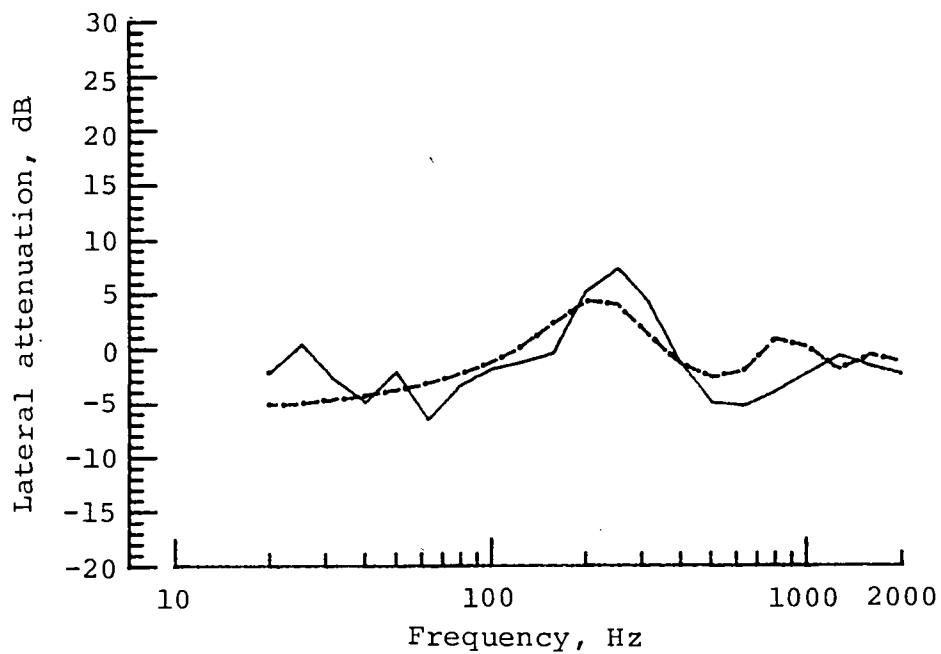
(b) Run 21; altitude, 80 m.

Figure 11.- Continued.

Mic. 8
SR 1355 m
β   3.2 deg

Mic. 11
SR 1826 m
β   2.4 deg

(b) Concluded.

Figure 11.- Continued.

Mic. 4
SR 433 m
β 5.0 deg

Mic. 6
SR 884 m
β 2.5 deg
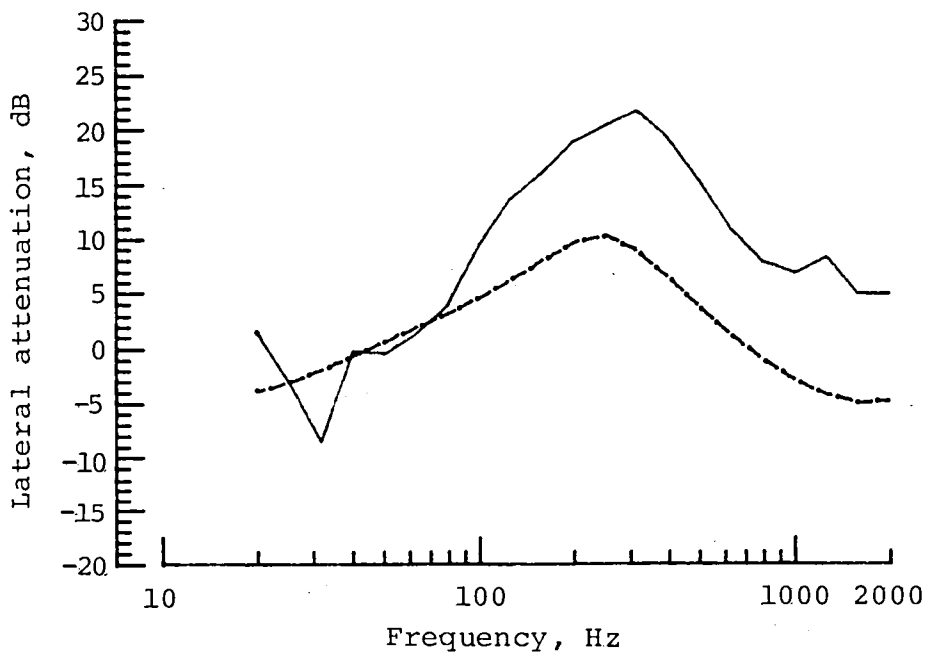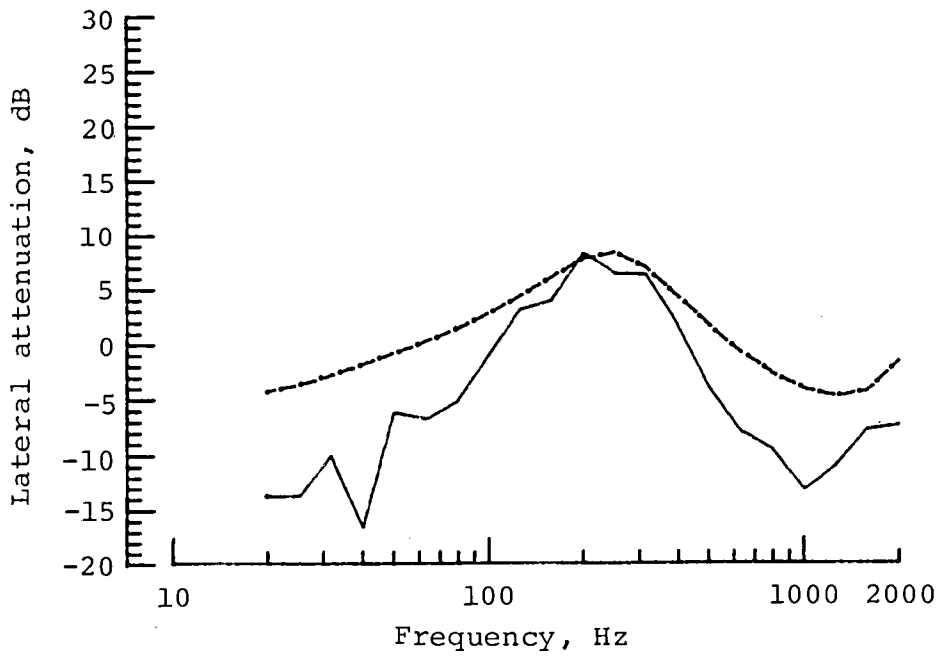
(c) Run 17; altitude, 40 m.

Figure 11.- Continued.

Mic. 8
SR 1351 m
β 1.6 deg

Mic. 11
SR 1819 m
β 1.2 deg

(c) Concluded.

Figure 11.- Continued.
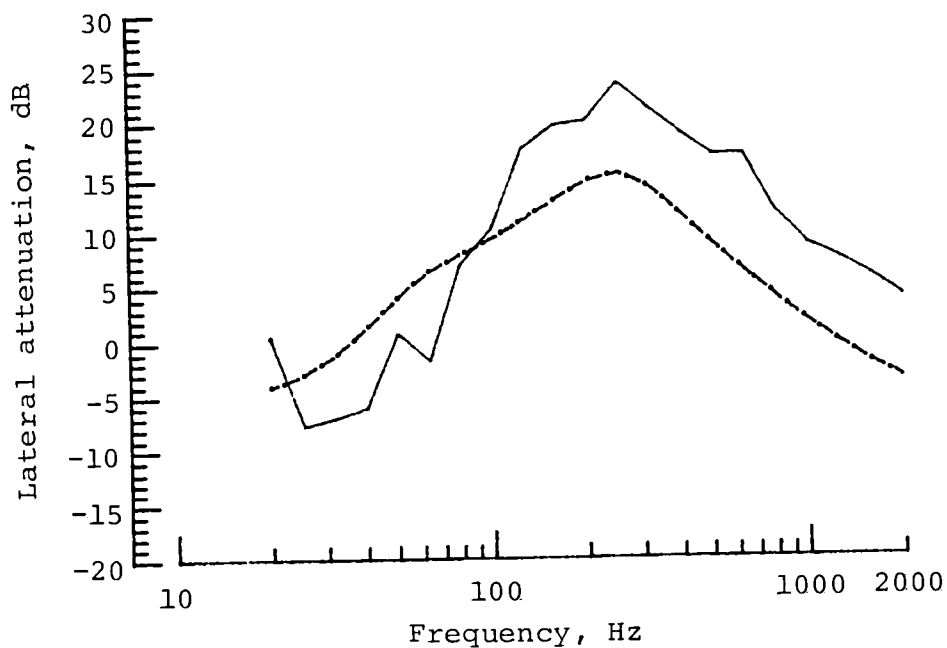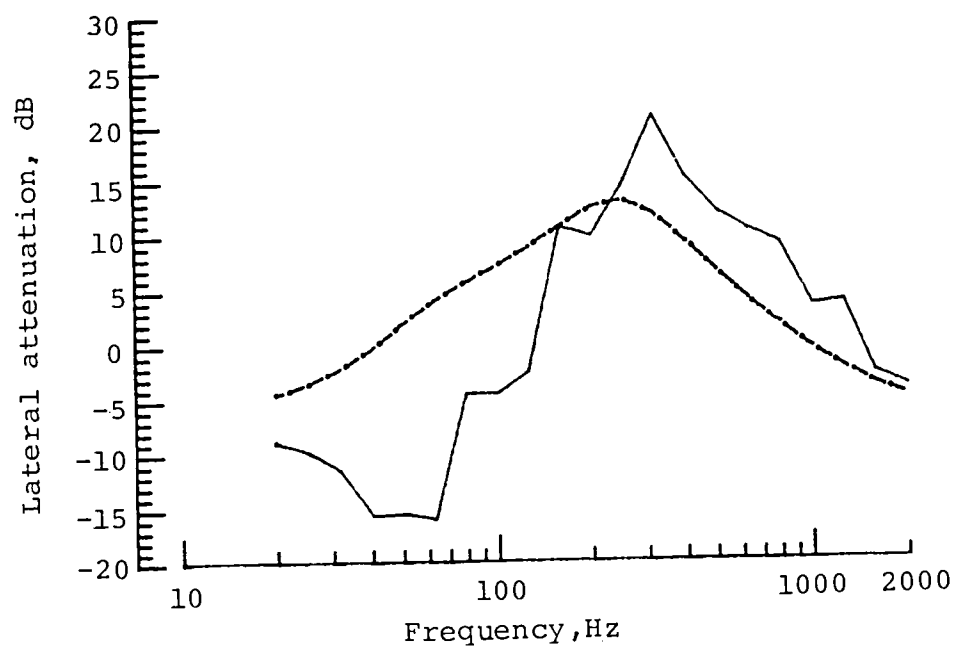
Mic. 4
SR 435 m
β 3.0 deg
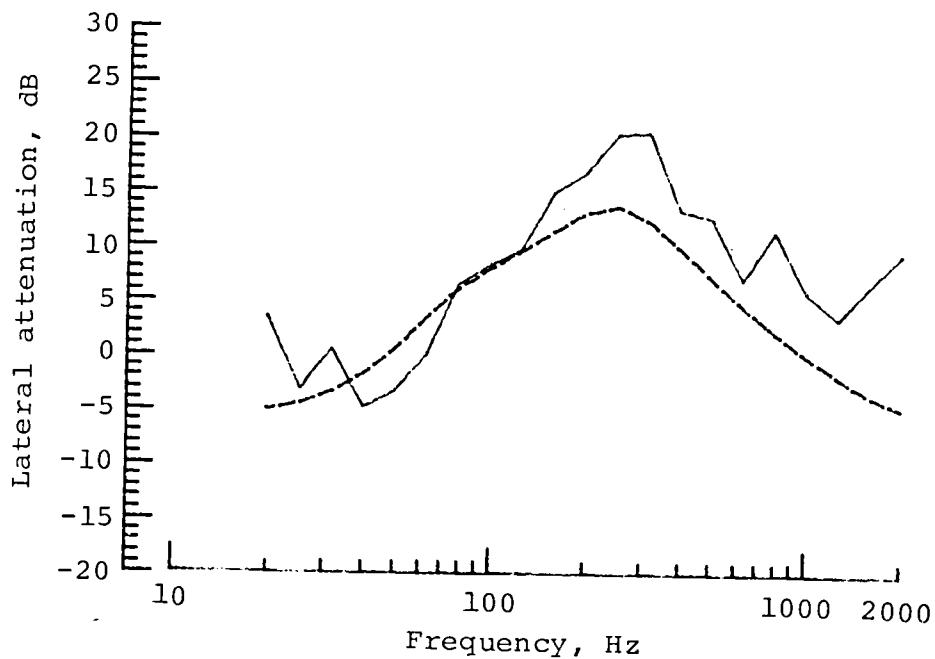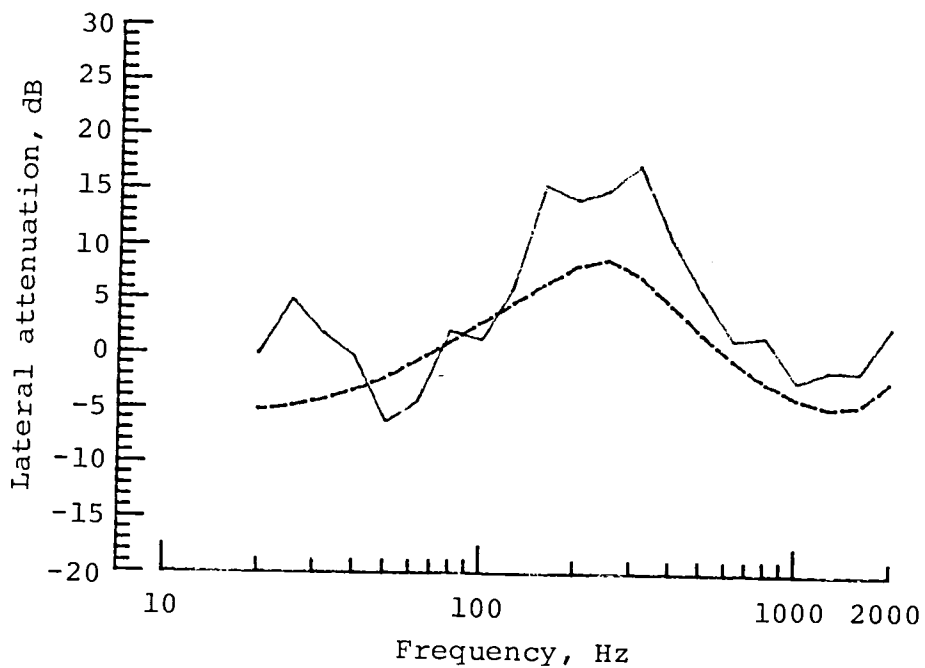
Mic. 6
SR 885 m
β 1.4 deg

(d) Run 27; altitude, 20 m.

Figure 11.- Continued.
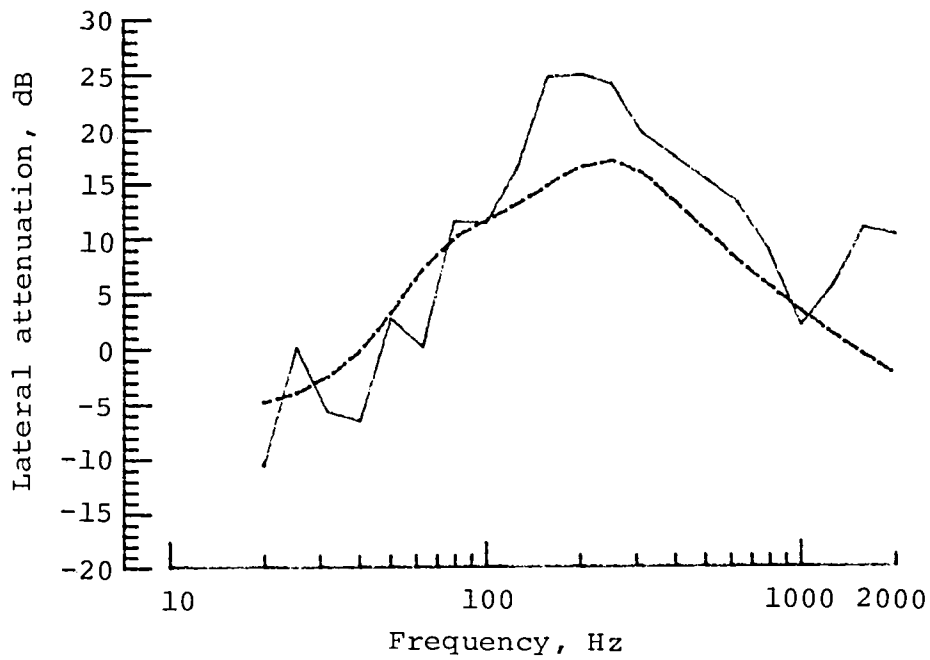
Mic. 8
SR 1351 m
β 1.0 deg
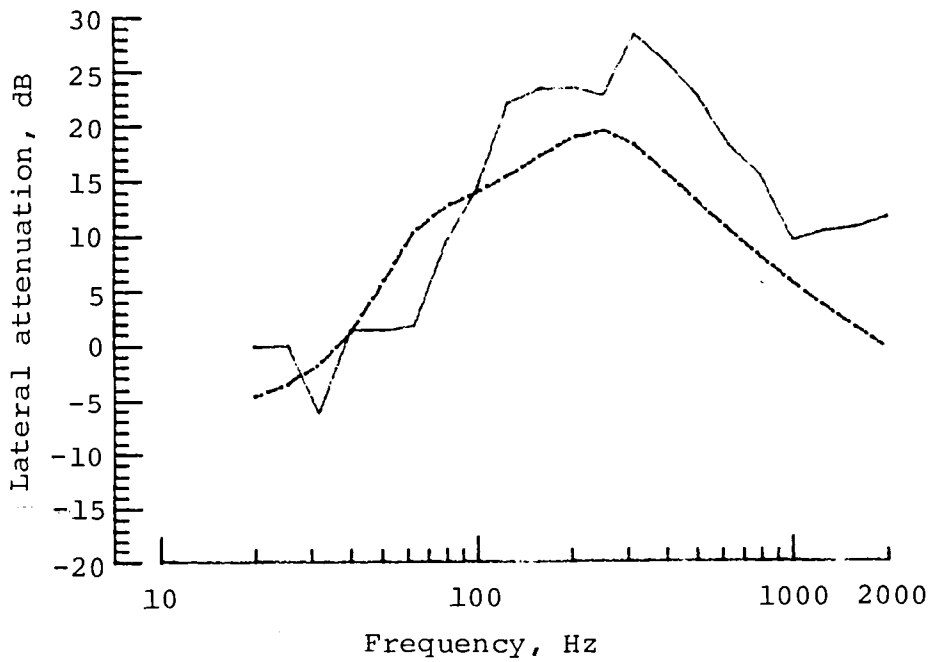
Mic. 11
SR 1818 m
β 0.7 deg

(d) Concluded.

Figure 11.- Continued.
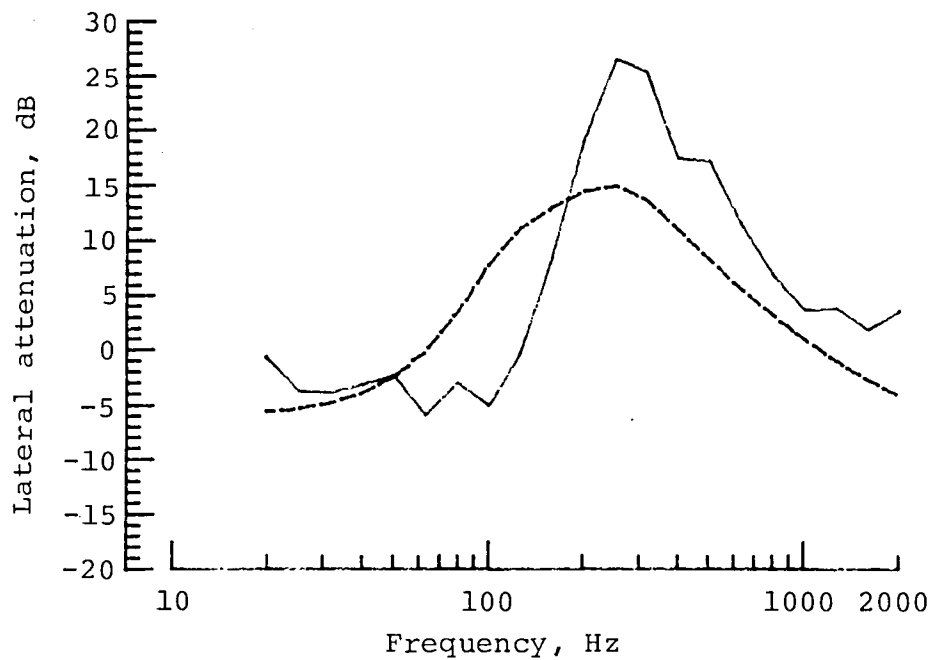
Mic. 4
SR 435 m
β 1.2 deg
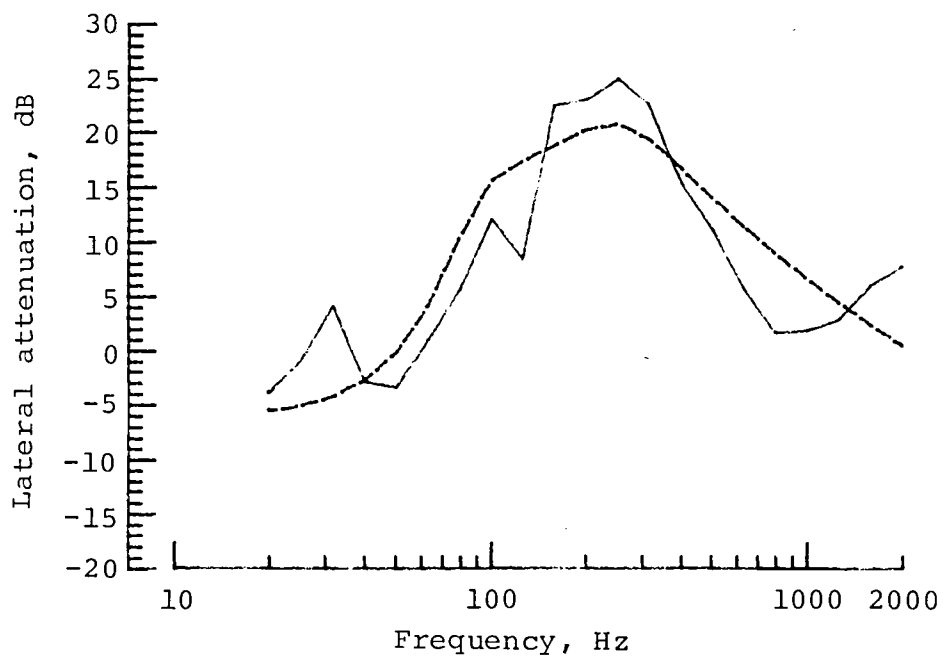
Mic. 6
SR 887 m
β 0.6 deg

(e) Run 26; altitude, 10 m.

Figure 11.- Continued.
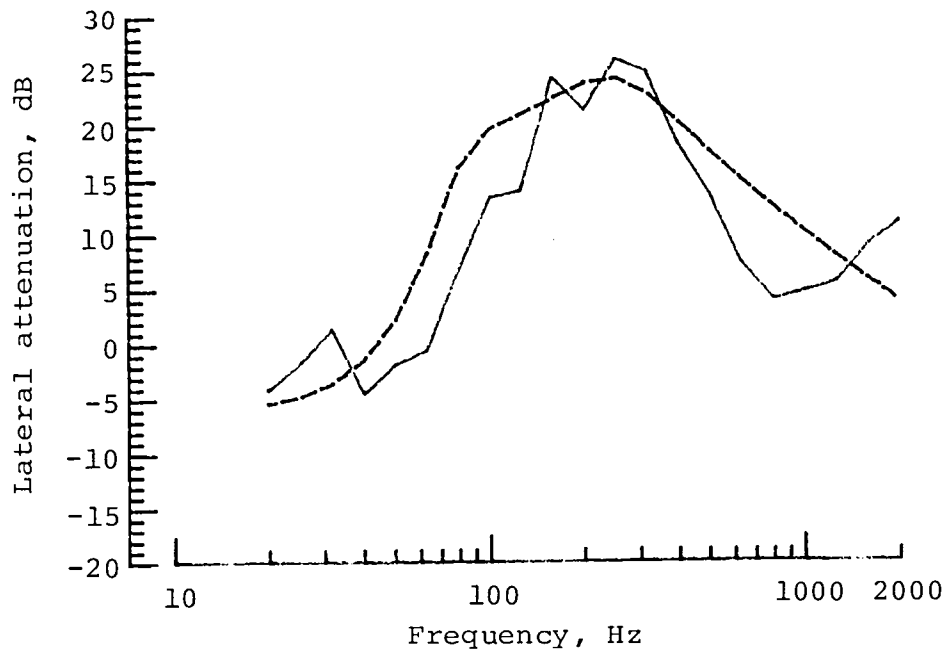
Mic. 8
SR 1355 m
β 1.0 deg
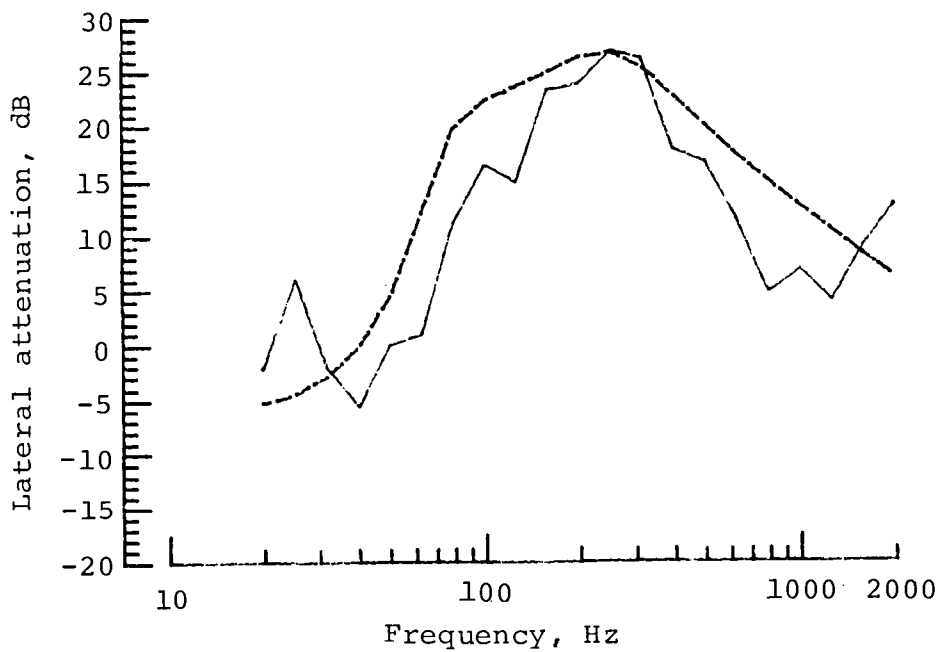
Mic. 11
SR 1823 m
β 0.3 deg

(e) Concluded.

Figure 11.- Concluded.

Mic. pair 2-14

SR 285 m

β 30.8 deg

Mic. pair 9-19

SR 1601 m

β 5.2 deg
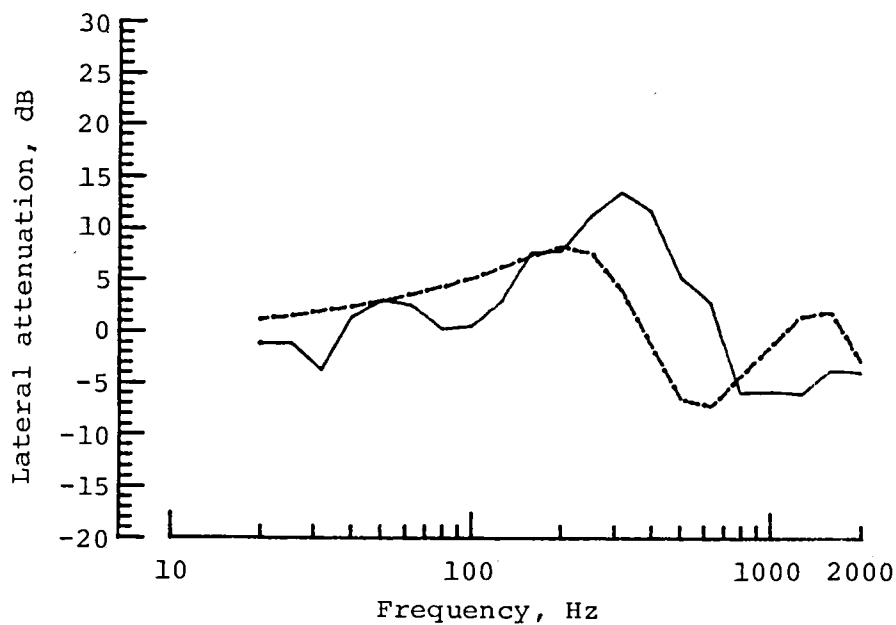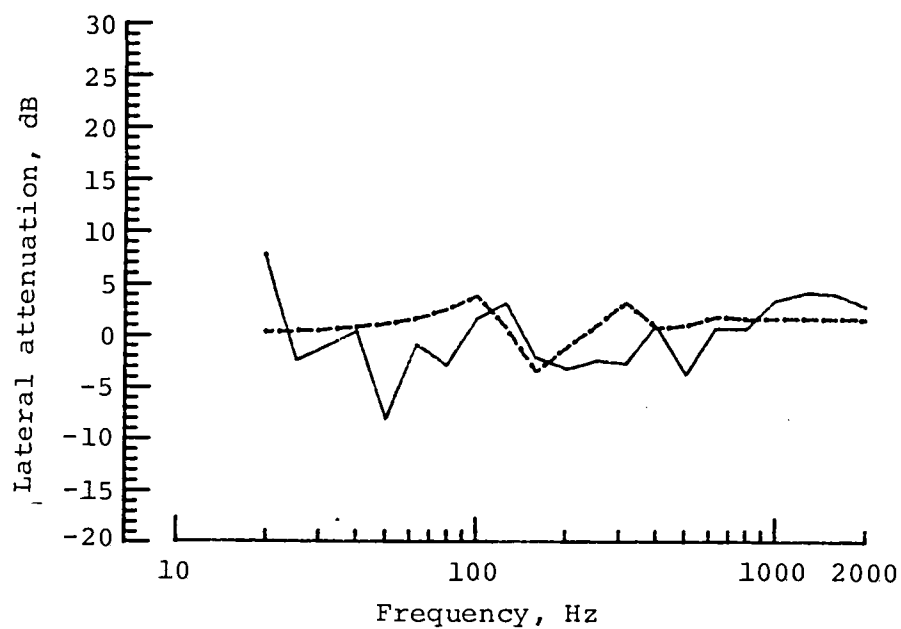
(a) Run 24; altitude, 160 m.

Figure 12.- Direct results. Solid curve, measured results; dashed curve, predicted results.

Mic. pair 2-14
SR 237 m
β 18.7 deg

Mic. pair 9-19
SR 1601 m
β 2.7 deg
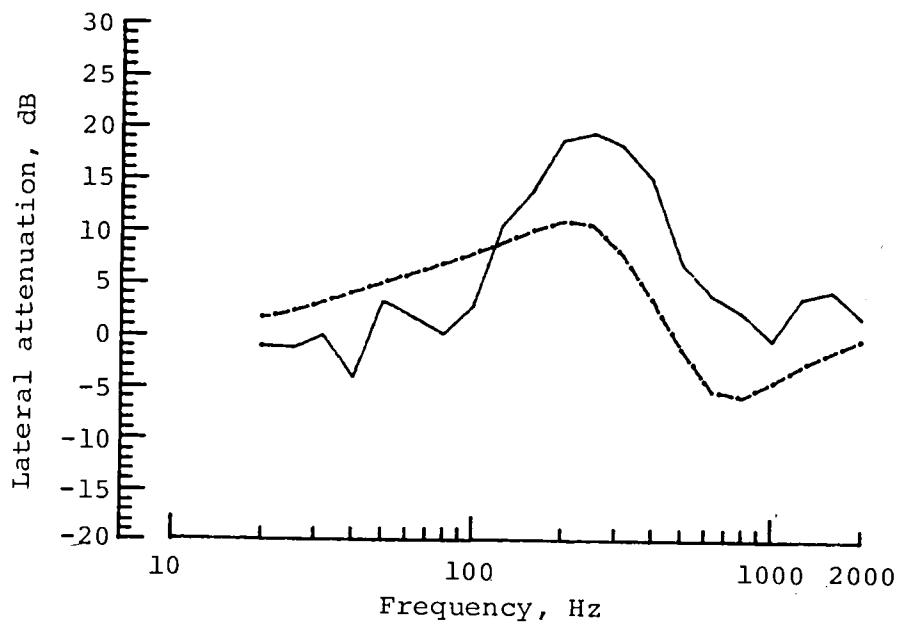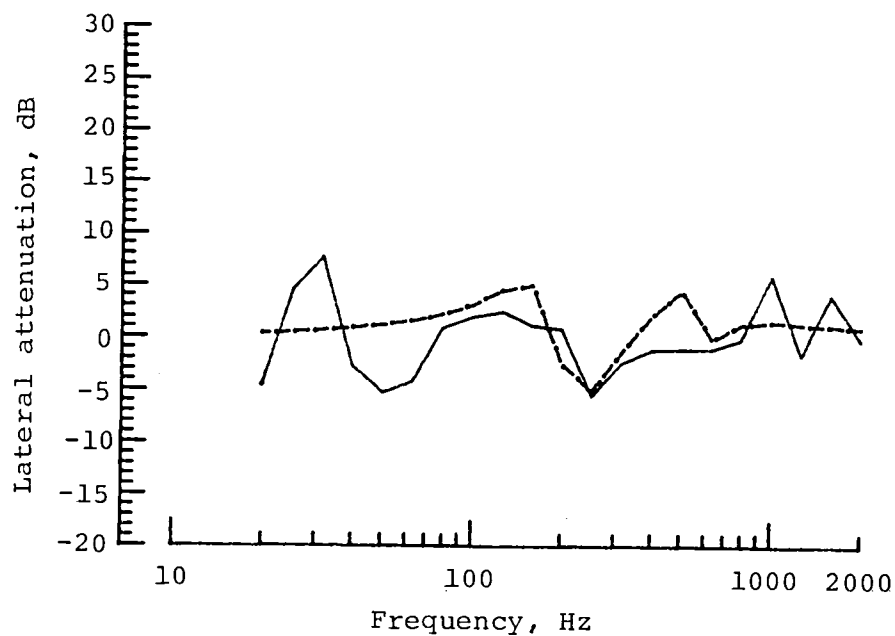
(b) Run 21; altitude, 80 m.

Figure 12.- Continued.

Mic. pair 2-14

SR 233 m

β 9.4 deg

Mic. pair 9-19

SR 1596 m

β 1.4 deg
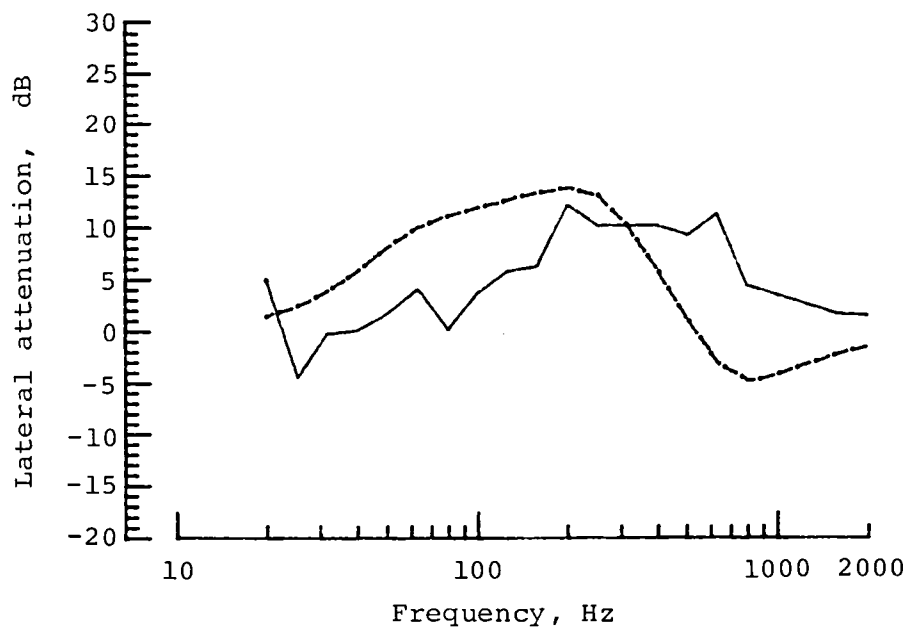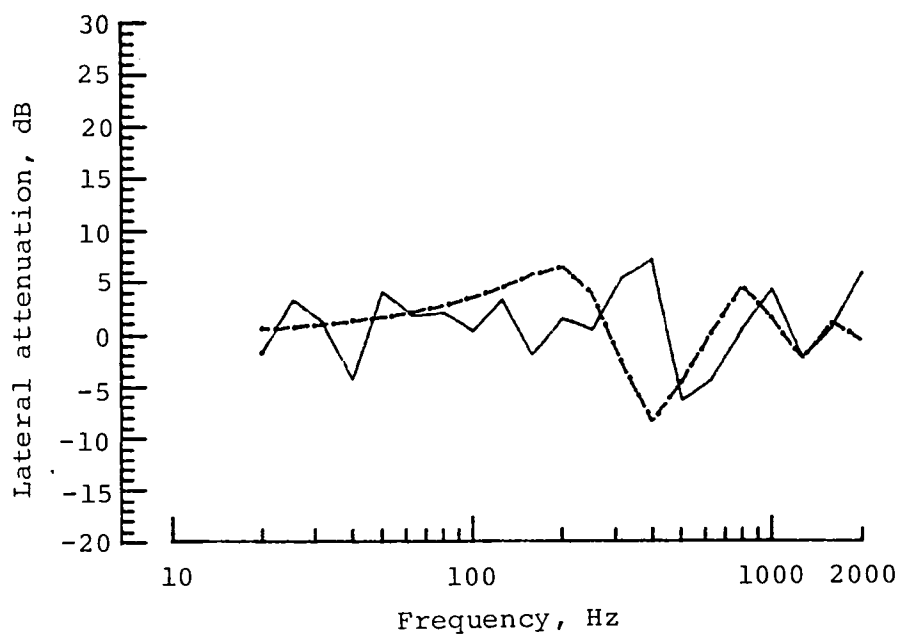
(c) Run 17; altitude, 40 m.

Figure 12.- Continued.

Mic. pair 2-14

SR 235 m

β 5.5 deg

Mic. pair 9-19

SR 1596 m

β 0.8 deg
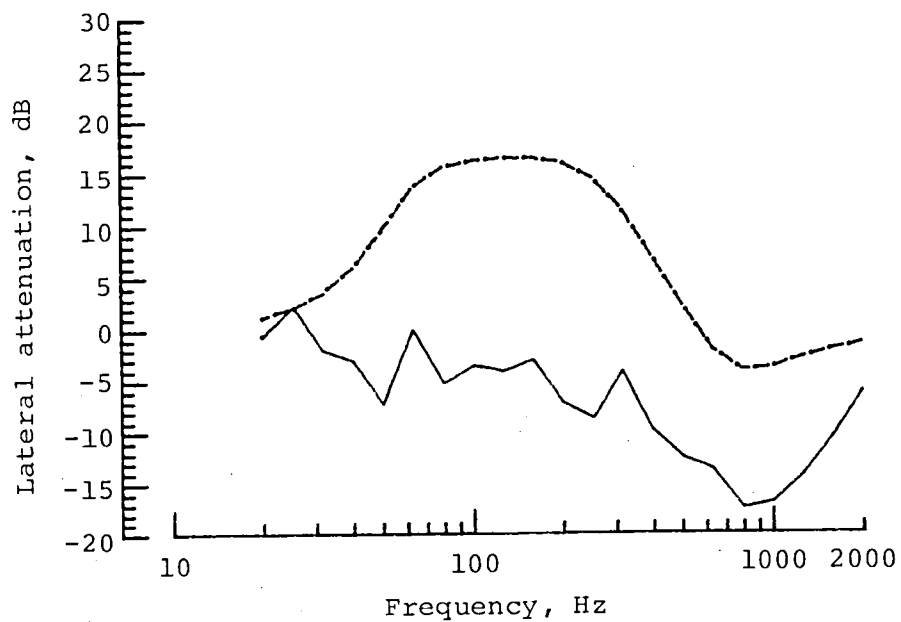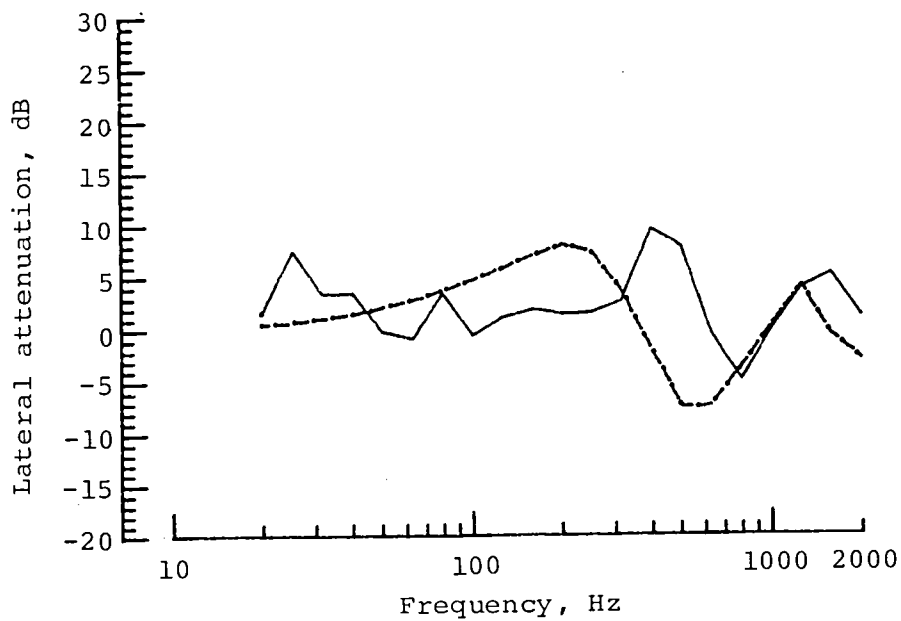
(d) Run 27; altitude, 20 m.

Figure 12.- Continued.

Mic. pair 2-14
SR 233 m
β 2.3 deg

Mic. pair 9-19
SR 1600 m
β 0.3 deg
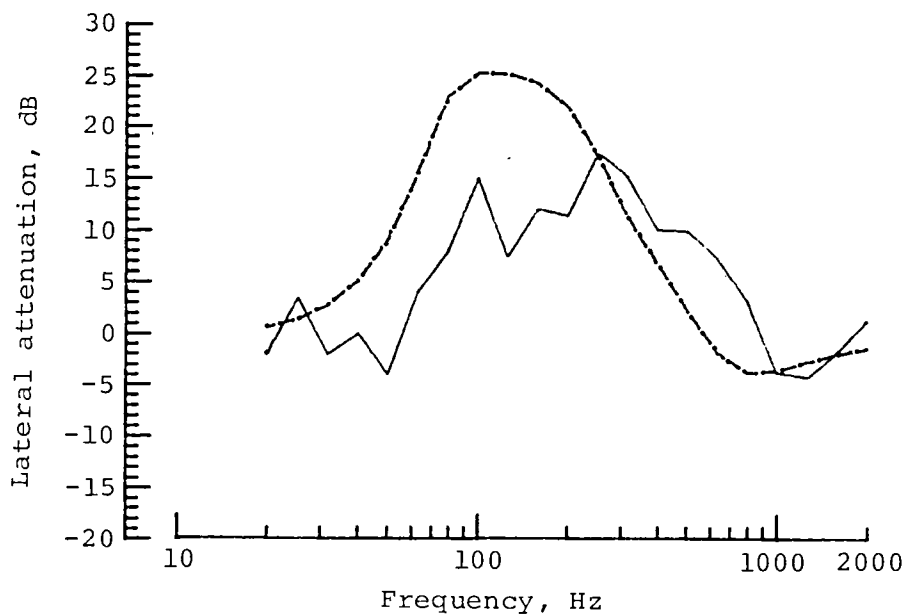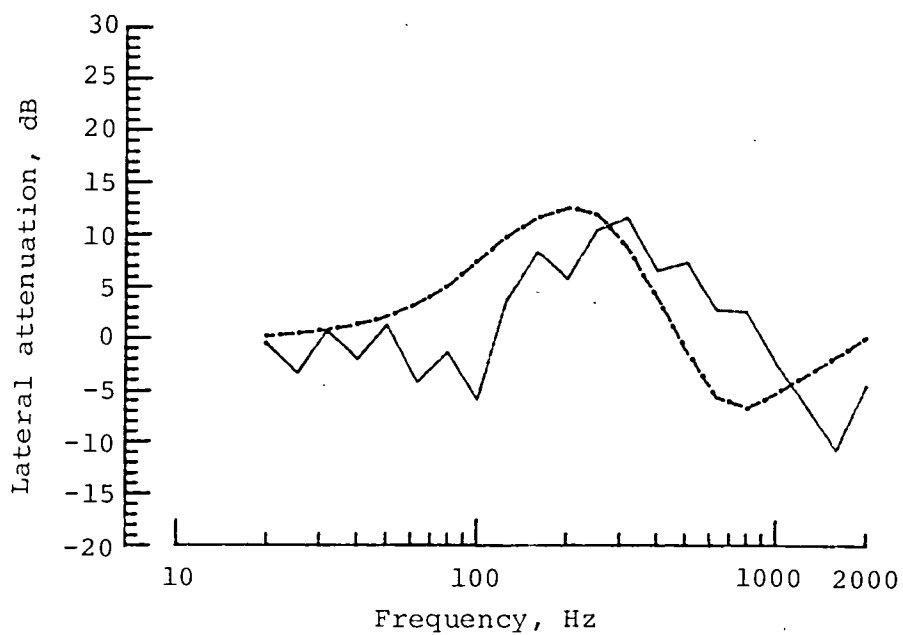
(e) Run 26; altitude, 10 m.

Figure 12.- Concluded.
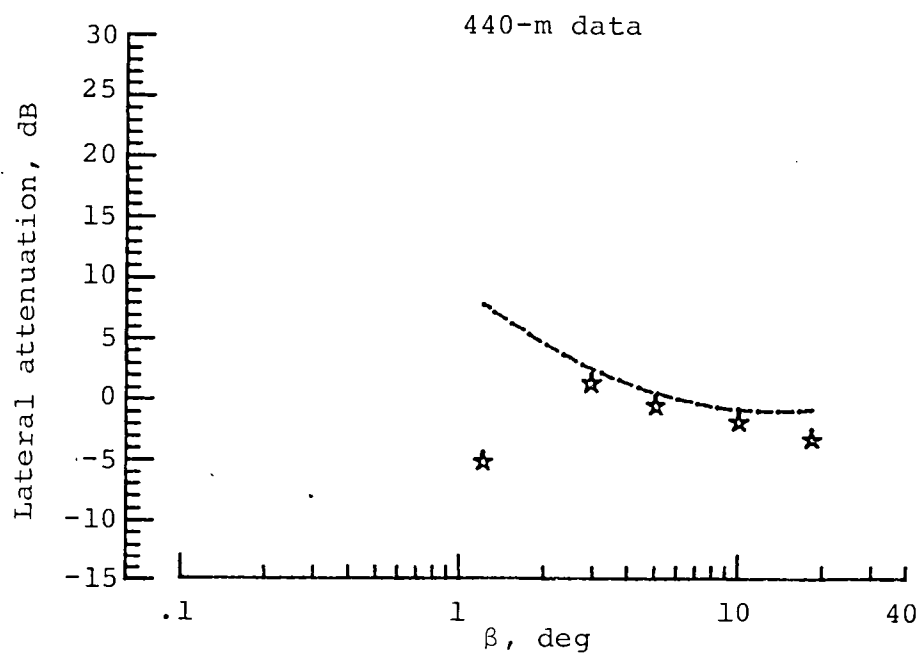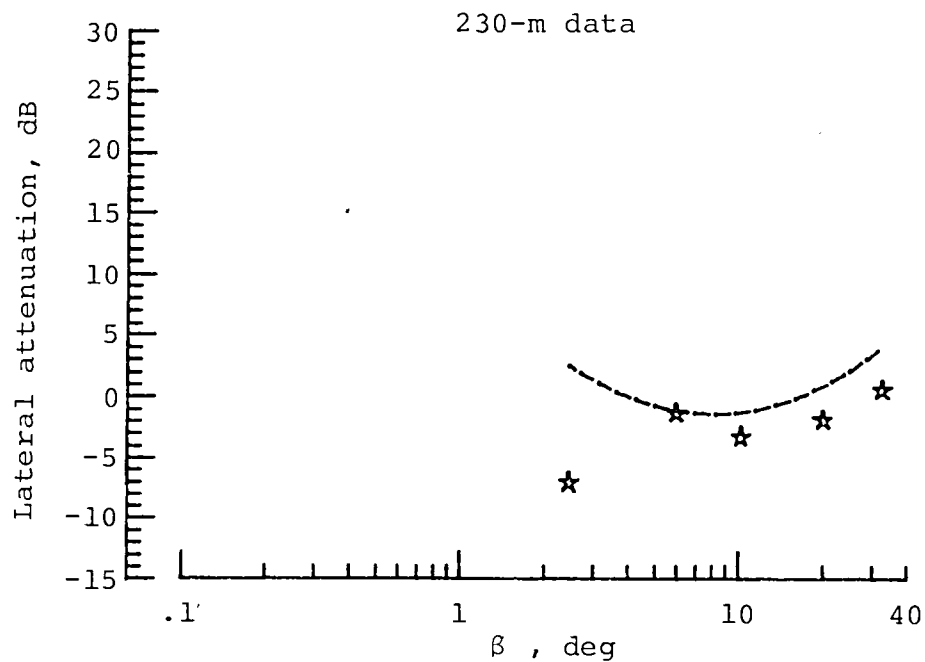
(a) 100 Hz.

Figure 13.- Near/far results. Symbols, measured results;
curves, predicted results.

900-m data

1600-m data

(a) Concluded.

Figure 13.- Continued.

230-m data

440-m data
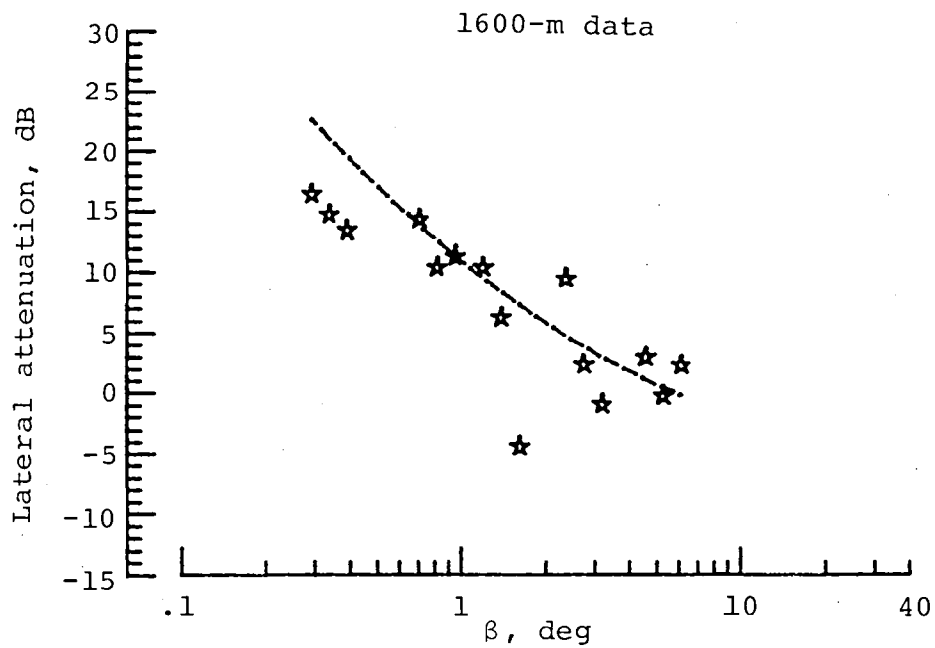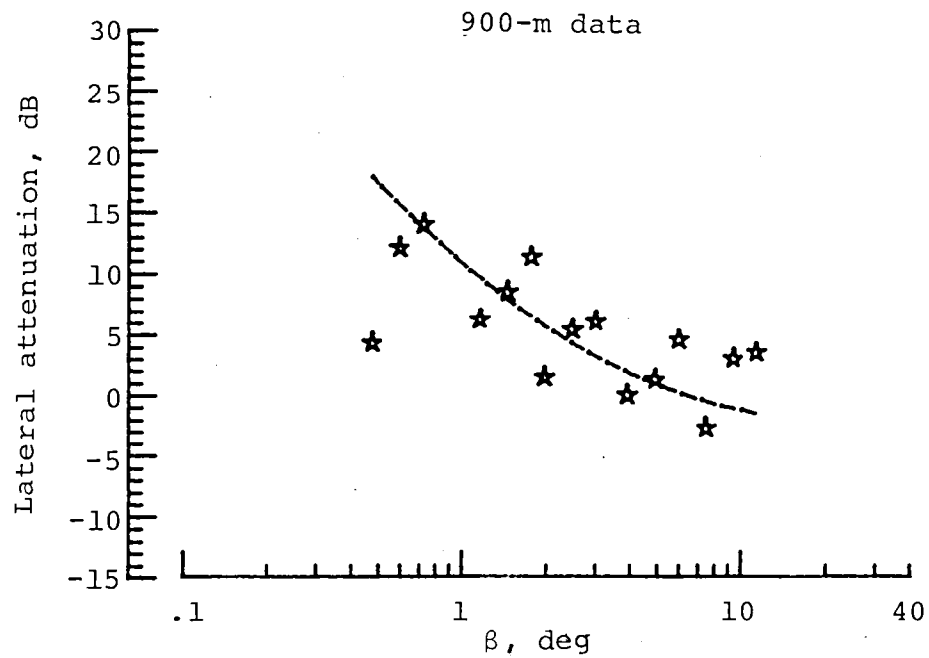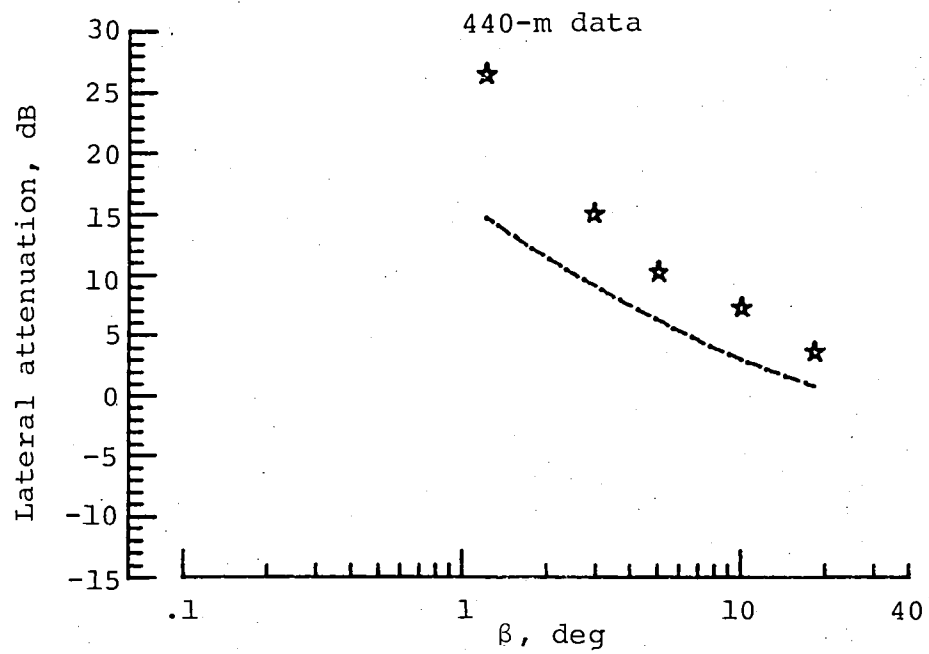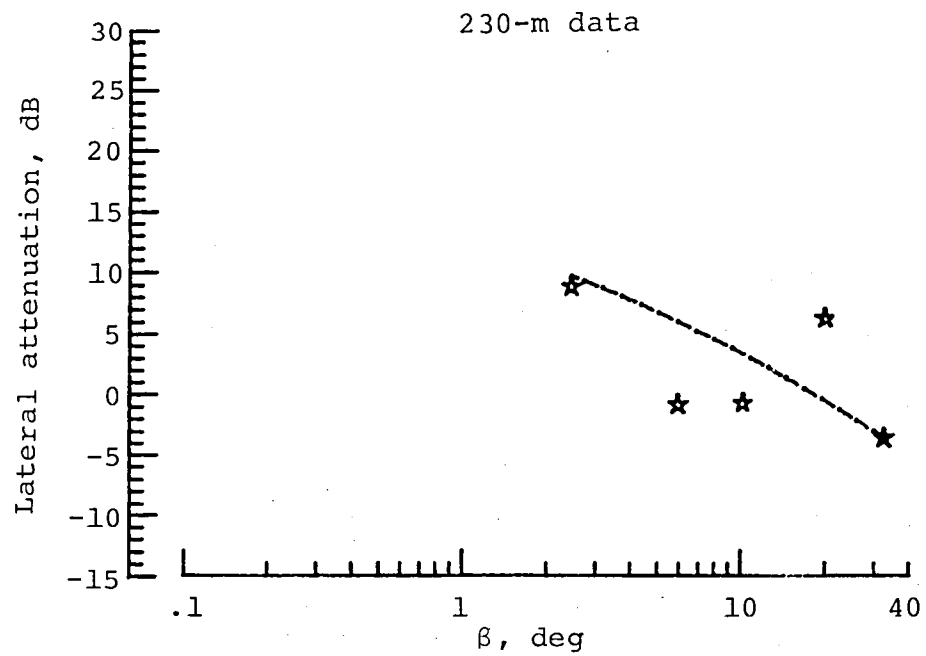
(b) 250 Hz.

Figure 13.- Continued.
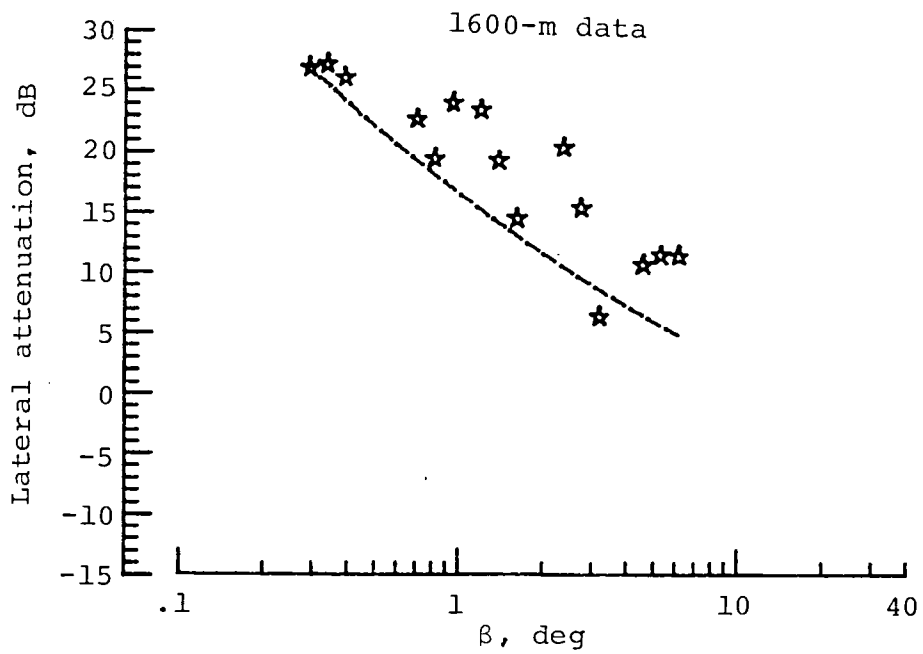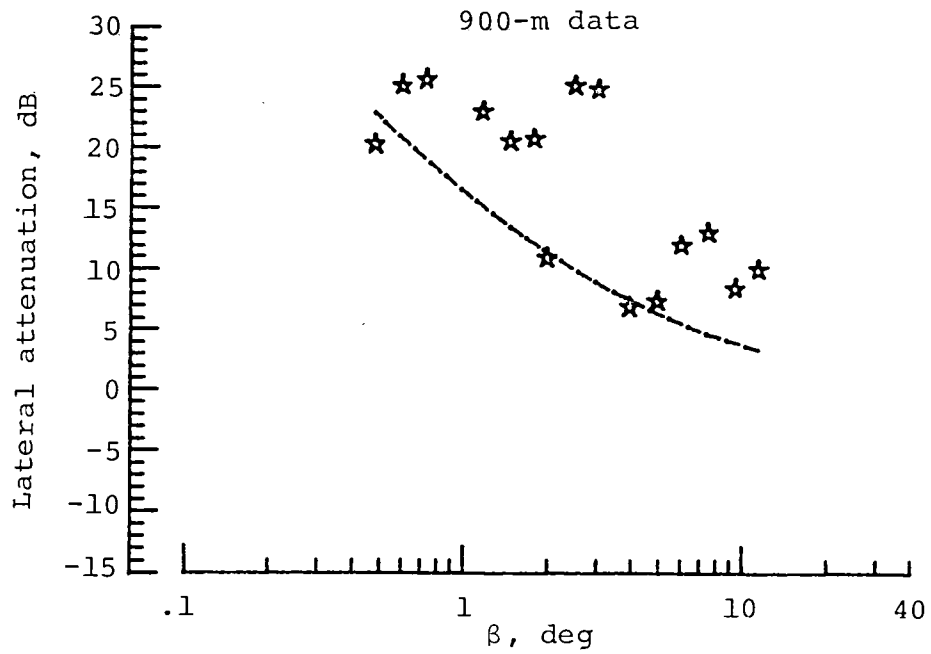
(b) Concluded.

Figure 13.- Continued.

(c) 300 Hz.

Figure 13.- Continued.

900-m data

1600-m data

(c) Concluded.

Figure 13.- Continued.

230-m data

440-m data
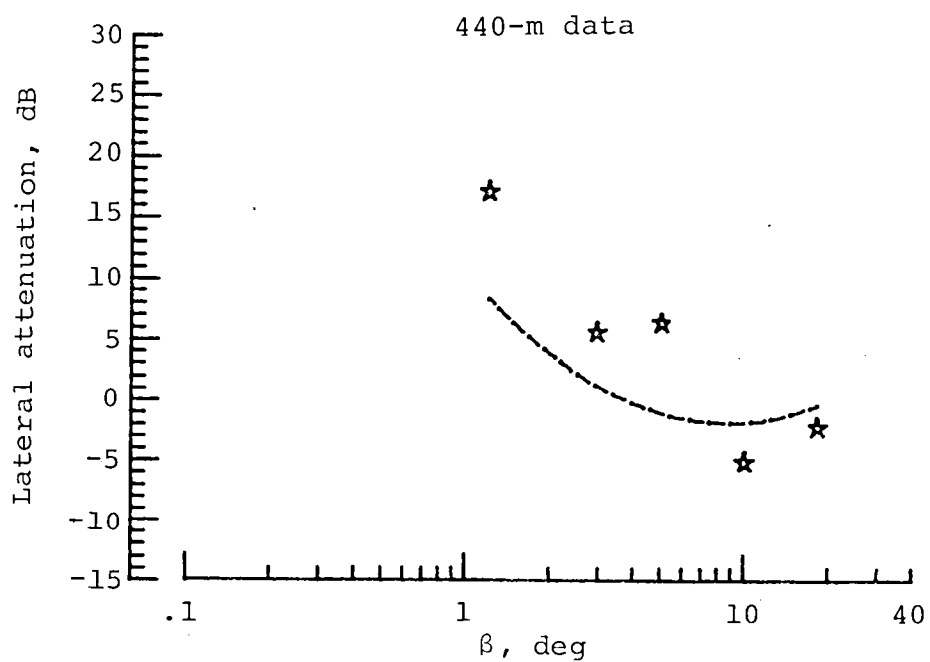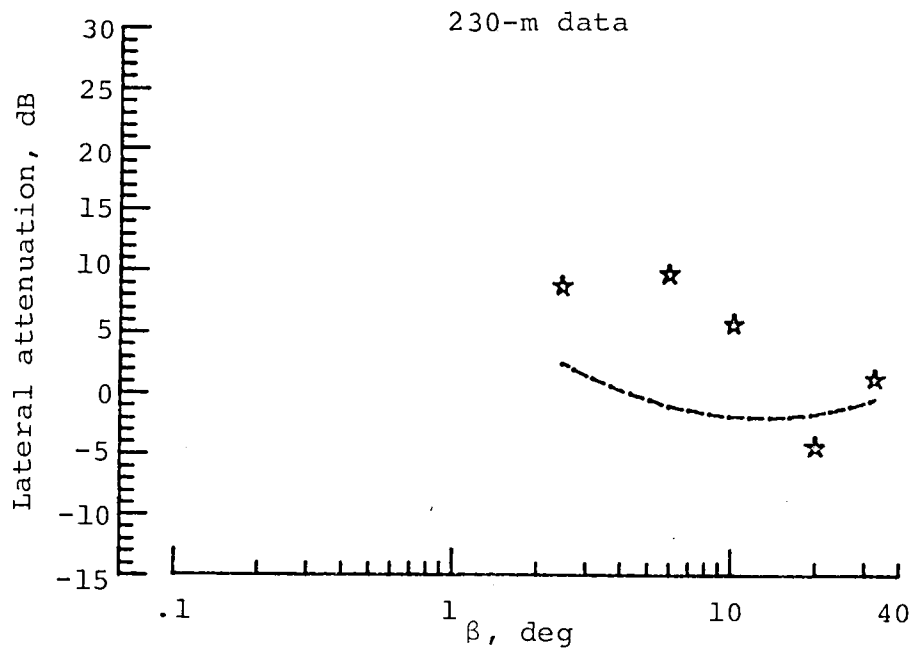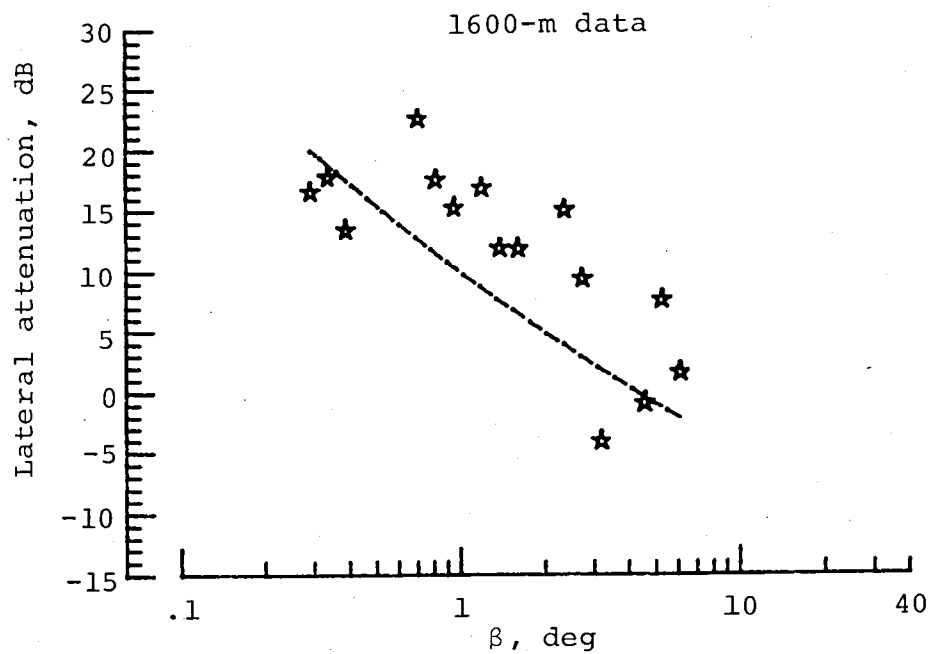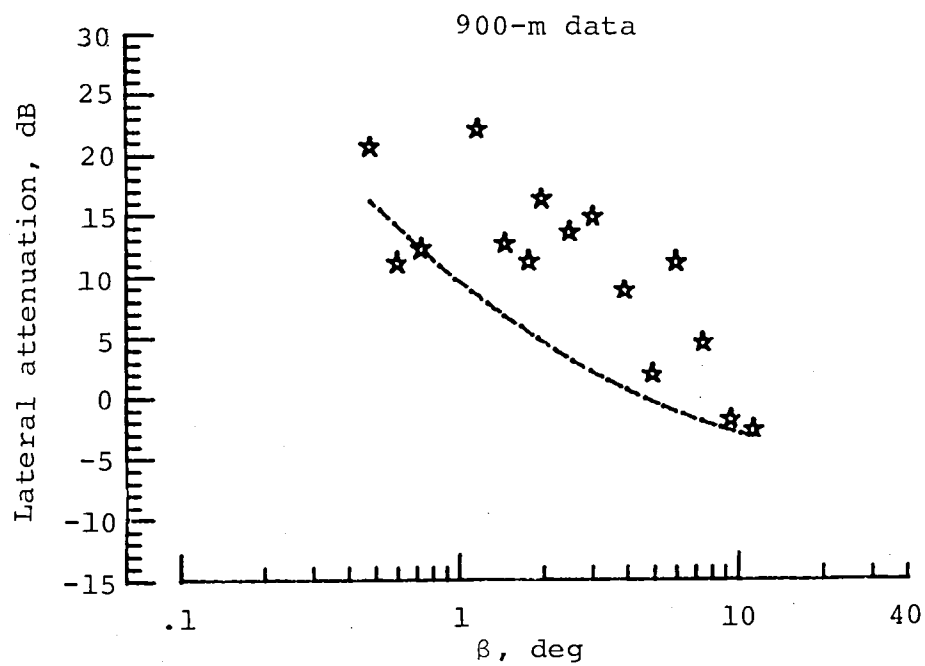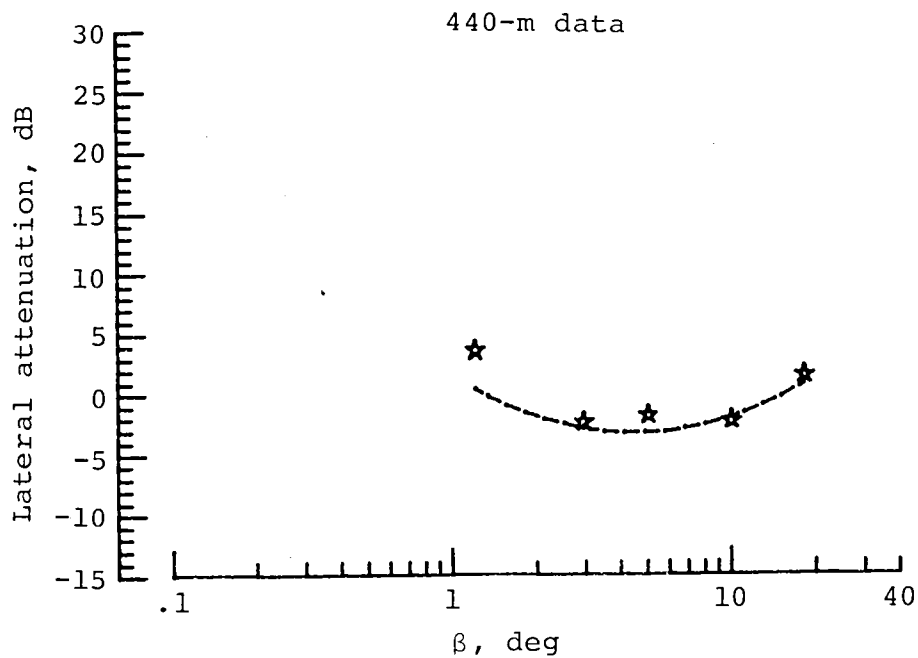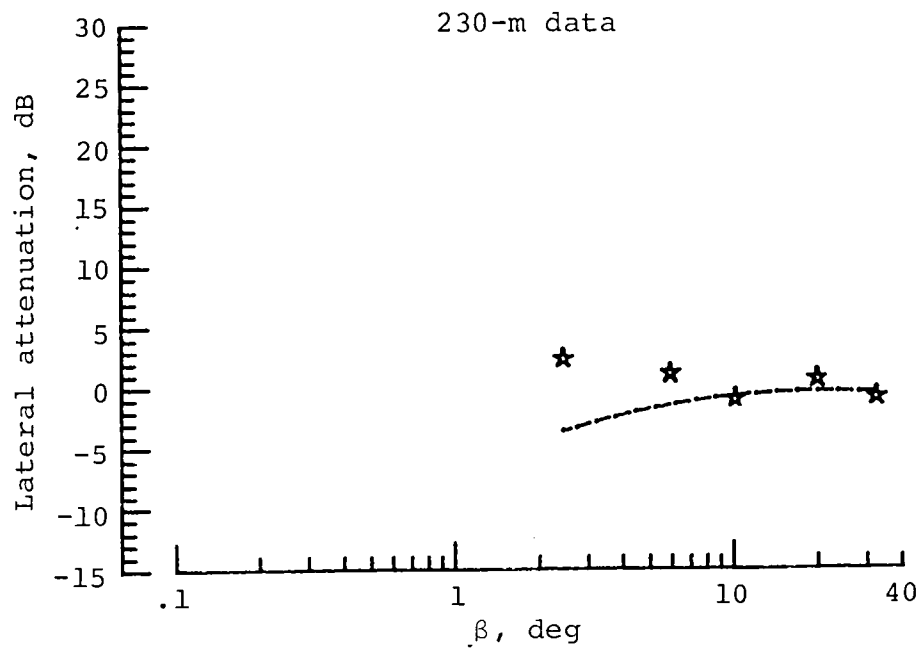
(d) 1000 Hz.

Figure 13.- Continued.
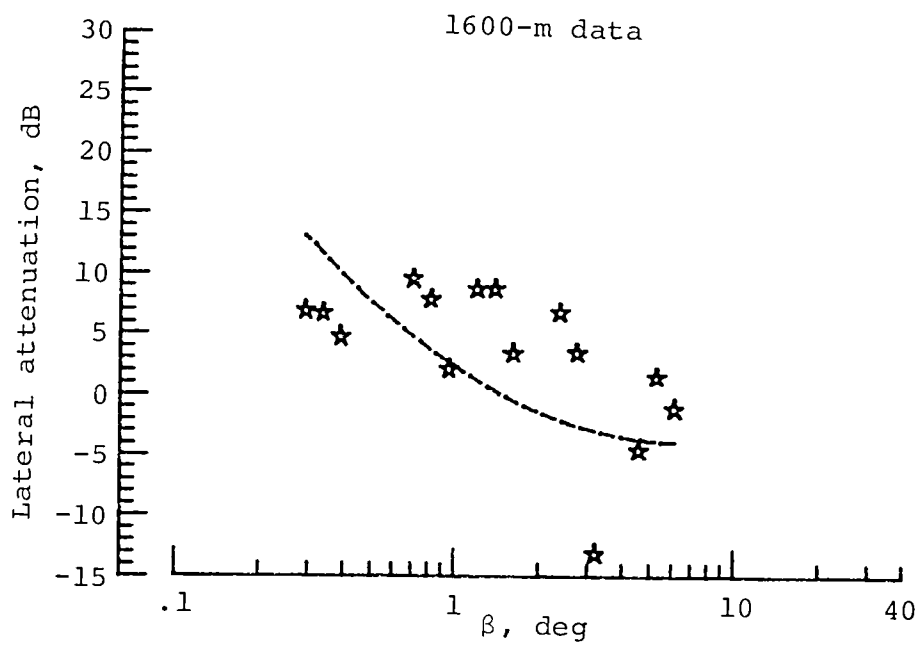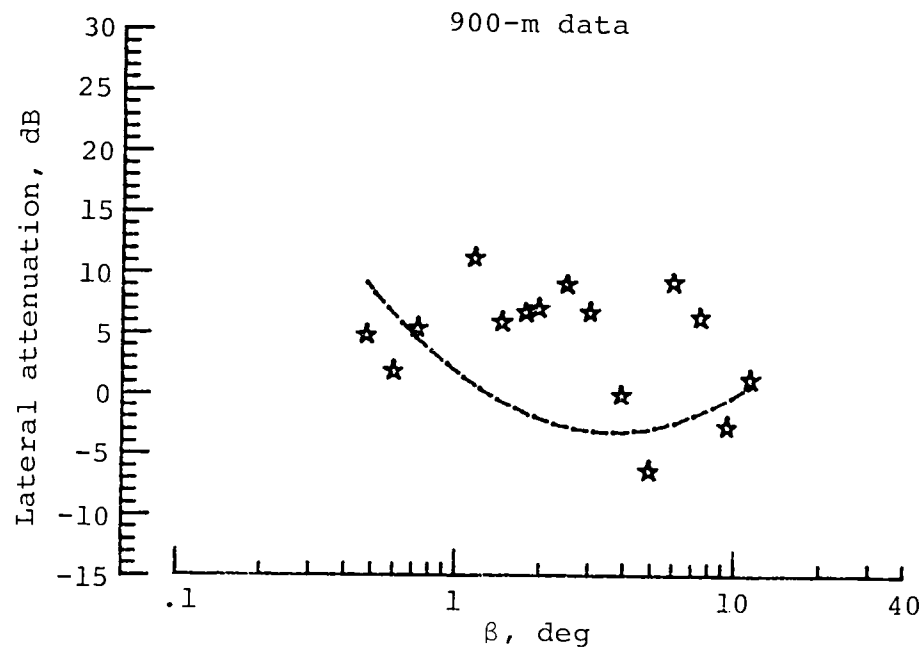
(d) Concluded.

Figure 13.- Concluded.
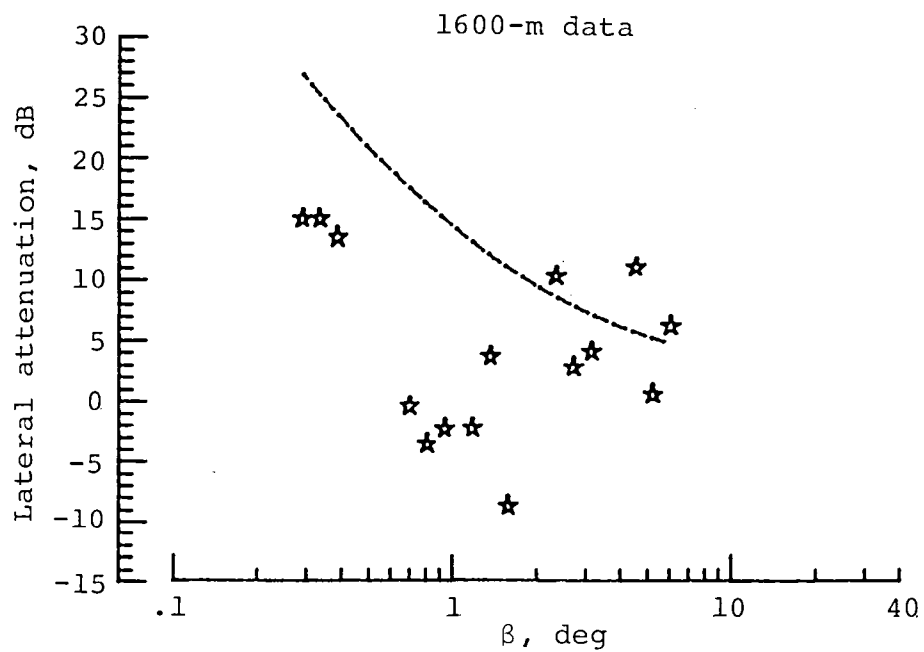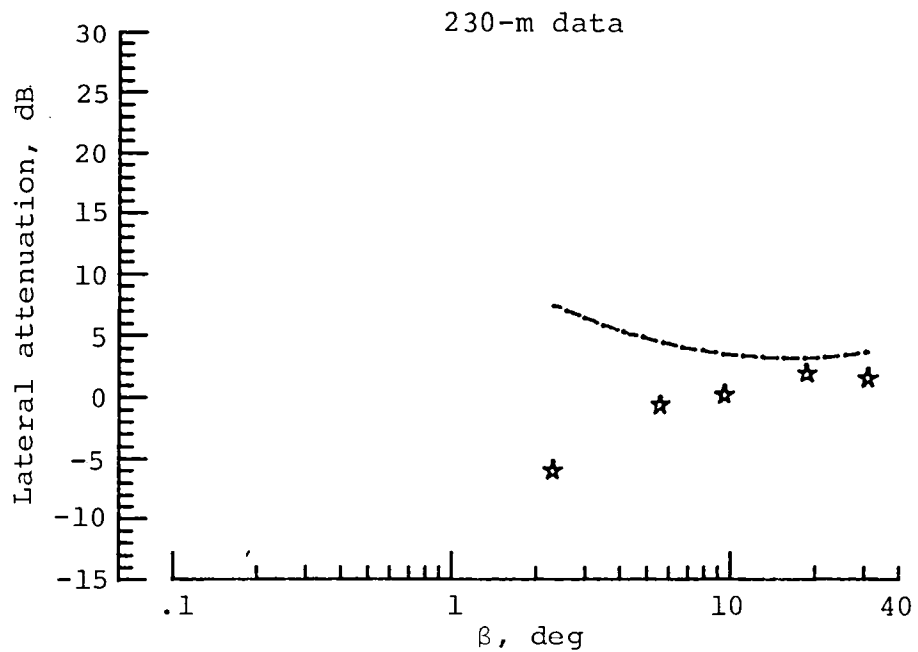
(a) 100 Hz.

Figure 14.- Direct results. Symbols, measured results;
curves, predicted results.
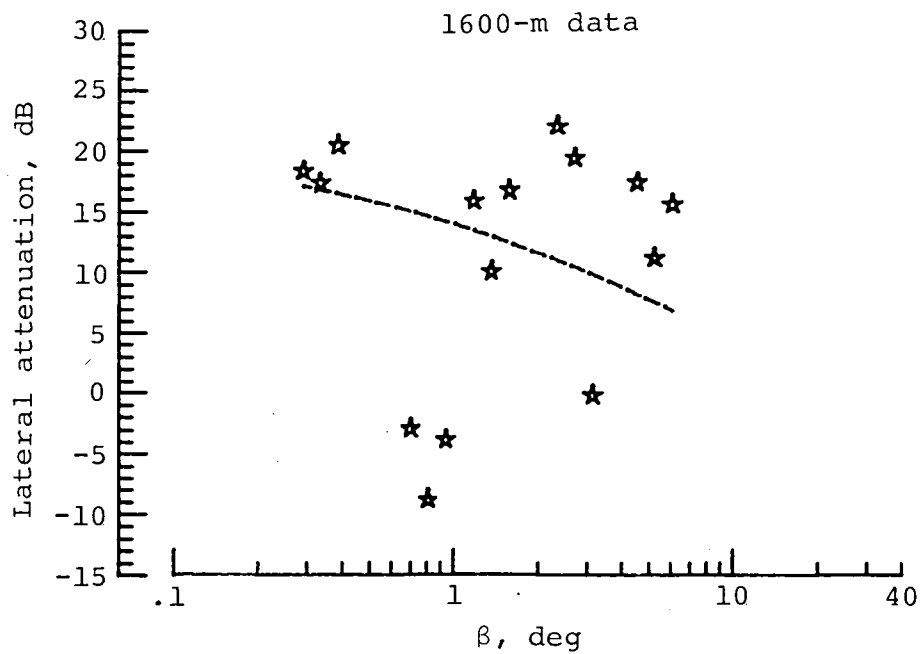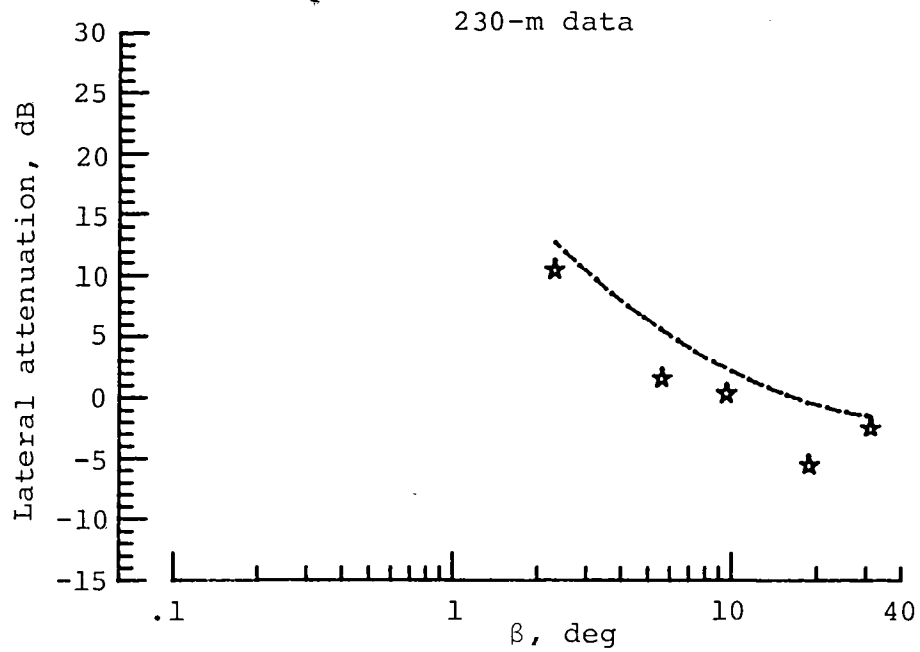
(b) 250 Hz.

Figure 14.- Continued.

230-m data

1600-m data
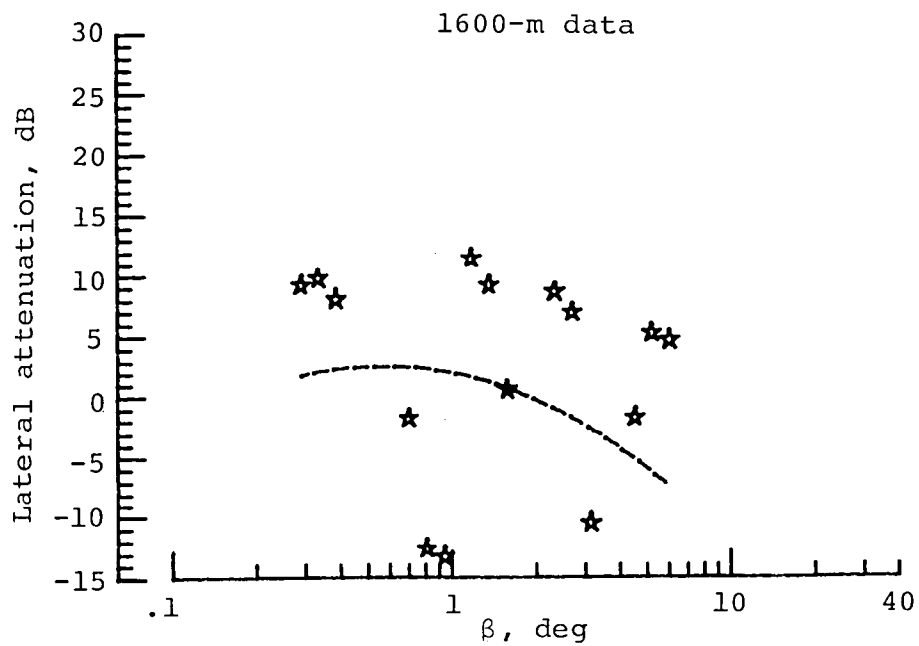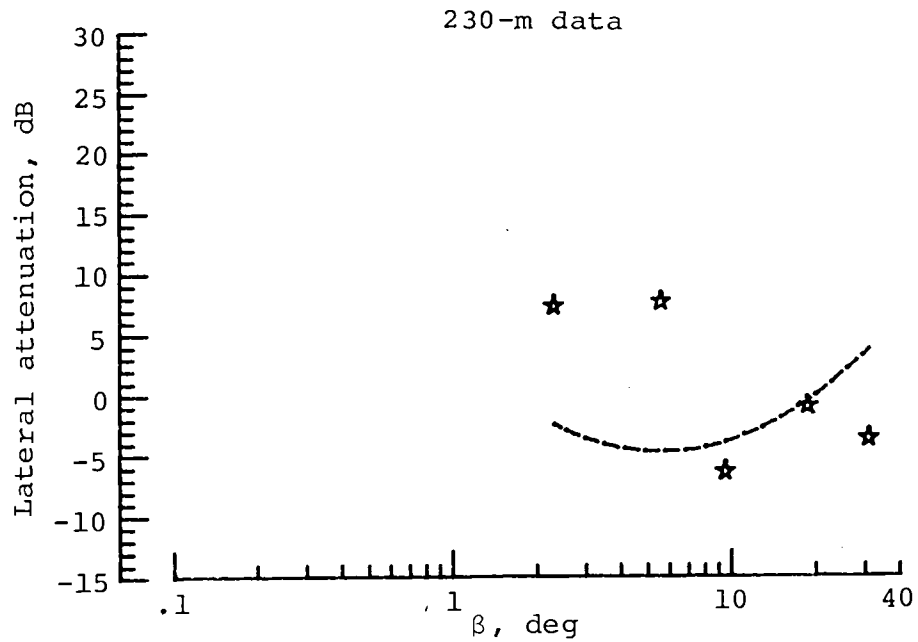
(c) 500 Hz.

Figure 14.- Continued.

230-m data

1600-m data
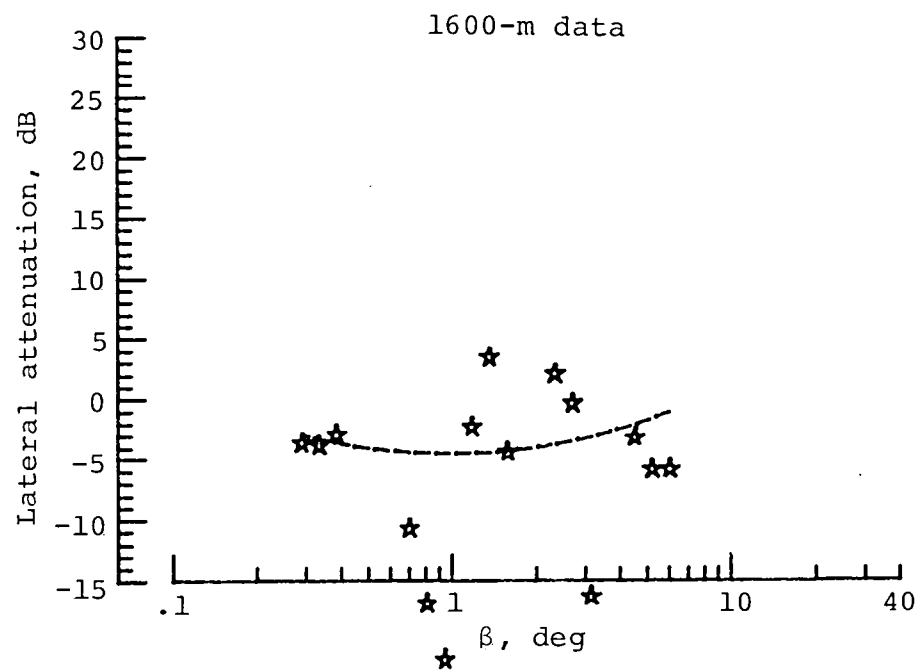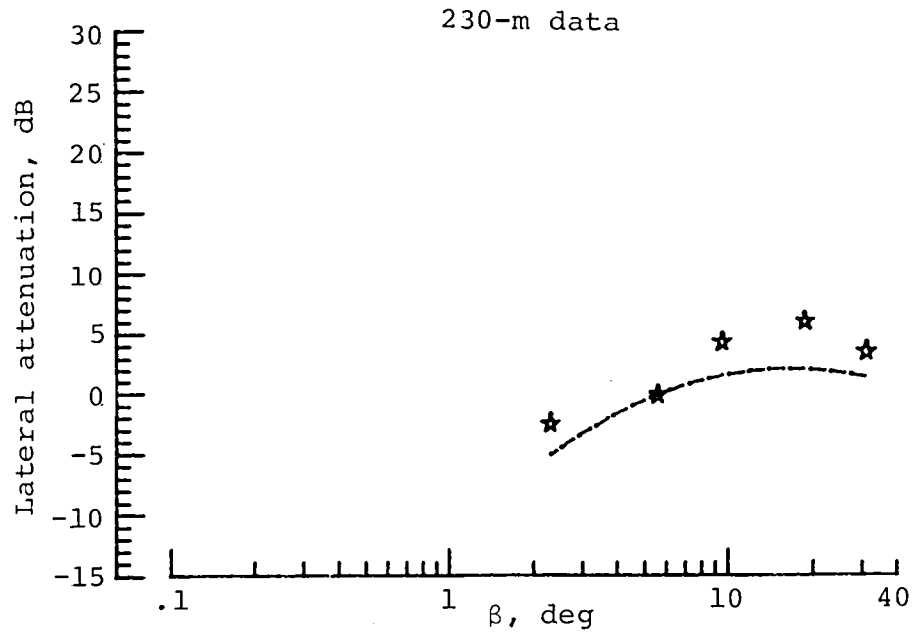
(d) 1000 Hz.

Figure 14.- Concluded.
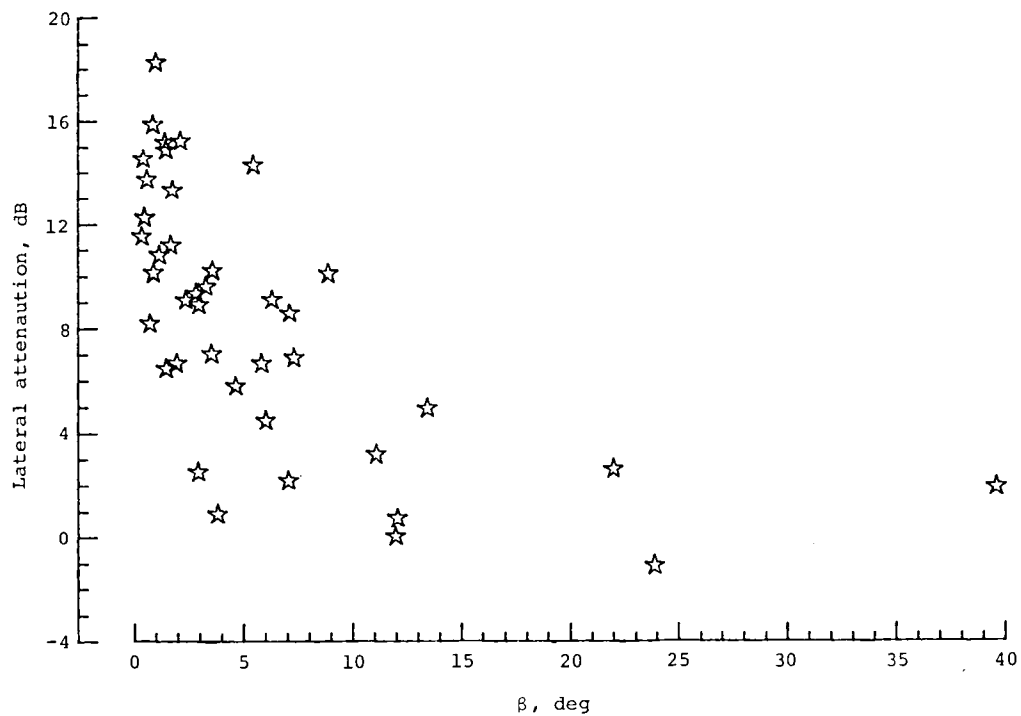
Figure 15.- Near/far results in EPNL units.
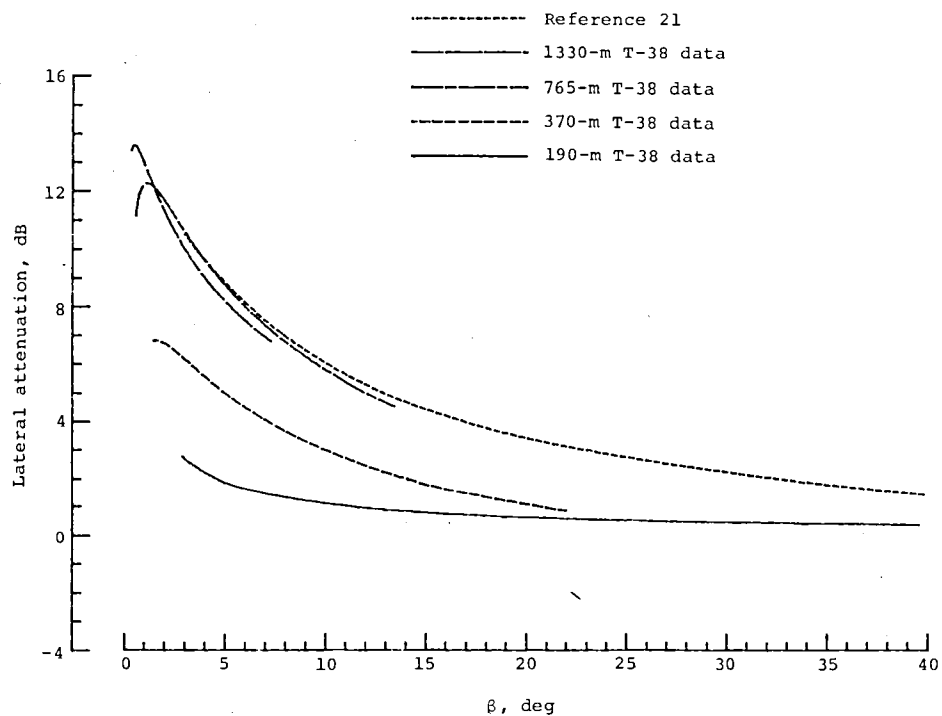
Figure 16.- Near/far results in EPNL units. Dependence on slant range.

1. Report No. NASA TP-1747	2. Government Accession No.	3. Recipient's Catalog No.
4. Title and Subtitle ASSESSMENT OF GROUND EFFECTS ON THE PROPAGATION OF AIRCRAFT NOISE: THE T-38A FLIGHT EXPERIMENT		5. Report Date December 1980
		6. Performing Organization Code 505-32-03-01
7. Author(s) William L. Willshire, Jr.		8. Performing Organization Report No. L-13765
		10. Work Unit No.
9. Performing Organization Name and Address NASA Langley Research Center Hampton, VA 23665		11. Contract or Grant No.
		13. Type of Report and Period Covered Technical Paper
12. Sponsoring Agency Name and Address National Aeronautics and Space Administration Washington, DC 20546		14. Sponsoring Agency Code

15. Supplementary Notes

16. Abstract

A flight experiment was conducted to investigate air-to-ground propagation of sound at grazing angles of incidence. A turbojet-powered airplane was flown at altitudes ranging from 10 to 160 m over a 20-microphone array positioned over grass and concrete. Acoustic, tracking, and weather data are presented in the appendices.

The dependence of ground effects on frequency, incidence angle, and slant range has been determined using two analysis methods. In one method, a microphone close to the flight path is compared to down-range microphones. In the other method, comparisons are made between two microphones which were equidistant from the flight path but positioned over the two surfaces. In both methods, source directivity angle was the criterion by which portions of the microphone signals were compared.

The ground effects were largest in the frequency range of 200 to 400 Hz and were found to be dependent on incidence angle and slant range. Ground effects measured for angles of incidence greater than 10° to 15° were near zero. Measured attenuation increased with increasing slant range for slant ranges less than 750 m. Theoretical predictions were found to be in good agreement with the major details of the measured results.

17. Key Words (Suggested by Author(s)) Ground effects Excess ground attenuation Flight experiment Noise propagation outdoors	18. Distribution Statement Unclassified - Unlimited Subject Category 71		
19. Security Classif. (of this report) Unclassified	20. Security Classif. (of this page) Unclassified	21. No. of Pages 125	22. Price A06

National Aeronautics and
Space Administration

Washington, D.C.
20546

THIRD-CLASS BULK RATE

U.S.MAIL

NASA